# RDCK FLOODPLAIN AND STEEP CREEK STUDY

# Kaslo River

**Final**
**March 31, 2020**

BGC Project No.:
**0268007**

BGC Document No.:
**RDCK2-CW-003F**

Prepared by BGC Engineering Inc. for:
**Regional District of Central Kootenay**

**BGC ENGINEERING INC. 500-980 Howe Street, Vancouver, BC Canada V6Z 0C8**
**Tel: 604.684.5900 Fax: 604.684.5909**

# TABLE OF REVISIONS

| ISSUE | DATE | REV | REMARKS |
|---|---|---|---|
| DRAFT | February 25, 2020 | | Issued for Client review. |
| FINAL | March 31, 2020 | | Final issue. |

# LIMITATIONS

BGC Engineering Inc. (BGC) prepared this document for the account of Regional District of Central Kootenay. The material in it reflects the judgment of BGC staff in light of the information available to BGC at the time of document preparation. Any use which a third party makes of this document or any reliance on decisions to be based on it is the responsibility of such third parties. BGC accepts no responsibility for damages, if any, suffered by any third party as a result of decisions made or actions based on this document.

As a mutual protection to our client, the public, and ourselves, all documents and drawings are submitted for the confidential information of our client for a specific project. Authorization for any use and/or publication of this document or any data, statements, conclusions or abstracts from or regarding our documents and drawings, through any form of print or electronic media, including without limitation, posting or reproduction of same on any website, is reserved pending BGC's written approval. A record copy of this document is on file at BGC. That copy takes precedence over any other copy or reproduction of this document.

# EXECUTIVE SUMMARY

This report provides a detailed flood hazard assessment of the Kaslo River at the Village of Kaslo, British Columbia. This river was chosen as a high priority clear-water hazard amongst hundreds in the Regional District of Central Kootenay (RDCK) from a risk perspective because of its comparatively high hazards and consequences from flooding. This report describes hydrological conditions and details the methods applied to create flood construction level (FCL) and hazard maps for the Kaslo River. This work is the foundation for possible future quantitative risk assessments or conceptualization of mitigation measures such as potential upgrades to existing dikes.

Flood mapping is used for estimating the extent and depth of different magnitude floods for application in community planning, policy development, and emergency response planning in areas subject to flood hazards. A two-dimensional (2D) hydraulic model was developed for an approximately 2-km length of the Kaslo River and provides hydraulic results to support identification of flood inundation extents and river hazards, and establishment of FCLs. In this report, FCLs are based on the 200-year return period event or annual exceedance probability (AEP) of 0.5% with consideration for climate change and include a freeboard allowance for planning purposes.

The following types of results were produced for the Kaslo River:

- Flood depth, velocity and intensity maps for the 20-, 50-, 100-, 200- and 500-year return period events
- Designated floodplain maps depicting the 200-year flood levels including a freeboard allowance of 0.6 m. The floodplain maps also incorporate results from a dike breach assessment
- Aerial photograph interpretation and channel change mapping.

Flood mapping developed by BGC Engineering Inc. (BGC) provides an update to historical floodplain mapping previously conducted for the Kaslo River. Flood extents are similar to the 1984 designated floodplain maps created by the BC Ministry of Forests, Lands and Natural Resource Operations and Rural Development (BC MFLNRORD). FCLs are higher than the historic floodplain maps, but some areas previously within the designated floodplain are no longer within the FCL. This is likely due to a combination of increased 200-year return period flood event that accounts for climate change, improved topography resolution and accuracy, and the application of more advanced modelling methods. Implementation of the Kaslo River FCLs, combined with community planning to control development within high hazard areas will lead to greater flood resiliency within the Village of Kaslo. Flood mapping results are also provided digitally through a BGC web application called Cambio™.

Channel change mapping conducted by BGC indicates that the Kaslo River channel has experienced progressive bank erosion, indicating that the flood hazard assessment and modelling should be updated over time. Furthermore, the assumptions made on changes in runoff due to climate change will likely need to be updated periodically as scientific understanding evolves.

Table E-1 provides key observations derived from the hazard assessment.

**Table E-1. Summary of key hazard assessment results.**

| Process | Key Observations |
|---|---|
| Bank erosion and channel changes | • Aerial photo interpretation and channel change mapping results indicate that the identified channel reaches have experienced bank erosion over the reviewed period (1957-2019). The channel protection works installed on the left bank downstream of Highway 31 have controlled the magnitude of these changes. However, high flows have the potential to exacerbate existing erosion processes. The sections where bank erosion has the potential to continue are: 1) where shear stresses concentrate (e.g., outside of meander bends) relevant to reaches upstream of the Highway 31 bridge; 2) where the banks are unprotected and erodible (e.g. local sections in reaches upstream of the Highway 31 bridge); and 3) where ongoing slope instability of the banks have been identified (e.g. within the 200 m upstream of the Highway 31 bridge). |
| Clear-water inundation | • Overland flooding occurs during the 20-year and higher return period floods on the vegetated bars upstream of the Village of Kaslo near the bike skills park. There appears to be limited infrastructure in the affected areas but flooding may impact recreational trails (e.g., Lettrari Trail).<br>• Flooding up to and including the 500-year event do not overtop the dikes, assuming no log jams occur.<br>• During the dike breach scenarios (200- and 500-year floods) overland flooding occurs in the residential area northwest of Kaslo River, approximately as far as D Ave.<br>• Recreational areas along the Kootenay Lake foreshore are flooded during the 50-year and higher return period floods by Kaslo River. |
| Hydraulic Structures (Bridges) | • The flood elevations for all scenarios modeled did not reach the low cord of the Highway 31 or Kaslo River Trail pedestrian bridges over Kaslo River.<br>○ There is approximately 1.4 m of clearance between the lower chord of the Highway 31 bridge and the 200-year return period flood.<br>○ There is greater than 1.5 m of clearance between the lower chord of the Kaslo River Trail pedestrian bridge and the 200-year return period flood. |
| Flood Protection Structures (Dikes) | • The dikes were designed with a 1 m freeboard and current modelling indicates that the crest is greater than 1 m above the 200-year flood elevation. |

# TABLE OF CONTENTS

**TABLE OF REVISIONS** ..... i
**LIMITATIONS** ..... i
**TABLE OF CONTENTS** ..... iv
**LIST OF TABLES** ..... v
**LIST OF FIGURES** ..... vi
**LIST OF APPENDICES** ..... vii
**LIST OF DRAWINGS** ..... vii
**1. INTRODUCTION** ..... 1
**1.1. Scope of Work** ..... 4
**1.2. Terminology** ..... 5
**1.3. Deliverables** ..... 5
**1.4. Study Team** ..... 5
**2. STUDY AREA CHARACTERIZATION** ..... 7
**2.1. Physiography** ..... 7
**2.2. Alluvial Fan and Floodplain Morphology** ..... 8
**2.3. Hydroclimatic Conditions** ..... 8
**2.4. Climate Change Impacts** ..... 11
**2.5. Glacial History and Surficial Geology** ..... 11
**3. SITE HISTORY** ..... 12
**3.1. Area Development** ..... 12
**3.2. Historical Flood Events** ..... 12
**3.3. Flood Protection and Hydraulic Structures** ..... 15
3.3.1. Bridges ..... 15
3.3.2. Dikes ..... 17
**3.4. Previous Mitigations** ..... 18
**3.5. Bank Erosion and Avulsion History** ..... 18
**4. METHODS** ..... 21
**4.1. Field Data, Topographic Data and River Bathymetric Surveys** ..... 21
4.1.1. Fieldwork and Site Investigations ..... 21
4.1.2. Topographic Mapping ..... 21
4.1.3. Ground and Bathymetric Surveying ..... 23
4.1.4. Survey Equipment, Accuracy and Processing Software ..... 23
4.1.5. Terrain Creation ..... 24
**4.2. Channel Change and Bank Erosion Analysis** ..... 24
4.2.1. Data Sources ..... 25
4.2.2. Methods ..... 25
4.2.3. Limitations and Uncertainties ..... 27
**4.3. Hydrological Analysis** ..... 28
4.3.1. Flood Frequency Analysis ..... 28
4.3.2. Climate Change Considerations ..... 29

**4.4. Hydraulic Modelling ..... 30**
4.4.1. General Approach ..... 30
4.4.2. Model Inputs ..... 30
4.4.2.1. Terrain Model ..... 31
4.4.2.2. Dike Breach ..... 31
4.4.2.3. Model Domain ..... 31
4.4.2.4. Boundary Conditions ..... 32
**4.5. Hazard Mapping ..... 32**
4.5.1. Hazard Scenario Maps ..... 33
4.5.2. Flood Construction Level Mapping ..... 33
**5. RESULTS ..... 35**
**5.1. Channel Change Mapping and Bank Erosion ..... 35**
**5.2. Hydrological Modelling ..... 38**
5.2.1. Historical Peak Discharge Estimates ..... 38
5.2.2. Accounting for Climate Change ..... 38
**5.3. Hydraulic Modelling ..... 40**
**5.4. Flood Hazard Mapping ..... 41**
**5.5. Flood Construction Level Mapping ..... 41**
**6. SUMMARY AND RECOMMENDATIONS ..... 42**
**6.1. Hazard Assessment ..... 42**
6.1.1. Channel Change Mapping and Bank Erosion Analysis ..... 42
6.1.2. Peak Discharge Estimates ..... 43
6.1.3. Hydraulic Modelling ..... 43
6.1.4. Flood Hazard Mapping ..... 43
**6.2. Limitations and Uncertainties ..... 43**
**6.3. Considerations for Hazard Management ..... 44**
**6.4. Recommendations ..... 45**
**7. CLOSURE ..... 46**

## LIST OF TABLES

Table E-1. Summary of key hazard assessment results ..... iii
Table 1-1. List of study areas. ..... 1
Table 1-2. Study team. ..... 6
Table 2-1. Watershed characteristics of Kaslo River ..... 7
Table 2-2. Historical (1961 to 1990) annual climate statistics ..... 10
Table 2-3. Projected change (RCP 8.5, 2050) from historical conditions ..... 11
Table 3-1. Bridge dimensions surveyed by Midwest Survey Inc., July 2019. ..... 16
Table 3-2. Relevant historical bank erosion and avulsion information. ..... 19
Table 4-1. Summary of survey equipment. ..... 24
Table 4-2. Aerial photographs and satellite imagery used in the analysis. ..... 25
Table 4-3. Geomorphic features used for geomorphic floodplain and channel mapping. ..... 26

Table 4-4. Levels of activity assigned to the geomorphic features. 26
Table 4-5. Channel change classes. 27
Table 4-6. WSC hydrometric station information for prorated FFA. 29
Table 4-7. Modelling scenarios and return period classes. 30
Table 4-8. Summary of HEC RAS modelling inputs. 31
Table 4-9. Flow impact force values shown on the flood hazard scenario maps 33
Table 5-1. Channel reaches characterization and average bank retreat. 36
Table 5-2. Summary of key changes observed within the analyzed periods. 36
Table 5-3. Trend analysis results. 38
Table 5-4. Historical and climate-adjusted peak discharge estimates for the Kaslo River 39
Table 5-5. Summary of modelling results. 40

## LIST OF FIGURES

Figure 1-1. Hazard areas prioritized for detailed flood and steep creek mapping 3
Figure 1-2. Federal Flood Mapping Framework (NRCan, 2017). 4
Figure 2-1. Historical (1961 to 1990) MAP (a), MAT (b), PAS (c) averaged 9
Figure 2-2. Annual maximum peak instantaneous flows at Kaslo River 10
Figure 3-1. Kaslo River flooding in 1894 (source: Kootenay Lake Archives). 13
Figure 3-2. Summary of recorded flood history, mitigation, and development history 14
Figure 3-3. Highway 31 bridge over Kaslo River looking upstream (west). 15
Figure 3-4. Standing upstream of the Kaslo River Trail pedestrian bridge. 16
Figure 3-5. Kaslo dike looking upstream towards the Highway 31 bridge. 17
Figure 3-6. Kaslo River dike locations. Image: Google Earth. 18
Figure 3-7. Bank erosion and slope instability upstream of the Highway 31 bridge 19
Figure 3-8. Tilted trees at the left (north bank) indicating bank instability processes 20
Figure 4-1. Lidar coverage for clearwater study sites. 22
Figure 4-2. Kaslo River study area modelling domain. 32
Figure 4-3. Definition of design flood levels (DFL) in the presence of a dike. 34
Figure 5-1. Identified channel reaches within the Kaslo River floodplain 37
Figure 5-2. Historical peak discharge estimates based on regional FFA 39
Figure 5-3. Model profile showing channel bed, 200-year water surface elevation 41

# LIST OF APPENDICES

APPENDIX A TERMINOLOGY
APPENDIX B SITE PHOTOGRAPHS
APPENDIX C REGIONAL FLOOD FREQUENCY ANALYSIS
APPENDIX D CLIMATE CHANGE IMPACTS ON HYDROLOGY
APPENDIX E HYDRAULIC ASSESSMENT METHODS

# LIST OF DRAWINGS

DRAWING 01 SITE LOCATION MAP
DRAWING 02 WATERSHED OVERVIEW MAP
DRAWING 03 SURVEY LOCATIONS
DRAWING 04 AERIAL PHOTOGRAPHS COMPARISON
DRAWING 05 HISTORICAL CHANNEL CHANGE MAP
DRAWING 06 FLOOD HAZARD MAP
DRAWING 07 FLOOD CONSTRUCTION LEVEL MAP

# 1. INTRODUCTION

The Regional District of Central Kootenay (RDCK, the District) is located in a mountainous region in southeastern British Columbia (BC) that is subject to damaging floods, which have resulted in impacts to communities and infrastructure. In 2018, RDCK retained BGC Engineering Inc. (BGC) to carry out a regional geohazard risk prioritization study for the District (BGC, March 31, 2019). Supported by National Disaster Mitigation Program (NDMP) Stream 1 funding, the objective of the study was to characterize and prioritize flood and steep creek (debris-flood and debris-flow) geohazards. Through the regional study, BGC identified and prioritized 427 flood and steep creek hazard areas within the RDCK, of which, six floodplains and ten steep creeks in the District were selected for further detailed assessment (Table 1-1, Figure 1-1).

**Table 1-1. List of study areas.**

| Site Classification | Geohazard Process | Hazard Code | Jurisdiction | Name |
|---|---|---|---|---|
| Floodplain | Clear-water Flood | 340 | Village of Salmo | Salmo River |
| | | 372 | Village of Slocan | Slocan River |
| | | 393 | Town of Creston | Goat River |
| | | 408 | RDCK Electoral Area A | Crawford Creek |
| | | 375 | RDCK Electoral Area K | Burton Creek |
| | | 423 | Village of Kaslo | Kaslo River |
| Steep Creek | Debris Flood | 212 | RDCK Electoral Area F | Duhamel Creek |
| | | 252 | RDCK Electoral Area F | Kokanee Creek |
| | | 248 | RDCK Electoral Area D | Cooper Creek |
| | | 137 | RDCK Electoral Area H | Wilson Creek |
| | | 242 | RDCK Electoral Area E | Harrop Creek |
| | | 95 | RDCK Electoral Area K | Eagle Creek |
| | | 238 | RDCK Electoral Area F | Sitkum Creek |
| | Hybrid Debris Flood/Debris Flow | 116 | RDCK Electoral Area E | Procter Creek |
| | | 251 | RDCK Electoral Area E | Redfish Creek |
| | Debris Flow | 36 | RDCK Electoral Area A | Kuskonook Creek |

The six clear-water hazard areas were prioritized either for development of new flood maps or modernization of existing historical flood maps. Flood maps provide information on the hazards associated with defined flood events, such as water depth, flow velocity, and the probability of occurrence. These maps are critical decision-making tools for local and regional governments to inform flood mitigation, land use planning, emergency management, and public awareness. Generally, the historical flood maps in the District are at least twenty years out-of-date and lack consideration of more robust hydraulic models, additional hydrological data, changes in land use such as urban development or the impacts of climate change. In response, updated floodplain

mapping was conducted by BGC for each of the six prioritized clear-water hazard areas and provided under separate cover along with digital deliverables through a BGC web application called Cambio™[1].

This report details the approach used by BGC to conduct detailed floodplain mapping for the Kaslo River at the Village of Kaslo, BC (Drawing 01). The Kaslo River flows into Kootenay Lake and has an approximate watershed area of 449 $km^2$ at the Village of Kaslo, as described in Section 2. The Kaslo River poses a flood hazard to properties and infrastructure constructed on the adjacent floodplain and low-gradient alluvial fan of the river. The river has a history of damaging flood events and has been diked through the Village, as described in Section 3.

Flood mapping developed by BGC provides an update to historical floodplain mapping conducted previously for Kaslo River in 1984 (BC Ministry of Forests, Lands and Natural Resource Operations [BC MFLNRO], 2016). The historical mapping lacks a design report to document the methods and assumptions used to create the maps. The BGC update is based on a two-dimensional (2D) hydraulic model, which was developed for about a 2-km length of the river using methods described in Section 4. Modelling results described in Section 5 provide estimated flood inundation extents and establishes flood construction levels (FCLs) based on the 200-year return period event or annual exceedance probability (AEP) of 0.5% and includes a freeboard allowance of 0.6 m for planning purposes.

An outcome of the study is an improved basis for community planning, bylaw development, and emergency response planning in developed areas subject to flood hazards, with consideration of climate change. Recommendations are provided in Section 6 and include considerations for next steps from the study such as possible future quantitative risk assessments (QRAs) or conceptualization of mitigation measures such as potential upgrades to existing dikes.

BGC is providing a summary report for the entire assessment, *RDCK Floodplain and Steep Creek Study Summary* Report (referred to herein as the “Summary Report”). Readers are encouraged to read the Summary Report to obtain context about the objectives, scope of work, deliverables, and recommendations of the larger study.

[1] *www.cambiocommunities.ca.*

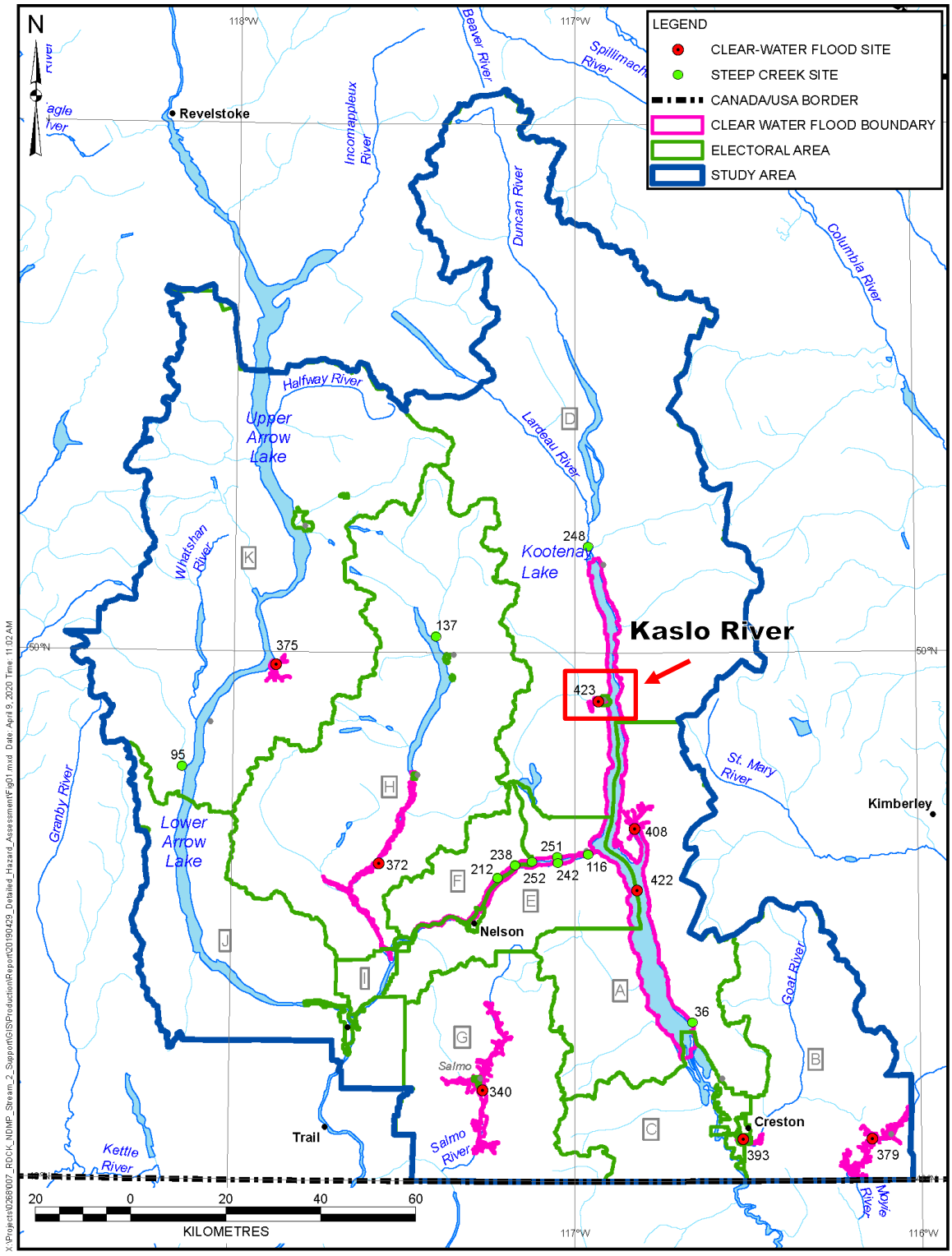


**Figure 1-1. Hazard areas prioritized for detailed flood and steep creek mapping. Site labels correspond to hazard identification numbers in Cambio. Kaslo River (No. 423) is labelled on the figure.**

## 1.1. Scope of Work

BGC's scope of work is outlined in the proposed work plan (BGC, May 24, 2019), which was refined to best meet RDCK's needs as the project developed (BGC, November 15, 2019). It was carried out under the terms of contract between RDCK and BGC dated June 20, 2019. The work scope was funded by Emergency Management BC (EMBC) and Public Safety Canada under Stream 2 of the NDMP.

For the Kaslo River, the scope of work included:

- Characterization of the study area including regional physiography and hydroclimate, and local watershed characteristics, geology and site characteristics.
- Development of a comprehensive site history of floods and mitigation activity.
- Compilation of data and baseline analyses required as inputs for flood geohazards assessment. This included topographic and river bathymetry data collection, terrain, hydrologic, hydraulic, and fluvial geomorphologic analyses, and consideration of climate change impacts.
- Complete hazard mapping and assessment according to provincial and national standards, including mapping of inundation areas, flow velocity, and flow depth for a range of return periods, including a dike breach scenario.
- Integrate flood mapping results with the regional study and disseminate flood hazard mapping and data in web-accessible formats amenable to incorporation into policy and risk-informed decision making.

The study scope was informed by Engineers and Geoscientists of British Columbia (EGBC, 2018) professional practice guidelines, *Legislated Flood Assessments in a Changing Climate in BC,* and EGBC (2017) guidelines for flood map preparation. The assessment is consistent with the *Federal Floodplain Mapping Framework* (Natural Resources Canada [NRCan], 2017). Within the NRCan framework, this study provides the foundation to risk assessment and mitigation (Figure 1-2).

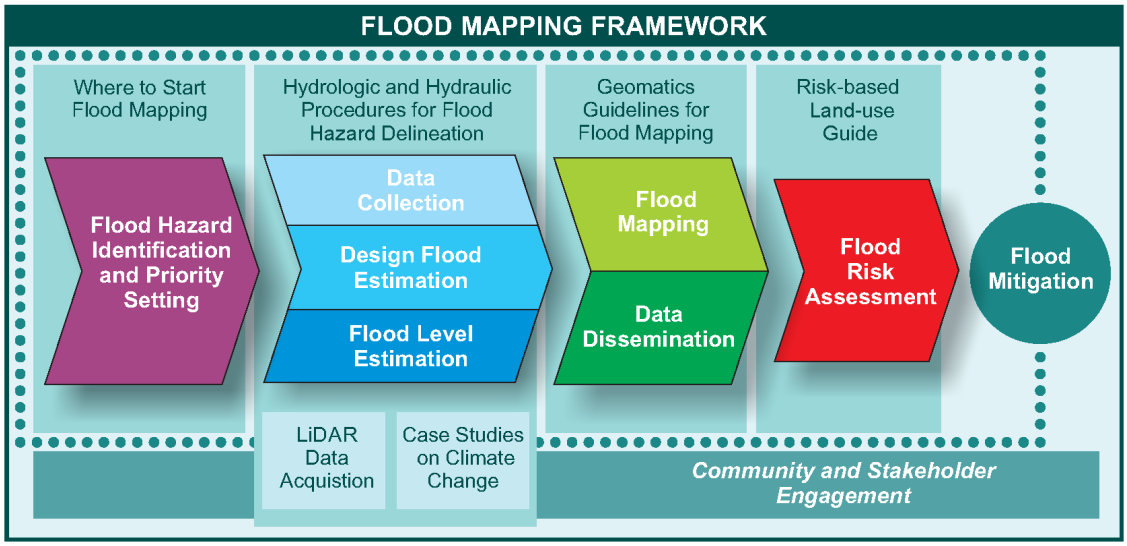


**Figure 1-2. Federal Flood Mapping Framework (NRCan, 2017).**

## 1.2. Terminology

This assessment uses specific hazard terminology, which is defined in Appendix A.

## 1.3. Deliverables

The deliverables of this study include this assessment report and digital deliverables (hazard maps) provided via the Cambio web application and as geospatial data provided to the RDCK.

This report is best read with access to a web application. Cambio displays the results of both the NDMP Stream 1 and Stream 2 studies. The application can be accessed at www.cambiocommunities.ca, using either Chrome or Firefox web browsers. The Summary Report provides a Cambio user guide.

## 1.4. Study Team

This study was multidisciplinary. Contributors are listed below, and primary authors and reviewers are listed in Table 1-2.

- Kris Holm, M.Sc., P.Geo., Principal Geoscientist
- Sarah Kimball, M.A.Sc., P.Eng., P.Geo., Senior Geological Engineer
- Rob Millar, Ph.D., P.Eng., P.Geo., Principal Hydrotechnical Engineer
- Hamish Weatherly, M.Sc., P.Geo., Principal Hydrologist
- Betsy Waddington, M.Sc., P.Geo., Senior Geoscientist
- Patrick Grover, M.A.Sc., P.Eng., Senior Hydrotechnical Engineer
- Elisa Scordo, M.Sc., P.Geo., P.Ag., Senior Hydrologist
- Pascal Szeftel, Ph.D., P.Eng., Senior Hydrotechnical Engineer
- Marc Oliver Trottier, M.A.Sc., P.Eng., Intermediate Hydrotechnical Engineer
- Melissa Hairabedian, M.Sc., P.Geo., Senior Hydrologist
- Hilary Shirra, B.A.Sc., EIT, Junior Hydrotechnical Engineer
- Toby Perkins, M.A.Sc., P.Eng., Senior Hydrotechnical Engineer
- Kenneth Lockwood, Ph.D., EIT, Junior Civil Engineer
- Beatrice Collier-Pandya, B.A.Sc., EIT, Geological Engineer
- Matthias Busslinger, M.A.Sc., P.Eng., Senior Geotechnical Engineer
- Carie-Ann Lau, M.Sc., P.Geo., Intermediate Geoscientist
- Phil LeSueur, M.Sc., P.Geo., Geological Engineer
- Lauren Hutchinson, M.Sc., P.Eng., Intermediate Geotechnical Engineer
- Anna Akkerman, B.A.Sc., P.Eng., Senior Hydrotechnical Engineer
- Matthew Buchanan, B.Sc., GISP, A.D.P., GIS Analyst
- Vanessa Cuervo, M.Sc., Geohazard Specialist
- Sophol Tran, B.A., A.D.P., GIS Analyst
- Lucy Lee, B.A., A.D.P., GISP, GIS Analyst/Developer
- Matthew Williams, B.Sc., A.D.P., GIS Analyst.
- Alistair Beck, B.S.F., Dip CST, Database/Web Application Developer
- Michael Porter, M.Eng., P.Eng., Director, Principal Geological Engineer.

**Table 1-2. Study team.**

| | | |
|---|---|---|
| **Project Director** | Kris Holm | |
| **Project Manager** | Sarah Kimball | |
| **Overall Technical Reviewer(s)** | Rob Millar<br>Hamish Weatherly | |
| **Section** | **Primary Author(s)** | **Peer Reviewer(s)** |
| 1 | Elisa Scordo | Kris Holm |
| 2 | Toby Perkins | Melissa Hairabedian<br>Betsy Waddington |
| 3 | Toby Perkins<br>Vanessa Cuervo | Melissa Hairabedian<br>Elisa Scordo |
| 4.1 | Elisa Scordo | Patrick Grover |
| 4.2 | Vanessa Cuervo | Betsy Waddington |
| 4.3 | Toby Perkins | Patrick Grover<br>Melissa Hairabedian |
| 4.4 | Toby Perkins | Marc Oliver Trottier<br>Pascal Szeftel |
| 4.5 | Toby Perkins | Marc Oliver Trottier<br>Pascal Szeftel |
| 5.1 | Vanessa Cuervo | Betsy Waddington |
| 5.2 | Toby Perkins | Marc Oliver Trottier<br>Pascal Szeftel |
| 5.3 – 5.5 | Toby Perkins | Marc Oliver Trottier<br>Pascal Szeftel |
| 6.0 | Toby Perkins<br>Vanessa Cuervo | Patrick Grover<br>Melissa Hairabedian |
| Appendix A | Hilary Shirra | Elisa Scordo |
| Appendix B | Toby Perkins | Elisa Scordo |
| Appendix C | Melissa Hairabedian<br>Patrick Grover | Hamish Weatherly |
| Appendix D | Melissa Hairabedian<br>Patrick Grover | Hamish Weatherly |
| Appendix E | Kenneth Lockwood<br>Toby Perkins | Patrick Grover<br>Pascal Szeftel |

# 2. STUDY AREA CHARACTERIZATION

The following section provides a characterization of the study area including physiography, hydroclimatic conditions and projected impacts of climate change, glacial history and surficial geology, and a description of the Kaslo River channel and floodplain.

## 2.1. Physiography

The Kaslo River watershed is in the Montane Cordillera Ecozone and Central Columbia Mountains Ecosection (Demarchi, 2011). Originating in the Kokanee Range of the Selkirk Mountains, Kaslo River flows southeast towards Kokanee Lake, with headwaters near the peaks of Mount Jardine and Mount Carlyle at elevations exceeding 2,500 m. Keen Creek is a major tributary to Kaslo River with a similar watershed area above their confluence. The headwaters of Keen Creek are the glaciated Kokanee Mountain with an elevation of 2,790 m. The confluence of Keen Creek and Kaslo River is approximately 5 km upstream of the Village of Kaslo, which is located on the west side of Kootenay Lake. The lake has an approximate normal elevation of 532 m. Kaslo River has a total watershed area of 449 $km^2$ above the alluvial fan described in Section 2.2 (Drawing 02).

The watershed contains a few small unnamed lakes. Glaciers are present in the headwaters of Keen Creek, but currently represent less than 1% of the total watershed area. The Kaslo River watershed boundary is presented in Drawing 02 and key physiographic parameters of the watershed are listed in Table 2-1.

**Table 2-1. Watershed characteristics of Kaslo River.**

| Characteristic | Value |
|---|---|
| Watershed area ($km^2$) | 449 |
| Maximum watershed elevation (m) | 2,790 |
| Minimum watershed elevation (m) | 532 |
| Watershed relief (m) | 2,258 |
| Watershed centroid elevation (m) | 1,280 |
| Typical mainstem channel gradient above Village of Kaslo[1] (%) | 1.9 |
| Average channel gradient through the Village of Kaslo (%) | 1.9 |

Note:
1. Typical mainstem channel gradient is the average gradient between near Retallak and Village of Kaslo. Sub reaches may be steeper or flatter.

## 2.2. Alluvial Fan and Floodplain Morphology

Downstream of the Kaslo River and Keen Creek confluence, the river is confined in a narrow valley for approximately 5 km (Drawing 01 and 02). Highway 31A is on the left (north) bank of the river through this section. In this reach, the valley bottom is approximately 100 m wide and the channel meanders slightly within the valley before reaching the apex of the fan (Drawing 04), a moderate-gradient cone-shaped depositional feature formed where the river becomes unconfined within the wide valley of the Kootenay River. This fan has formed through sediment transport during post-glaciation flood events over the last 10,000 years after Quaternary glaciation receded from the area. Contemporary sediment transport rates do not appear to be particularly high, as indicated by the single-channel morphology of the river through the fan boundary. The coarse bed material and slumping banks indicate that the channel may be degrading (lowering in average channel elevation). However, large flood events may still transport substantial sediment volumes sourced from avalanches and debris-flow activity on small tributaries in the upper watershed. A smaller contemporary fan delta has developed where the Kaslo River meets Kootenay Lake due to deposition of fine-grained (predominantly sand and gravel) bedload at the confluence.

Where the river flows through the Village of Kaslo, the average bankfull width is approximately 20 to 30 m. The river is confined in the valley bottom or by dikes and displays a low sinuosity, single-channel morphology. The average channel gradient is approximately 2% (0.02 m/m). Sediment sampling in April 2019 indicates that bed material sizes within the active channel range from approximately 90 mm to 520 mm in diameter and the median diameter ($D_{50}$) is approximately 170 mm. Site photographs are provided in Appendix B.

## 2.3. Hydroclimatic Conditions

Large-scale airflows moving in from the Pacific bring moist, marine air to the BC Interior. The Columbia Mountains, lying perpendicular to the prevailing winds, influences the distribution of precipitation and temperatures within the Columbia River watershed. Air masses rising over the Columbia Mountains produce an area of increased precipitation in the form of rain in the summer and deep snow in the winter. Cold air from the arctic infrequently enters this area because it is protected by mountain ranges from all sides. Located within the Columbia Mountain range, the Kaslo River watershed rises to an elevation of approximately 2,790 m where the historical (1961 to 1990) mean annual precipitation (MAP) is approximately 1,900 mm (Wang et al, 2016). For comparison, the Village of Kaslo is located at an elevation of approximately 540 m and receives a MAP of approximately 800 mm.

Distributed across the watershed, the historical MAP is 1,312 mm, of which approximately 756 mm is snowfall (Table 2-2). The historical mean annual temperature (MAT) in the watershed is approximately 2.1ºC. The spatial distribution of historical average precipitation, temperature, and precipitation as snowfall (PAS) is depicted in Figure 2-1 based on climate data from Wang et. al. (2016). Precipitation occurs primarily as snowfall from November to April, and as rain throughout the remainder of the year. Precipitation is highest on average in November and lowest in August.

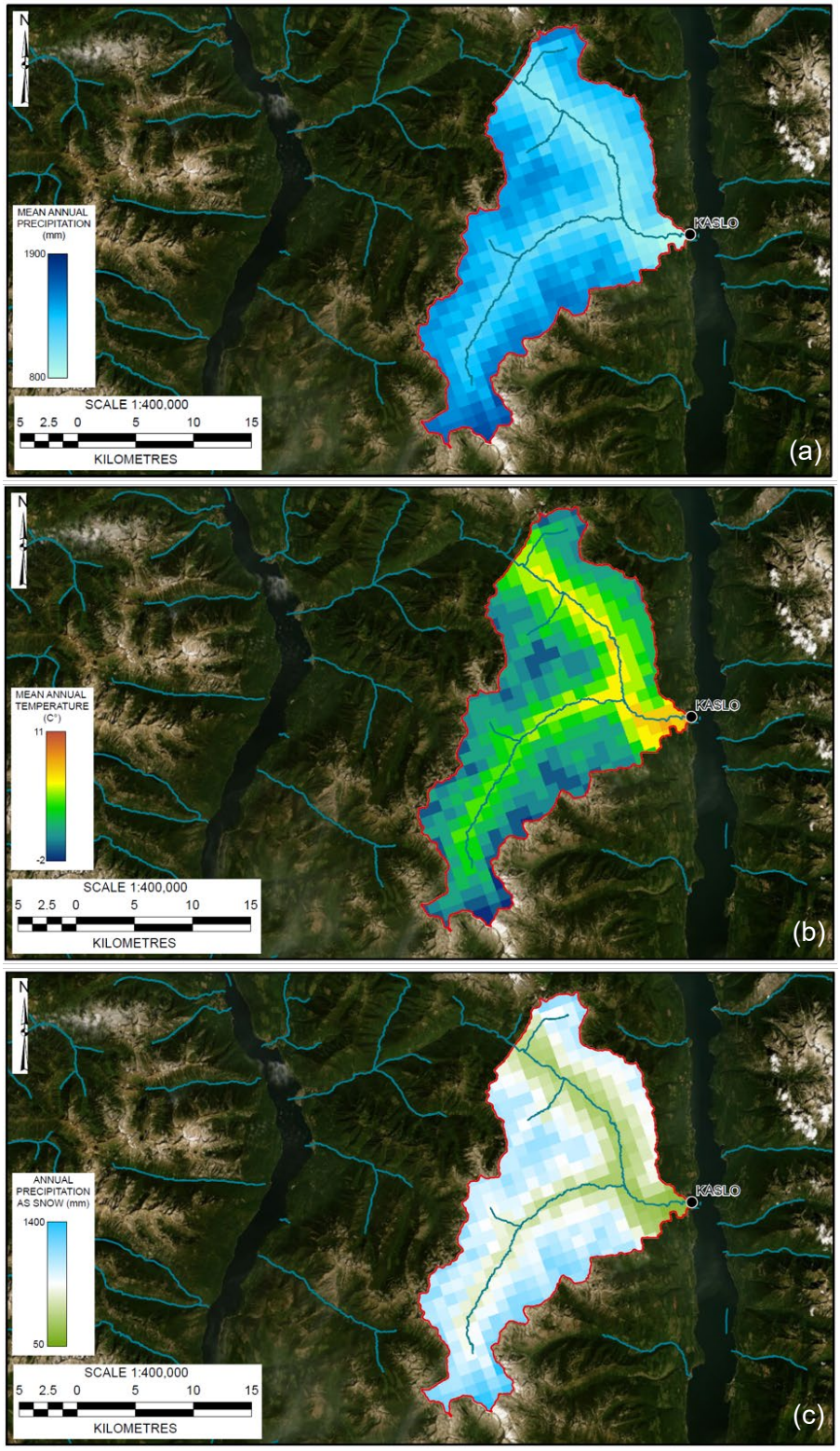


**Figure 2-1. Historical (1961 to 1990) MAP (a), MAT (b), PAS (c) averaged over the Kaslo River watershed (from Wang et. al., 2016).**

**Table 2-2. Historical (1961 to 1990) annual climate statistics for the Kaslo River watershed (from Wang et al., 2016).**

| Variable | Mean Annual Total | Percent of total annual precipitation (%) |
|---|---|---|
| Temperature | 2.1 ºC | - |
| Precipitation | 1312 mm | 100 |
| Precipitation as Snow | 756 mm | 58 |
| Precipitation as Rainfall | 556 mm | 42 |

The Kaslo River is currently gauged by the Water Survey of Canada (WSC) at hydrometric station *Kaslo River below Kemp Creek* (08NH005). This station has a record that extends from 1914 to 2018, although the station was inactive between 1920 and 1964. The hydrometric station is located near the outlet of the watershed just upstream from the Village of Kaslo, as shown on Drawing 02. Kaslo River is not regulated by dams. The timing of the peak flows generally occurs between May and June in response to spring snowmelt.

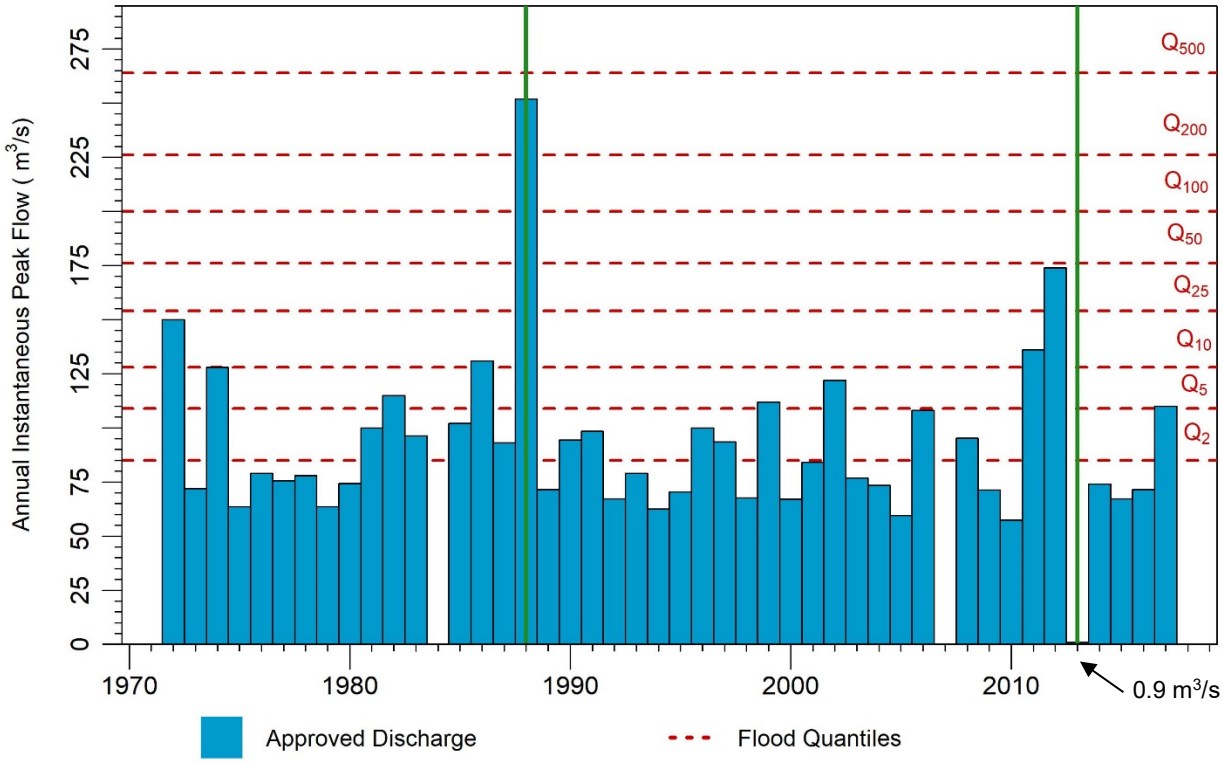


**Figure 2-2. Annual maximum peak instantaneous flows at Kaslo River below Kemp Creek (08NH005). Return period peak flow values do not include climate change. Green bars show records for 1988 and 2013 which were considered erroneous (see Section 4.3.1). Records were not provided by WSC for 1984 and 2007.**

## 2.4. Climate Change Impacts

The mean annual temperature in the Kaslo River watershed is projected to increase from 2.1°C (based on historical period 1961 to 1990) to 5.7 ºC by 2050 (based on period 2041 to 2070) assuming the representative carbon pathway 8.5 (RCP 8.5). MAP is projected to increase to 1390 mm while the component as snow is projected to decrease to 520 mm by 2050 in the Kaslo River watershed. Projected change in climate variables from historical conditions for the Kaslo River watershed are presented in Table 2-3.

Extreme flood events in the Montane Cordillera are often associated with rain-on-snow events in the spring (Harder et al., 2015). Although the effects of climate change on precipitation are not clear, projected increases in temperature are expected to have the largest impact on annual minimum temperatures occurring in the winter months (Harder et al., 2015). The effects of temperature change differ throughout the region. High elevation regions within the Montane Cordillera (e.g., Upper Columbia watershed) are projected to experience increases in snowpack due to increased precipitation and although temperatures increase, these areas remain above the freezing level. While at lower elevations, increased precipitation and temperature will result in increased winter runoff and smaller snowpack (Loukas & Quick, 1999; Schnorbus et al., 2014).

Changes in streamflow vary spatially and seasonally based on snow and rainfall changes and topography-based temperature gradients. Researchers anticipate that average streamflow conditions will increase in the winter and spring in this region due to earlier snowmelt and more frequent rain events. Peak flow timing is expected to be earlier in many rivers (Schnorbus et al., 2014; Farjad et al. 2016). Peak flows may increase or decrease depending on the watershed characteristics and the balance of temperature and precipitation changes described above.

**Table 2-3. Projected change (RCP 8.5, 2050) from historical conditions (1961 to 1990) for the Kaslo River watershed (Wang et al, 2016).**

| Climate Variable | Projected Change |
|---|---|
| MAT | +3.6 ºC |
| MAP | +76 mm |
| PAS | -233 mm |

## 2.5. Glacial History and Surficial Geology

Between 2 million and 10,000 years ago ice sheets advanced and retreated into the Kootenay region (Turner et al., 2009). The final glaciation which ended approximately 10,000 years ago is responsible for many of the surficial materials in the area. South-flowing glaciers carved deep troughs which now hold Kootenay, Arrow and Slocan Lakes. Ice dammed the outlet to Kootenay Lake during deglaciation, which resulted in lake levels approximately 150 m higher than present, and the deposition of silts and clays in isolated terraces near the lake shore. The processes of erosion and deposition have continued since deglaciation creating the younger deposits, such as the fluvial materials found along the streams. The river valley sides are bedrock with a thin, discontinuous cover of glacial till and colluvium (Fulton et al., 1984). Fluvial sediments are present in a narrow strip along the river and in the fan.

# 3. SITE HISTORY

## 3.1. Area Development

Prior to the arrival of European settlers on Kootenay Lake, the Kutenai (Ktunaxa) and Lakes (Sinixt) indigenous nations made this region their home and both likely camped on the Kaslo delta as part of their seasonal rounds. Ktunaxa nation today states that Kaslo was known to them as 'Qatsu,' meaning 'the land between the snow and the water.' (Kaslo Now, n.d.).

The Village of Kaslo is the oldest incorporated community in the Kootenay Region. The Village grew rapidly in the late 1800s during the mining boom and a mill was constructed as the watershed and surrounding areas were logged. It has been reported that Kaslo River was relocated towards the right (south) side of the fan, likely following the 1894 flood (MoE, 1981). However, no official documentation has been found to confirm. Today the Village of Kaslo has a population of approximately 1,000 people (Statistics Canada, 2016). The estimated total improvement value of parcels intersecting the Kaslo River hazard area based on the 2018 BC Assessment Data is $7,171,800 (BGC, March 31, 2019). The economy is largely resource-based with agriculture and forestry the primary industries along with tourism.

## 3.2. Historical Flood Events

Kaslo River has overtopped its banks several times since the founding of the Village in the late 1800s, the most significant being 1894 and 1948 (e.g. Figure 3-1.). These events also consisted of lake flooding from Kootenay Lake. High water levels in Kaslo River and a debris flood on Kemp Creek occurred in 2012. The 2012 flows in the Village of Kaslo were approximately equivalent to a 50-year (0.02% AEP) flood (Figure 2-2). Riverine flooding combined with a concern about log jam flooding within the Village prompted the construction of dikes along the north side of the river as described in Section 3.3. A timeline summary of floods and mitigation history for Kaslo River is presented in Figure 3-2. The historical event inventory is based upon a variety of sources including newspaper articles, government records and consulting reports. Some sources may not be completely accurate or only provide partial records of flood events but are provided to present an overview of historic events.

The provincial floodplain mapping program began in BC in 1974 aimed at identifying flood risk areas. This was in part due to the large Fraser River flood of 1972, which resulted in damage in the BC Interior. From 1975 to 2003, the province managed development in designated floodplain areas under the Floodplain Development Control Program. In 2003, the Program ended resulting in a significant change in how MFLNRO participated in land use regulation in flood-prone areas. The responsibility for developing and applying floodplain mapping tools was transferred to local governments, with the requirement that provincial guidelines be taken into consideration (EGBC 2017).


**Figure 3-1. Kaslo River flooding in 1894 (source: Kootenay Lake Archives).**

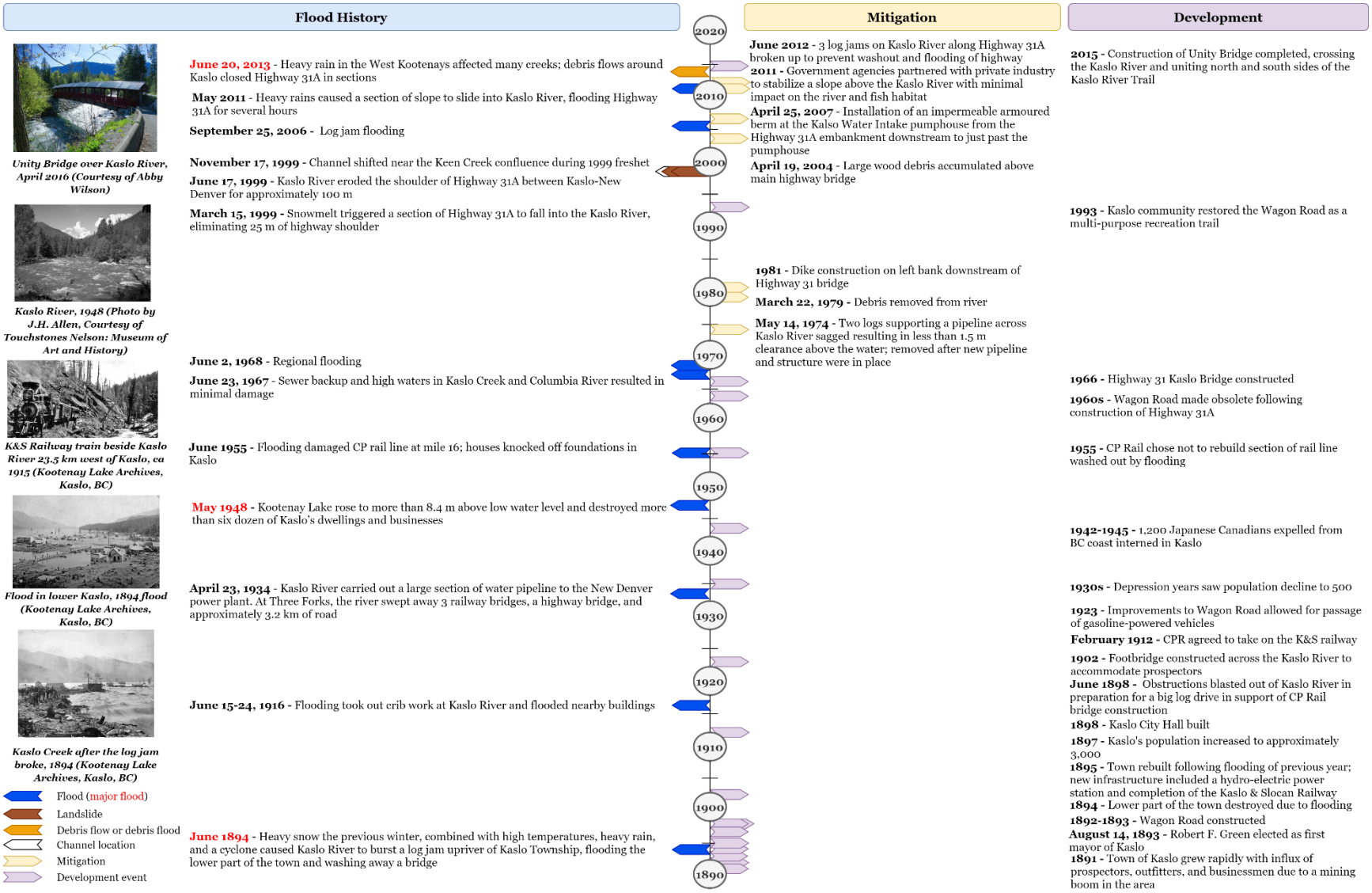


**Figure 3-2. Summary of recorded flood history, mitigation, and development history at the Kaslo River.**

## 3.3. Flood Protection and Hydraulic Structures

### 3.3.1. Bridges

Two bridges cross Kaslo River within the Village of Kaslo. The Highway 31 bridge crosses Kaslo River approximately 600 m upstream (west) of Kootenay Lake, while the Kaslo River Trail pedestrian bridge is a further 200 m upstream (west). The pedestrian bridge is a new structure, just completed in 2017. The Highway 31 bridge was constructed in 1966 but is currently scheduled for replacement in 2021. Key dimensions of the pedestrian bridge and existing Highway 31 bridge (Figure 3-3 and Figure 3-4) were measured by Midwest Survey Inc. (Midwest) and are presented in Table 3-1.

**Figure 3-3. Highway 31 bridge over Kaslo River looking upstream (west). Photo: BGC, April 18, 2019.**

**Figure 3-4. Standing upstream of the Kaslo River Trail pedestrian bridge looking downstream (east). Photo: BGC, July 25, 2019.**

**Table 3-1. Bridge dimensions surveyed by Midwest Survey Inc., July 2019.**

| Bridge | Top Deck Elevation (m) | Bottom Deck Elevation (m) | Pier Thick-ness (m) | Number of Piers | Shape of Piers | Deck Span (m) | Deck Width (m) |
|---|---|---|---|---|---|---|---|
| Highway 31 | 545.7 - 547[1] | 544.4 – 545.2[1] | 0.7 | 3 | Circular wooden piles | 40.5 | 11.8 |
| Kaslo River Trail Pedestrian | 549.1 | 548.1 | - | 0 | - | 33.5 | 4.5 |

Note:
1. Bridge deck is sloped from north (low) to south (high).

### 3.3.2. Dikes

Approximately 450 m of dike have been constructed on the left (north) bank of Kaslo River, which are managed by the Village of Kaslo and regulated under the Dike Maintenance Act (Figure 3-4). The dikes were designed with 2H:1V slopes on the riverside and a 1 m thick layer of riprap. The riprap size specification is not known, but a Wolman count in April 2019 estimated the $D_{50}$ to be approximately 500 mm. The design flood was the 200-year peak instantaneous discharge, which at the time was estimated to be 229 $m^3/s$. Due to concerns over bedload deposition and log jams, a freeboard of 1 m above the design flood level was recommended (MoE, 1981). The dikes were constructed in the mid 1980's. Another small section of diking is located on the right (south) bank near the location of the pedestrian bridge, but details about the design of this section are not known. The location of all Kaslo River dikes is shown on Drawing 01 and on Figure 3-6.

**Figure 3-5. Kaslo dike looking upstream towards the Highway 31 bridge. Photo: BGC, July 4, 2019.**

**Figure 3-6. Kaslo River dike locations. Image: Google Earth.**

## 3.4. Previous Mitigations

Limited official documentation has been found by BGC, but it appears that Kaslo River was relocated towards the right (south) side of the fan, likely following the 1894 flood. Additionally, Fearon (2002) notes that deposition of large woody debris in the channel has long been noted as a concern in Kaslo River, in particular the reach downstream of the Keen Creek confluence. Various actions have been taken over the years to remove large woody debris from the channel upstream of Kaslo to mitigate direct impacts to Highway 31A and reduce the potential for log jams occurring that might impact flooding in the Village of Kaslo (e.g., Boyer, 2000; Masse Environmental, 2012).

## 3.5. Bank Erosion and Avulsion History

Channel migration caused by bank erosion is a typical process in rivers. This process may occur as gradual erosion at the outside of river bends, or as sudden widening of the river during floods. Gradual bank erosion occurs as material is eroded of the outer bank of a meander bend and is deposited (as a point bar) inside of the meander bend (Charlton, 2007). There are no specific studies investigating avulsion and channel changes within the study area. However, some relevant information can be obtained from the review of the historical documentation (Table 3-2).

**Table 3-2. Relevant historical bank erosion and avulsion information.**

| Year | Reported observations | Reference |
|---|---|---|
| 2016 | Four sections of the riverbank and one section of the flood protection dike were identified for remediation work following bank degradation. These sections were defined as follow: sections 1 and 2 were upstream of the pedestrian bridge, section 3 located downstream of the pedestrian bridge, and sections 4 and 5 located downstream of the Highway 31 bridge crossing. All sections were identified as unstable banks with active bank failure processes. Figure 3-7 and Figure 3-8 display 2019 photographs at two of these locations. | Austin Engineering (2016) |

**Figure 3-7. Bank erosion and slope instability upstream of the Highway 31 bridge (left bank). The depth of the undercutting is unknown, but local testimonials and previous reports suggest that it is a gradual process and has exacerbated for the past five years.**

**Figure 3-8. Tilted trees at the left (north bank) indicating bank instability processes (80 m upstream of the Highway 31 bridge.**

# 4. METHODS

This section summarizes the assessment methods applied to at the Kaslo River. Additional details are summarized in Appendices C, D, and E.

## 4.1. Field Data, Topographic Data and River Bathymetric Surveys

### 4.1.1. Fieldwork and Site Investigations

Fieldwork on Kaslo River was conducted on July 4, 2019 and on July 31, 2019 by BGC personnel (Elisa Scordo, P.Geo., Marc Oliver Trottier, P.Eng., and Rob Millar, P.Geo., P.Eng.). Field work included measurement of bed material grain size to characterize the grain size distribution. Sampling was conducted at the Kootenay Lake shoreline following the method of Wolman (1954). Observations of infrastructure, including bridges and flood protection structures (e.g., dikes, riprap armouring), were noted. Field work was conducted to coordinate the survey extent and data collection with the survey crews. The watershed was flown by helicopter on July 6, 2019 by BGC personnel (Marc Oliver Trottier, P.Eng., Matthias Busslinger, P.Eng., and Matthias Jakob, P.Geo.).

A site visit was also conducted on April 18, 2019 by Evan Shih (BGC) as part of a Highway 31 Kaslo River bridge replacement study for the BC Ministry of Transportation and Infrastructure (MOTI). Additional information on dike and channel grain size, dike condition and bridge hydraulics observations were collected at that time (BGC, July 5, 2019).

### 4.1.2. Topographic Mapping

Detailed topographic data of the floodplain were available from a classified high-resolution lidar dataset obtained from RDCK and flown in October 2017. BGC was provided with tiles containing the classified point cloud and a 1 m bare-earth Digital Elevation Model (DEM). Lidar coverage provided by RDCK for the entire study area is shown in Figure 4-1.

The lidar data were provided with the following coordinate system:

- Horizontal Datum: NAD83 CSRS
- Projection: UTM Zone 11 North
- Vertical Datum: CGVD 2013
- Geoid Model: CGG2013.

As part of the lidar acquisition, orthophotos were not collected. As a result, the classification of the raw lidar point cloud contained inaccuracies particularly around gravel bars and the location of the river shoreline. In order to account for this, BGC collected additional ground and bathymetric survey data to capture in-channel features that were not classified in the lidar survey.

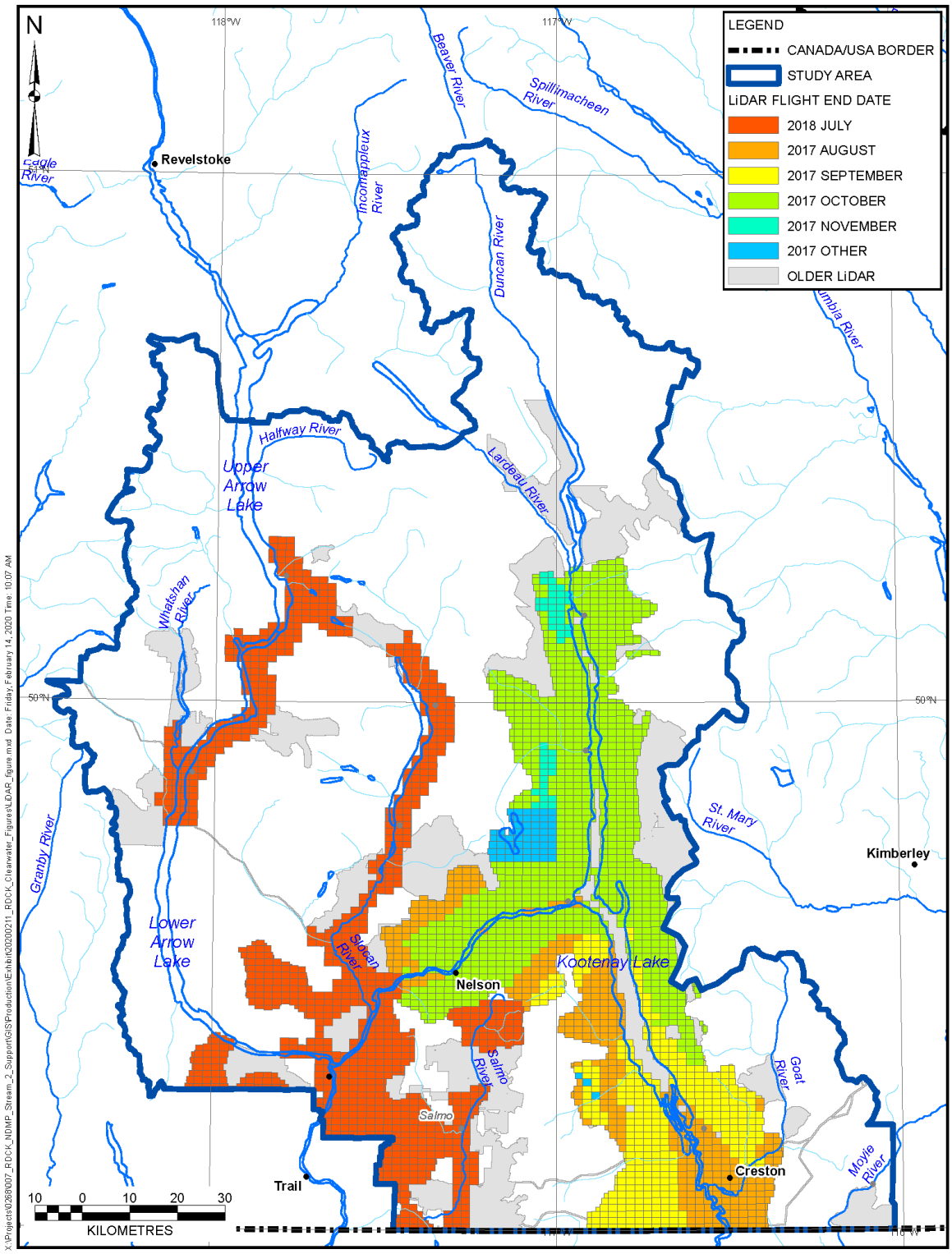


**Figure 4-1. Lidar coverage for clearwater study sites.**

### 4.1.3. Ground and Bathymetric Surveying

BGC contracted Midwest Surveys Inc. (MSI) to conduct a detailed survey of the Kaslo River and Kootenay Lake foreshore (Drawing 03). The scope of work included surveying of the channel bed, bridges, and dikes. A combination of Static Global Navigation Satellite System (GNSS) techniques, real-time kinematic (RTK) and real-time network (RTN) techniques were used to establish a precise, reliable Survey Control Network (SCN) for the length of the project. The SCN was integrated with existing BC Survey Control and/or the Canadian Base Network. The survey data were provided in the 3TM NAD 83 (CSRS) UTM 11 North coordinate system with elevation in the CGVD2013 Vertical Datum.

The survey was conducted from August 9 to 11, 2019. The survey covered approximately 1.2 km of Kaslo River and 1 km of the Kootenay Lake foreshore. Surveying of the channels was completed using GNSS RTK GPS. The Kootenay Lake bathymetry was completed using a Single Beam echosounder (sonar) from a boat. A summary of locations collected using survey and sonar techniques is presented in Drawing 03. Channel cross-sections, extending from bank to bank and approximately perpendicular to the channel, were collected at a typical spacing of 20 to 25 m. Sonar data were collected along continuous transects collected at a density of 5 to 10 m.

The Highway 31 and pedestrian bridges were surveyed to collect details such as the length of the span, width of the bridge, top of curb elevation, low chord elevation and width of piers. A total of 450m of dikes along the left (north) bank were also surveyed including the crest elevation and length, type and general condition of the dike.

### 4.1.4. Survey Equipment, Accuracy and Processing Software

Table 4-1 provides a list of survey equipment and the reported accuracy. Hypack 2018 Hydrographic Software was used to correlate global position system (GPS) and hydrographic data together.

**Table 4-1. Summary of survey equipment.**

| Equipment Type | Reported Accuracy |
|---|---|
| **GPS** | |
| Trimble R10 GNSS | • Single Baseline: <30 km<br>• Horizontal (RTK): 8 mm + 1 ppm RMS<br>• Vertical (RTK): 15 mm + 1 ppm RMS<br>• Horizontal (Static GNSS): 3 mm + 0.1 ppm RMS<br>• Vertical (Static GNSS): 3.5 mm + 0.4 ppm RMS |
| **Total Station** | |
| Leica TCR 403<br>Trimble SX3 Robotic Scanning Total Station | • Angular Accuracy: +/- 3"<br>• EDM Range: 1 m – 2,500 m to single prism<br>• Reflectorless EDM Range: 1 m – 100 m<br>• Distance Accuracy: 2 mm + 2 ppm<br>• Distance Accuracy Scanning: 2 mm + 1.5 ppm |
| **Hydrographic Equipment** | |
| Odom Echotrac CV-100 | • Depth Range: <0.30 m to 600 m<br>• Accuracy (Corrected for Sound Velocity): 0.01 m +/-0.1 % depth |

### 4.1.5. Terrain Creation

Following completion of the survey, BGC integrated the bathymetry data with the lidar bare-earth DEM to generate a 1.0 m resolution continuous terrain model for use in 2D hydraulic modelling (HEC-RAS). A DEM for the channel was generated by creating a boundary around the survey points with a 1 m buffer zone on either side using lidar data. The lidar and survey data were then meshed together using an iterative finite difference interpolation method similar to the discretized thin plate spline technique (Wahba, 1990).

Hydraulic structures were not included in the terrain. Bridge decks for both the Highway 31 and Kaslo River Trail pedestrian bridges were removed from the DEM as they were sufficiently high above the water surface elevation of a 500-year flood to not have an impact on flow.

## 4.2. Channel Change and Bank Erosion Analysis

Floods induce high shear stresses on channel banks, which can promote bank erosion. Non-cohesive materials such as sands and gravels are more susceptible to this process than cohesive banks. Standard hydraulic models to simulate floods do not consider bank erosion and assume the channel geometry is static. BGC conducted a separate analysis to assess changes in the floodplain and channel and their potential influence on flooding.

Channel change mapping and bank erosion approaches using remote sensing have been widely used to detect variations in the position of channel geomorphology features (e.g., channels, banks, and bars) (Trimble & Cooke, 1991; Marcus, 2012). These methods have been reviewed and considered useful to quantify the rate of change over a study period (Lawler, 2006).

This section briefly describes the data and methods used to document planform channel changes within the study area and analyze the bank erosion processes observed between 1957 and 2019 (the period of available aerial photographs). It also outlines the limitations and uncertainties of the methodology. The investigated area for this analysis extends 3.2 km upstream from the outlet of the Kaslo River into Kootenay Lake (Drawing 04).

### 4.2.1. Data Sources

Aerial photographs and satellite imagery supported with lidar were used to assess historical changes in channel planform geomorphology and bank erosion within the 3.2 km study reach (Table 4-2). The channel mapping was also informed by the river bathymetric survey described in Section 4.1.

**Table 4-2. Aerial photographs and satellite imagery used in the analysis.**

| Imagery | Year | Roll / Frame | Photo Number | Nominal Scale | Source |
|---|---|---|---|---|---|
| Aerial photographs | 1957 | BC2329 | 60 | - | BC Government |
| Aerial photographs | 1997 | BC97094 | 219 -220 | 1:15,000 | BC Government |
| Orthophoto | 2017 | BC17507 | N/A | 1:6,250 | BC Government |

### 4.2.2. Methods

In this analysis, the following tasks were completed:

Data preparation:

This task involved the acquisition of historic aerial photographs and imagery for georeferencing and mosaics creation. All the imagery and photographs listed in Table 4-2 were georeferenced to the same coordinate systems (NAD 1983 CSRS UTM, Zone 11N).

Geomorphic analysis:

The geomorphic analysis involved three steps. First, distinct channel reaches were delineated (i.e., length of the channel with similar physical characteristics). These reaches were then used to quantify the average net erosion recorded in the analyzed period.

Second, the channel thalweg and planform were delineated. The channel planform refers to the form of a river as viewed from above (Charlton, 2007). The 2019 thalweg was generated from the river bathymetric survey data. The historical channel thalwegs were interpreted from the photographs and manually digitized on-screen. Third, geomorphic features were mapped. The criteria for geomorphic mapping are provided in Table 4-3 and Table 4-4.

**Table 4-3. Geomorphic features used for geomorphic floodplain and channel mapping.**

| Feature | Type | Map Symbol | Description |
|---|---|---|---|
| Channel | Main-channel | Fmc | Flowing channel with distinct banks that carries most of the river discharge. This feature is always active. |
| | Side-channel | Fsc | Flowing channel with distinct banks that carries a portion of the river discharge less than the main-channel. This feature is active. |
| | Back-channel | Fbc | Abandoned-channel with distinct banks whose downstream end is connected to the river but whose upstream end is plugged. This feature is always active. |
| | Flood-channel | Ffc | Channel with distinct banks connected to a main- or side-channel only in overbank flood conditions. |
| | Abandoned-channel | Fac | Inactive channel remnant(s). No longer directly connected to active flow (e.g., oxbow lake). |
| Bars | Lateral and point-bars | Flb | Deposition and accumulation of sediments against the bank (lateral or side bars) and on the inside of a meander bend (point-bars). |
| | Mid-channel bar | Fmb | Feature characterized by the accumulation of sediments within the main channel. When the position of the bar become stable and vegetated during decades, they are commonly called islands. |
| Plain | Floodplain | Fp | Includes the level-ground area susceptible to overbank flow or flooding during high-flow events. |
| Fan | Alluvial fan/delta | Ff | A fan is a relatively smooth sector of a cone with a slope gradient from apex to toe up to and including 15°, and a longitudinal profile that is either straight, or slightly concave or convex (Howes and Kenk, 1997). |
| Terrace | Terrace | Ft, FGt<br>LGt | Flat or gently sloping areas bounded by an adjacent scarp. Fluvial terrace (Ft) deposits consist of channel deposits that may include some overbank materials. |

**Table 4-4. Levels of activity assigned to the geomorphic features.**

| Activity Class | Map Symbol | Description |
|---|---|---|
| Active | A | This indicates that the fluvial processes were active on the identified geomorphic feature at the time when the remote sensing data were collected. The lateral point or mid-channel bars are considered active until vegetation cover is established. Less than 75% of vegetation coverage or isolated patches of vegetation were classified as active. |
| Dormant/ Inactive | D | This indicates that there is no observable evidence of fluvial processes being active on the identified geomorphic feature at the time when the remote sensing data were collected. The lateral point or mid-channel bars are considered dormant when at least 75% of the mapped feature is covered by vegetation. |

Channel Change and Bank Erosion Analysis

The channel banks and geomorphic features delineated in the previous stage were used to quantify net bank erosion between the analyzed periods (Table 4-5). A spatial analysis using ArcGIS software by ESRI (version 10.6.1) was applied to estimate the net change in riverbank positions between each set of imagery. The following steps were completed:

- A numerical value of 1 (active) or 2 (dormant/inactive) was assigned to each mapped feature in the map attribute table. The values were determined based on the activity criteria described in Table 4-4. The general assumption was that unvegetated bars are active and would be submerged during bankfull conditions and, therefore, part of the active channel. A raster layer consisting of 1 and 2 values was created for each year of analysis.
- Then, the map algebra tool was used to subtract any two raster layers and estimate net change within the period. Negative values indicate bank erosion. Zero values indicate no change within the period and positive values indicate either bar stabilization, lateral accretion or deposition.

**Table 4-5. Channel change classes.**

| Map Algebra Results | Class | Definition |
|---|---|---|
| -1 | Bank Erosion, Channel Migration | Lateral migration of the channel due to the removal of bank material has occurred at raster cell. |
| 0 | No Change | The channel features remained the same at the raster cell between the reviewed periods. |
| 1 | Stabilization, Bank Accretion | Two conditions are possible for this result. First, pre-existing channel bars have remained stable during the period, allowing for vegetation to grow (stabilization). Second, the fluvial processes acting during the reviewed timeframe have promoted the sideway deposition along channel meanders (lateral accretion). |

### 4.2.3. Limitations and Uncertainties

Some limitations of the interpretation of remote sensing data to the quantification of channel change include:

- The scale and resolution of available aerial photographs, which affects the level of detail that can be identified for a given year.
- The geometric distortion that results from terrain and imagery acquisition method (e.g., camera tilt in aerial photographs). These factors may result in a displacement of the geomorphic features from its true position.
- The degree to which the historical photographs represent relevant channel changes within the investigated timeframe to within tolerable levels of accuracy.
- Challenges related to the quantification of the error during the process. Possible sources of error in this analysis include scanning, georeferencing error and on-screen digitizing errors.

- The discharge at the time of image capture. At higher discharges, most gravel bars would be inundated.

These errors were reduced in this study by applying common procedures including:

- Focusing on the central part of each aerial photograph
- Scanning the paper photographs at a high resolution
- Conducting geometric corrections on ArcGIS 10.6.1 software using the spline transformation tool which is commonly used when local accuracy is required.

## 4.3. Hydrological Analysis

### 4.3.1. Flood Frequency Analysis

Peak discharge estimates at the Village of Kaslo were calculated using a pro-rated flood frequency analysis (FFA) using historical streamflow data recorded at the *Kaslo River below Kemp Creek* (08NH005) WSC hydrometric station and are based on an assessment completed for the Highway 31 Kaslo River Bridge Replacement (BGC, July 5, 2019).

Peak discharge estimates were calculated at the hydrometric station (08NH005) based on the recorded peak annual instantaneous discharges (i.e., annual maximum series). Key hydrometric station information is presented in Table 4-6. Published maximum annual peak instantaneous flow data for the station were reviewed. The June 2013 data record was excluded from the FFA as the published instantaneous peak flow (0.9 $m^3/s$) was significantly less than the recorded maximum annual daily flow (145 $m^3/s$) on the same day and much less than the mean annual discharge, so it is therefore obviously erroneous. Similarly, the June 1988 data record was also deemed erroneous as the published instantaneous peak flow (252 $m^3/s$) was substantially larger than the corresponding maximum annual daily flow (67 $m^3/s$). The instantaneous peak flow to maximum annual daily flow ratio for that event was approximately 3.7, compared to an average ratio of 1.1 for all other events on record. Based on a review of historical climate data (from Kaslo climate station), there were no indications of significant rainfall having occurred during that period. Similarly, the peak instantaneous discharge in 1988 at regional WSC stations, including Keen Creek, were less than average. Therefore, the June 1988 record was excluded from the FFA.

Several statistical distributions were reviewed and a Log Pearson Type III distribution, with the parameters of the distribution calculated using the L-moments was selected.

**Table 4-6. WSC hydrometric station information for prorated FFA.**

| Station Name | Kaslo River Below Kemp Creek |
|---|---|
| **Station ID** | 08NH005 |
| **Real Time Gauge** | Yes |
| **Latitude** | 49° 54' 27" N |
| **Longitude** | 116° 57' 12" W |
| **Drainage Area (km$^2$)** | 442 |
| **Record Period** | 1914 – 1920, and 1964 – 2019 |
| **Record Length (Complete years of data)** | 63 |
| **# Years of published peak instantaneous flows** | 44 |
| **Approximate Elevation (masl)** | 645 |
| **Regulation Type** | Natural |
| **Location with Respect to Village of Kaslo** | 3.6 km upstream (west) |

The peak discharge estimates at the hydrometric station were transferred to the ungauged location by relating the return period peak instantaneous discharges at the hydrometric station to the ungauged site using watershed area. The equation used for this relation is as follows (Eq. 4- 1):

$$\frac{Q_U}{Q_G} = \left(\frac{A_U}{A_G}\right)^n \quad \text{[Eq. 4-1]}$$

where $Q_U$ and $Q_G$ are the annual maximum peak instantaneous discharges (m$^3$/s) at the ungauged site and the hydrometric station respectively, $A_U$ and $A_G$ are the watershed areas (km$^2$) for the ungauged and gauged sites respectively, and $n$ is a site-specific exponent related to peak discharges data at both sites (Watt, 1989). Typically, a value for n is chosen based on the watershed area size (Watt, 1989) and hydroclimatic conditions (e.g., frontal versus convective storms). In the case of Kaslo River, an exponent of 0.65 was used in the calculation, although the difference in watershed area between the gauge and Village is less than 2% so the exponent has little impact on the predicted flows.

The pro-rated estimates for Kaslo River were also compared to peak discharges estimated using a regional FFA based on the index-flood method and estimates published by previous studies (e.g., MoE, 1981; Fearon, 2002). As part of the regional FFA, the Kaslo River watershed was assigned to the Cluster 4 East hydrologic region for watersheds less than 500 km$^2$ based on its characteristics. Hydrologic regions are made up of hydrometric stations that share similar watershed characteristics. The hydrologic regions that cover the RDCK include Cluster 1 West, Cluster 4 East, and Cluster 7. The methodology for the regional FFA is described in Appendix C.

### 4.3.2. Climate Change Considerations

Engineers and Geoscientists British Columbia (EGBC) offer guidelines that include procedures to account for climate change when flood magnitudes for protective works or mitigation procedures are required (EGBC, 2018). The impacts of climate change on peak discharge estimates in Kaslo

River were assessed using statistical and processed-based methods (Appendix D). The statistical methods included a trend assessment on historical flood events using the Mann-Kendall test as well as the application of climate-adjusted variables (mean annual precipitation, mean annual temperature, and precipitation as snow) to the Regional FFA model. The process-based methods included the trend analysis for climate-adjusted flood data offered by the Pacific Climate Impacts Consortium (PCIC).

## 4.4. Hydraulic Modelling

### 4.4.1. General Approach

The preparation of flood hazard maps requires the development of a hydraulic model. The two-dimensional (2D) hydraulic model HEC-RAS (Version 5.0.7) was used to simulate the flood scenarios summarized in Table 4-7. HEC-RAS is a public domain hydraulic modelling program developed and supported by the United States Army Corps of Engineers (Brunner & CEIWR-HEC, 2016).

Six scenarios were selected to assess a range of conditions. Each scenario was modelled with climate-change adjusted discharges to represent projected future conditions as described below. Dike breach scenarios were also assessed at Kaslo Creek. Although the dikes appear to have sufficient freeboard for the climate-adjusted 200-year flood event, FLNRORD and others have noted concern about large woody debris either damaging the dike riprap and/or causing a log jam that results in flood flows overtopping the dike.

**Table 4-7. Modelling scenarios and return period classes.**

| Scenario | Return Period (years) | AEP | Dike Breach Included | Modelling Objective |
|---|---|---|---|---|
| 1 | 20 | 5% | No | Determine FCL |
| 2 | 50 | 2% | No | Assess flood hazards |
| 3 | 200 | 0.5% | No | Assess flood hazards |
| 4 | 200 | 0.5% | Yes | Determine FCLs with dike breach |
| 5 | 200 | 0.5% | No | Sensitivity analysis (+25% Manning's n) |
| 6 | 500 | 0.2% | Yes | Assess flood hazards |

Further details on modelling methods are presented in Appendix E and summarized in the sections below.

### 4.4.2. Model Inputs

Key model inputs include: (1) the topographic model to represent the floodplain and in-channel terrain, and (2) the boundary conditions at the upstream and downstream end of the study extent. Table 4-8 summarizes the key numerical modelling inputs selected for the HEC-RAS 2D model. Additional description of the topographic model and boundary conditions are provided in the sections below and in Appendix E

**Table 4-8. Summary of HEC RAS modelling inputs.**

| Variable | HEC-RAS |
|---|---|
| Topographic Input | Lidar (2017); Bathymetry (2019) |
| Mesh resolution | Variable (1- 10 m) |
| Manning's n | 0.06 (channel), 0.1 (urban areas). |
| Upstream boundary condition | Steady Flow ($Q_{20}$, $Q_{50}$, $Q_{200}$ and $Q_{500}$) |
| Downstream boundary condition | Steady stage at Kootenay Lake (535 m) |

Note: The downstream boundary condition is an intermediate scenario between BC Hydro's minimum and maximum flood scenarios; and 0.5 m above the approximate peak recorded reservoir level (July 4, 2012) since commissioning of the Libby Dam (BGC, January 15, 2020).

#### 4.4.2.1. Terrain Model

Following completion of the survey, BGC integrated the bathymetry data and surveyed cross sections with the lidar to generate a DEM for use in hydraulic modelling using the process described in Section 4.1.2.

Within the Kaslo River modelling extents there are two bridges. The Highway 31 bridge has piers that may affect hydraulic capacity at the crossing. The 2D model terrain was initially developed with the bridge decks removed from the terrain and no piers were included at the Highway 31 bridge crossing. Results indicated that the bridges provide over 1 m of clearance for a 500-year flow event. Because there was found to be sufficient capacity for clear-water flooding and because the Highway 31 bridge is scheduled for replacement in 2021, further analysis of the affect of the piers was not conducted.

#### 4.4.2.2. Dike Breach

Due to the potential of dike failure due to large woody debris either damaging the dike riprap and/or causing a log jam that overtops the dike, dike breach scenarios were assessed. Dike modelling followed the guidance provided in the Floodplain Mapping Guideline and Specifications (Water Management Consultants, March 19, 2004). A 200 m long breach was cut in the dike just downstream of the Highway 31 bridge. This location was selected as it provides the largest flood extent and FCL, but the following caveats should be noted:

1. The beach was not modelled dynamically. That is, the terrain was modified to include the final breach geometry and steady state conditions were determined. Velocities near the breach location could be higher than shown in the hazard maps as the breach develops.
2. Dike material eroded from the beach location are not included in the model and may affect flood conditions (inundation area and/or hazards).
3. A breach in other locations are expected to have a smaller inundation extent and FCL, but local flow depths and velocities could be higher than shown in the hazard maps.

#### 4.4.2.3. Model Domain

The model domain begins approximately 1.5 km upstream of the Highway 31 bridge, extending to Kootenay Lake and includes the Kaslo River fan, as shown on Figure 4-2. The upstream boundary was located well above the primary area of interest to avoid any boundary condition

affects. The downstream extends right along the lake foreshore and is far enough offshore where Kaslo River meets the lake that water depth is large, and velocities are negligible.

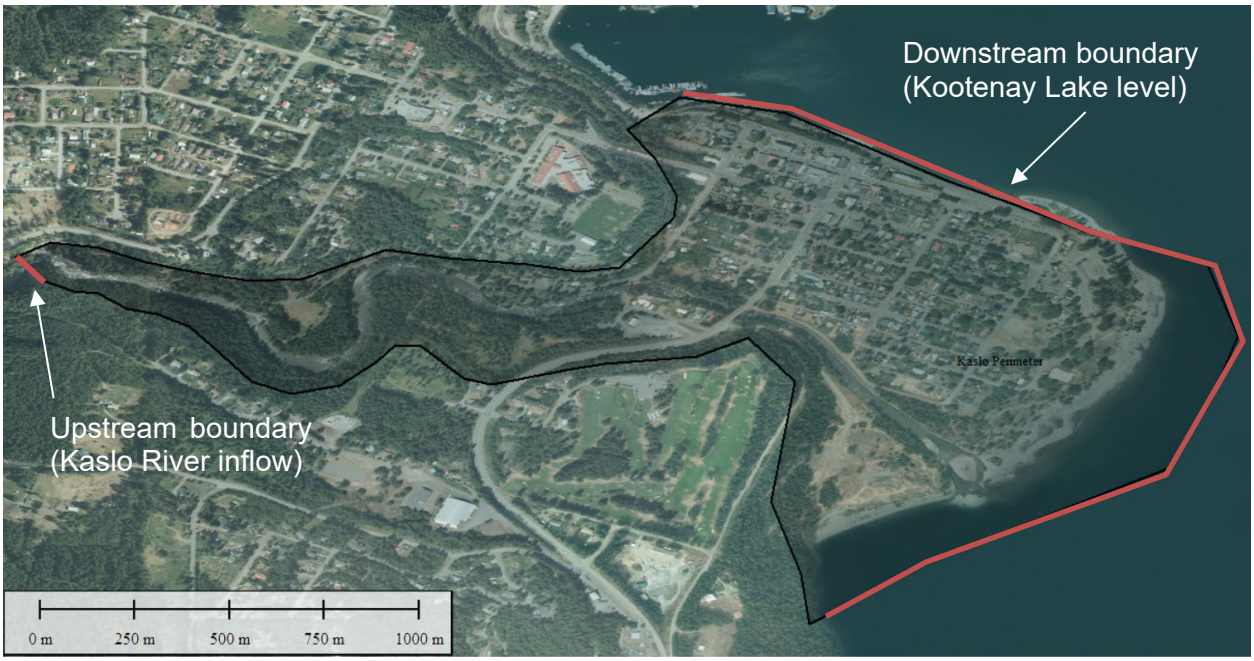


**Figure 4-2. Kaslo River study area modelling domain.**

#### 4.4.2.4. Boundary Conditions

The upstream boundary condition is the climate-adjusted peak flow for various return periods, as shown in Figure 4-2. The models were run with a warm-up period (approximately 4-6 hours) to ramp flows up to the target flow, then run at a steady flow for a sufficient period (2-4 hours) to allow steady state results (i.e., not changing with time).

Review of Kaslo River hydrometric station data and regional datasets indicate that the ratio of peak instantaneous flow to peak daily flow is approximately 1.1 in Kaslo River, indicating that flood hydrographs rise and fall relatively slowly. This finding is consistent with rain-on-snow events generated by frontal weather systems. The travel time of the model reach (the time it takes for a drop of water to travel through the model) is approximately 1 hour but is dependent on the flow rate. Consequently, modelling steady flows is considered appropriate.

The downstream boundary condition is Kootenay Lake levels. A steady lake level of 535 m was selected, which is an intermediate scenario between BC Hydro's minimum and maximum flood scenarios and 0.5 m above the approximate peak recorded reservoir level (July 4, 2012) since commissioning of the Libby Dam (BGC, January 15, 2020). However, adjusting the downstream boundary condition affects lake flooding but has limited influence on Kalslo River levels due to the rivers' steep gradient and near critical flow conditions.

## 4.5. Hazard Mapping

BGC prepared hazard maps based on the results from the numerical flood modelling. Specifically, BGC prepared two types of maps for Kaslo River: hazard scenario maps and FCL maps. The

scenario maps support emergency planning and risk analyses, and the FCL map supports communication and policy implementation, as described further below.

### 4.5.1. Hazard Scenario Maps

Hazard scenario maps display the hazard intensity (destructive potential) and extent of inundated areas for each scenario assessed. Two versions of the hazard scenario maps for each return period are provided: i) maps showing flood depth, and ii) maps showing flow impact force ($IF$), which is defined as the combination of fluid bulk density ($\rho$) , area of impact ($A$) and velocity ($v$) and shown in Equation 4-2:

$$IF \propto \rho\, A\, v^2 \qquad \text{[Eq. 4-2]}$$

For clearwater flooding, 1000 kg/m$^3$ was assumed for $\rho$. The area of impact represents the area of the object that is impacted or the portion thereof. For this level of study, depth of flow from modelling results is used as a proxy for the height of the area and the impact force is then represented as an impact force per unit width, in this case 1 m.

Maps displaying flow depth support assessments where inundation is the primary mechanism of damage. Flow impact force maps highlight locations where a combination of higher flow velocity and depth may warrant additional assessment (i.e., analyses of bank stability, erosion, or life safety). Table 4-9 provides a description of the flow impact force ranges and their impacts on life safety and impacts on the built environment. A flow depth map for the 200-year peak discharge is provided in this report in Drawing 06. Flow depth and flow impact force maps for all return periods are displayed on Cambio.

**Table 4-9. Flow impact force values shown on the flood hazard scenario maps (Cambio)**

| Impact Force (kN/m) | Description |
|---|---|
| ≤ 1 | Slow flowing shallow and deep water with little or no debris. High likelihood of water damage. Potentially dangerous to people in buildings, in areas with higher water depths. |
| 1 to 10 | Mostly slow but potentially fast flowing shallow or deep flow with some debris. High likelihood of sedimentation and water damage. Potentially dangerous to people in the basement or first floor of buildings without elevated concrete foundations. |
| 10-100 | Fast flowing water and debris. High likelihood of structural building damage and severe sediment and water damage. Dangerous to people on the first floor or in the basement of buildings. Replacement of unreinforced buildings likely required. |
| >100[1] | Fast flowing debris. High likelihood of building destruction. Very dangerous to people in buildings irrespective of floor. |

Note:
1. Flow intensities greater than 100 kN/m in clearwater creeks occur primarily in the steeper creeks within the main channel.

### 4.5.2. Flood Construction Level Mapping

FCLs are required for areas adjacent to river floodplains for consideration during planning. An FCL can be incorporated into regulation by authorities to provide guidance for new constructions on the extent and elevation of possible flooding in the area. In BC, FCLs have historically been calculated as the higher of the followings:

- Water surface profile for the design peak instantaneous flow plus 0.3 m of freeboard
- Water surface profile for the design daily flow plus 0.6 m of freeboard.

The freeboard is applied to the estimated water surface profile to account for uncertainties in the calculation of the water surface. As noted in EGBC (2017; 2018), for many BC rivers freeboard has been set higher than these minimum values to account for sediment deposition, debris jams, and other factors. Recently, several studies have recommended using 0.6 m of freeboard above the design peak instantaneous flow (KWL, 2014; 2017; NHC, 2008b; 2014; 2016; 2018). As such, we have selected to use this approach as well for the Kaslo River study area.

Depending on the situation, the presence of a dike may lead to a local rise in the flood levels as the dike constrains the flow within the channel rather than being distributed across the floodplain. Should a dike fail through overtopping or geotechnical failure, the resulting flooding depth and extent of flooding may be greater than if the dike was not present due to ponding of water on the landward side of the dike that cannot flow back into the river (e.g., Figure 4-3).

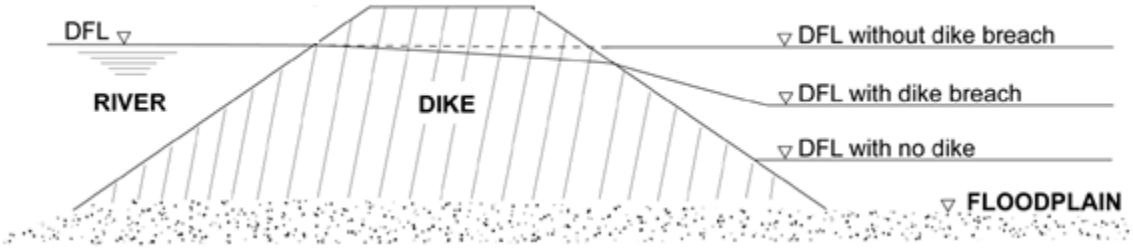


**Figure 4-3. Definition of design flood levels (DFL) in the presence of a dike. DFL refers to the estimated water levels from a design flood event such as the 200-year return period flood (Modified from Water Management Consultants March 19, 2004).**

The numerical modelling and mapping conducted for Kaslo River were based on existing conditions, including structural flood protection, and a dike breach scenario. As noted in Section 3.4, woody debris that causes a dike failure has been identified as a concern. Specifically, this means:

1. The elevations of the dikes were included within the model terrain for the 20-year and 50-year models.
2. It was assumed that a dike failure occurs during the 200-year and 500-year events.

For the Kaslo River, FCLs were generated by creating isolines from the predicted 200-year water surface (Scenario 4) plus a 0.6 m freeboard and extending the isolines across the limits of the floodplain generally perpendicular to the flow direction. Dike breach scenarios were conducted as part of the flood hazard assessment and used to determine FCLs. Additionally, because the Village of Kaslo is located on a fan, review of the terrain and extreme flow model scenarios identified that there is potential (e.g., considering dike breach material deposition, or terrain and model uncertainty) for flood flows to reach a low spot and flow northeast towards Front Street and Second Street. An FCL in this area was generated by assuming that approximately half of the flow that leaves the dike breach is able to flow in this direction.

# 5. RESULTS

## 5.1. Channel Change Mapping and Bank Erosion

The objective of the geomorphic and bank erosion analysis was to document historical changes in channel width and related geomorphic processes using remote sensing data, as described in Section 4.2. The mapped geomorphic units are illustrated in Drawing 04. Drawing 05 provides a summary of channel changes over the study period. The investigated area was divided into five reaches to facilitate the analysis of the observed changes (Figure 5-1). The relevant features of these reaches, including average bank retreat based on the planimetric study, are provided in Table 5-1. A summary of the key changes observed within the area is included in Table 5-2. A description of the interpreted channel changes observed within the reaches follows.

The first and most upstream reach (Reach-1) is a straight narrow channel that extends for about 950 m. The channel displays a riffle-pool morphology with some lateral deposition. The second reach (Reach-2) is a straight channel that extends for 390 m before the channel widens. This is a transitional channel between Reach-1 and -3 in which the vertical process (e.g., channel incision and bed scour) seems to dominate. The third reach (Reach-3) is about 760 m long. In this section, the channel widens and flattens, promoting channel meandering and deposition with the formation of lateral and point bars (Drawing 04). As is typical in meandering patterns, the observed erosion occurs at the outside of the meander bend. This is the reach that has experienced the most change within the 1957-1997 period. Between the 1997 and 2017 period the channel appeared more stable at this reach.

The fourth reach (Reach-4) extends for 600 m and starts about 535 m upstream of the Highway 31 bridge. In this section, the river channel straightens and steepens, resulting in a sinuous pattern. The change analysis shows significant bank retreat on the left bank within the 1957-1997 period, which caused the displacement of the channel towards the right bank. Between 1997 and 2017, most of the bank erosion was recorded on the right bank, creating an apparent stabilization or deposition on the left bank. However, during the field investigation the BGC crew identified a section of ongoing (local) erosion at a very steep bank (greater than 45°) on the left side, where local undercutting during high flows has caused instability. This site is located about 100 m upstream of the Kaslo River Highway 31 bridge (Drawing 04). In this section, the left bank (north) is steep, and the bank displays signs of slope instability, including tilted and damaged trees (Figure 3-8). The lidar data shows slope instability morphology extending 35 meters behind of the current stream bank. The slope instability processes occurring at this location has been highlighted in other studies (e.g. Austin Engineering, 2016) and are expected to continue. The inundation boundary of the estimated 20-year event overlap the toe of the bank. Bank failures can be reactivated or worsened under flooding conditions and restrict the channel cross-section limiting its ability to contain the flow.

The fifth reach (Reach-5) is straight and primarily controlled by the left bank dike (Drawing 04). The right bank (south) has not experienced significant changes during the observed period except for some minor deposition. The channel change display areas of change on the left bank indicating erosion. However, because of the uncertainties and limitations of the methodology (See

Section 4.2.3), it is unclear whether the observed change is related to inaccuracies with the georeferencing process or an actual removal of material from the toe of the dike. BGC did not conduct a stability analysis of the dike.

**Table 5-1. Channel reaches characterization and average bank retreat.**

| Reach | Length[1] (m) | Channel Width Variation (m) | Average Bank Retreat 1957-1997 (m) | Average Bank Retreat 1997-2019 (m) | Channel Pattern |
|---|---|---|---|---|---|
| Reach-1 | 950 | 18-32 | 10 | 7 | Straight |
| Reach-2 | 390 | 18-48 | 34 | 34 | Straight - Sinuous |
| Reach-3 | 760 | 12-56 | 32 | 17 | Meandering |
| Reach-4 | 600 | 17-47 | 19 | 1 | Straight - Sinuous |
| Reach-5 | 570 | 18-60 | 0 | 2 | Straight |

Note:
1. Based on 2019 lidar data.

**Table 5-2. Summary of key changes observed within the analyzed periods.**

| Period | Maximum Bank Retreat (m) | Highlighted observations |
|---|---|---|
| 1957-1997 | 30 ± 5 | Channel shifting towards the left bank in Reaches 1 and 3.<br>Reach 5 (alluvial fan) remained laterally stable during the analyzed period. |
| 1997-2019[1] | 32 ±2 | Bank failure and local erosion in Reach 4 (both banks). Field observations suggest that there is ongoing undercutting at this location, promoting bank instability. |

Note:
1. The analysis of the 2017 orthophoto was supplemented with the 2019 lidar and survey data.

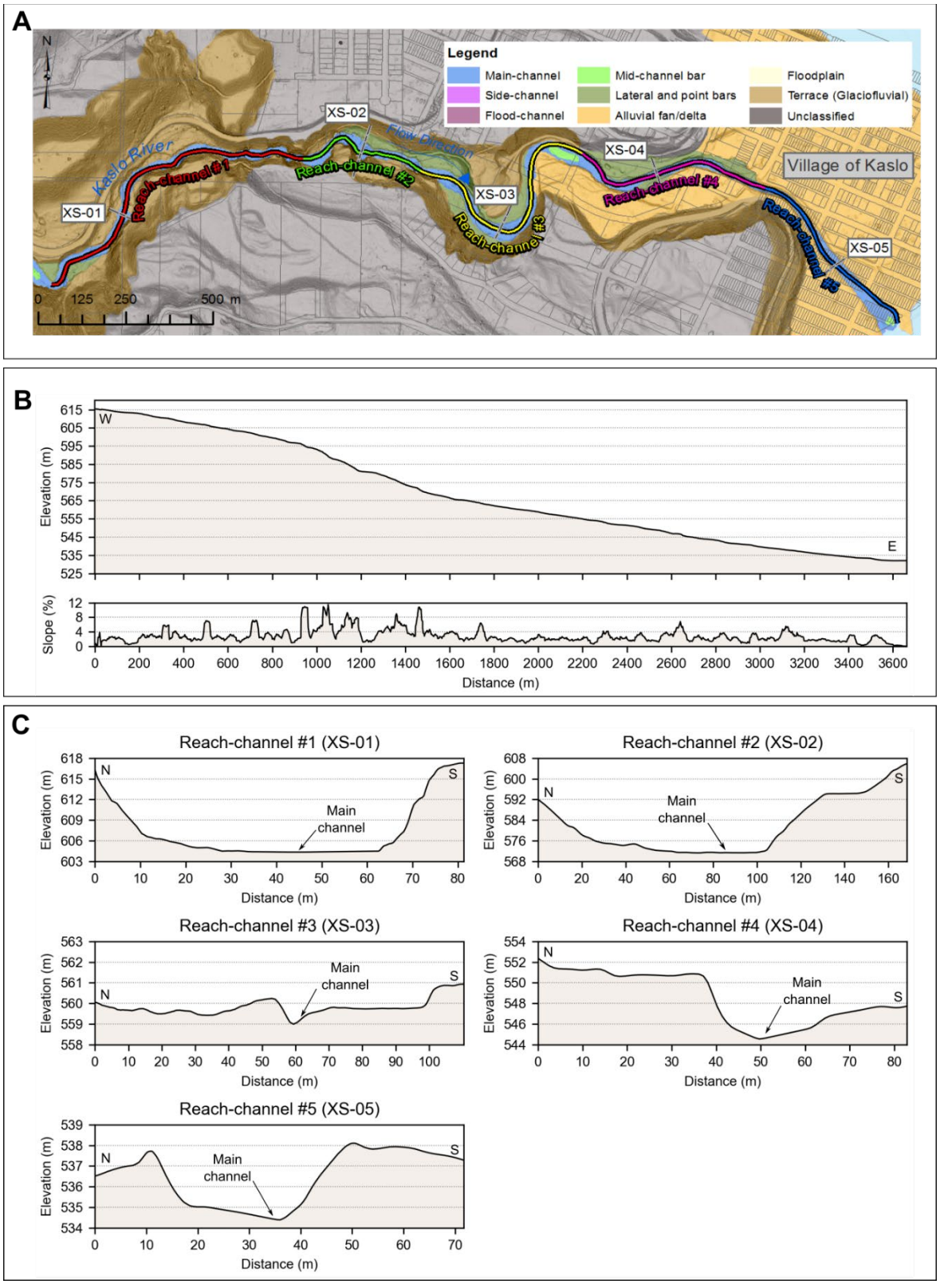


**Figure 5-1. Identified channel reaches within the Kaslo River floodplain. (A) Plan view of the river and floodplain. (B) Channel long-profile and slope gradient. Section lines are from left (north) to right (south) bank.**

## 5.2. Hydrological Modelling

### 5.2.1. Historical Peak Discharge Estimates

The historical peak discharge estimates for the Kalso River were based on the historical streamflow data recorded at the *Kaslo River below Kemp Creek* (08NH005) hydrometric station which were pro-rated to the downstream end of the model as discussed in Section 4.3.1. The peak discharges based on the historical data are presented in Table 5-4. A comparison of the estimates to results from previous reports and the Regional FFA is also presented in Figure 5-2. For comparison, the historical 200-year peak instantaneous discharge determined for the dike design (MoE, 1981) was estimated to be 229 $m^3/s$, while Fearon (2002) presented a value of 340 $m^3/s$. The historical peak discharge estimates based on the pro-rated calculation are considered more reliable than the regional FFA as they are based on 42 years of measured data just upstream of the study area.

### 5.2.2. Accounting for Climate Change

Statistical trend analysis results show that there is no significant trend in the historical peak flow time series for both *Kaslo River below Kemp Creek* (08NH005) and *Keen Creek below Kyawats* (08NH132) (Table 5-3).

**Table 5-3. Trend analysis results.**

| Hydrometric Station | Name | Start Year | End Year | p-value[1] | Trend Direction | Sen's Slope[2] |
|---|---|---|---|---|---|---|
| 08NH005 | Kaslo River Below Kemp Creek | 1972 | 2017 | 0.32 | - | -0.21 |
| 08NH132 | Keen Creek Below Kyawats Creek | 1974 | 2016 | 0.79 | - | 0.04 |

Notes:
1. A p-value of less than 0.05 is considered significant.
2. A positive Sen's slope indicates an increasing trend in the flow.

While these results suggest that the flood record may be stationary at these two hydrometric stations, the results of the statistical and process-based evaluation methods to assess climate change impacts on peak flows were found to be inconsistent across the RDCK by 2050. The climate change impact assessment results were difficult to synthesise in order to select climate-adjusted peak discharges on a site-specific basis. The assessment of the trends in the discharge records was inconclusive. The results of the statistical flood frequency modelling generally show a small decrease in the flood magnitude, while the results of the process-based discharge modelling generally show an increase with a wide range in magnitude. As a result, peak discharge estimates were adjusted upwards by 20% to account for the uncertainty in the impacts of climate change in the RDCK as per Appendix D.

The climate-adjusted peak discharge estimates for various return periods are listed in Table 5-4, and are based on the single-station FFA plus 20%.

**Table 5-4. Historical and climate-adjusted peak discharge estimates for the Kaslo River watershed.**

| Return Period (years) | AEP | Historical Peak Flows ($m^3/s$) | Climate-adjusted Peak Flows ($m^3/s$) |
|---|---|---|---|
| 2 | 0.5 | 85 | 110 |
| 5 | 0.2 | 110 | 130 |
| 10 | 0.1 | 130 | 160 |
| 20 | 0.05 | 150 | 180 |
| 50 | 0.02 | 180 | 210 |
| 100 | 0.01 | 200 | 240 |
| 200 | 0.005 | 230 | 270 |
| 500 | 0.002 | 270 | 320 |

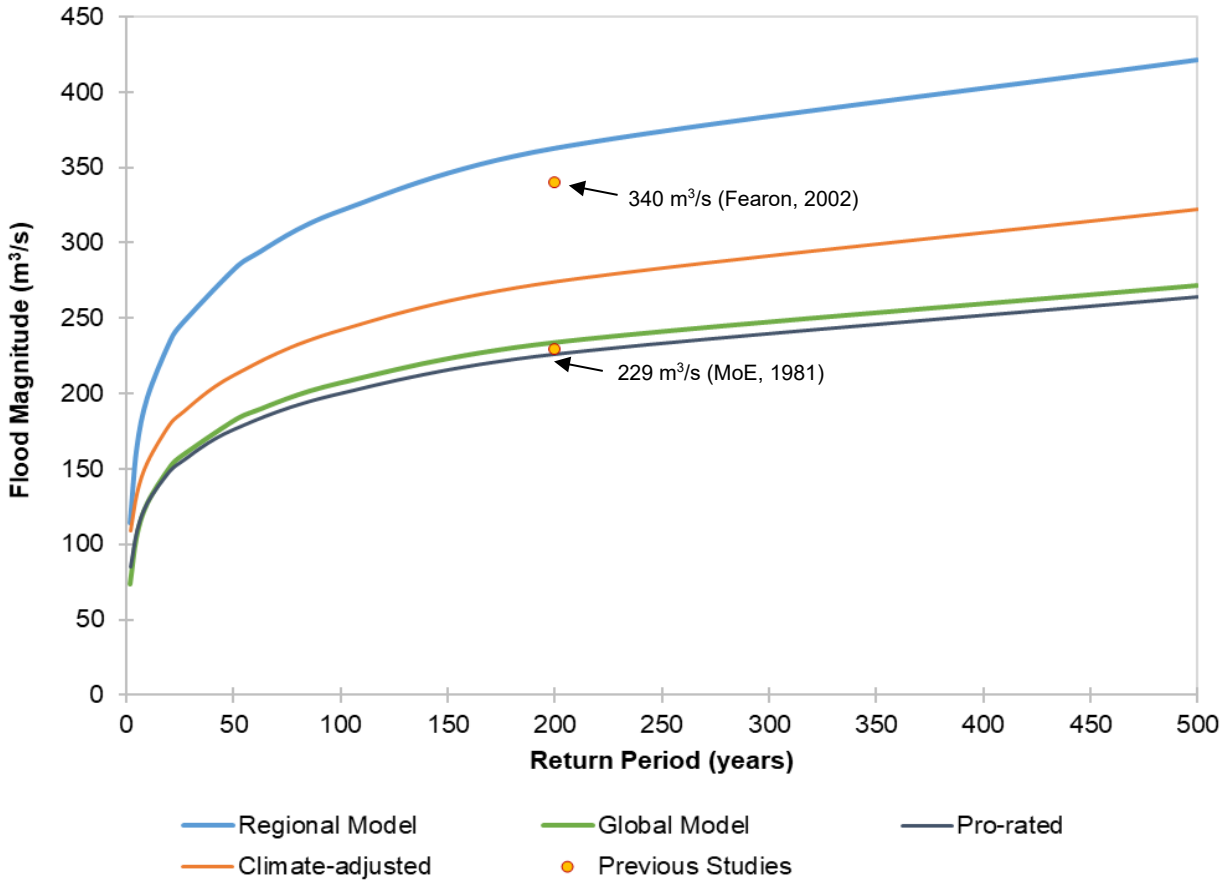


**Figure 5-2. Historical peak discharge estimates based on regional FFA, single-station FFA, and previous reports. Climate-adjusted flows are used in this study and are based on the single-station FFA plus 20%.**

## 5.3. Hydraulic Modelling

A summary of the key observations from the hydraulic modelling is included in Table 5-5. A channel profile showing the 200-year water surface and dike elevations are elevations are shown on Figure 5-3.

**Table 5-5. Summary of modelling results.**

| Process | Key Observations |
|---|---|
| Clear-water inundation | • Overland flooding occurs during the 20-year and higher return period floods on the vegetated bars upstream of the Village of Kaslo near the bike skills park. There appears to be limited infrastructure in the affected areas but may impact recreational trails (e.g., Lettrari Trail).<br>• Flooding up to and including the 500-year event do not overtop the dikes, assuming no log jams occur.<br>• During the dike breach scenarios (200- and 500-year floods) overland flooding occurs in the residential area northwest of Kaslo River, approximately as far as D Ave.<br>• Recreational areas along the Kootenay Lake foreshore are flooded during the 50-year and higher return period floods by Kaslo River. |
| Hydraulic Structures (Bridges) | • The flood elevations for all scenarios modeled do not reach the low cord of the Highway 31 or Kaslo River Trail pedestrian bridges.<br>  ○ There is approximately 1.4 m of clearance between the lower chord of the Highway 31 bridge and the 200-year return period flood.<br>  ○ There is greater than 1.5 m of clearance between the lower chord of the Kaslo River Trail pedestrian bridge and the 200-year return period flood. |
| Flood Protection Structures (Dikes) | • The dikes were designed with a 1 m freeboard and current modelling indicates that the crest is greater than 1 m above the 200-year flood elevation. |

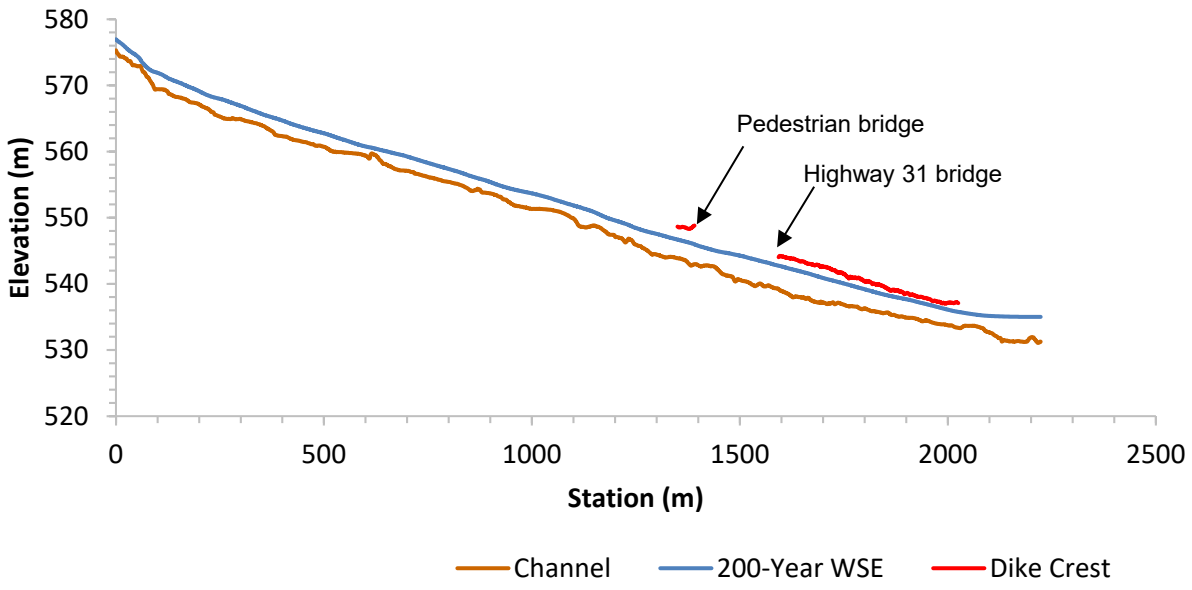


**Figure 5-3. Model profile showing channel bed, 200-year water surface elevation (WSE), and dike crest elevation.**

## 5.4. Flood Hazard Mapping

Hazard scenario results for the range of return periods modelled are presented in Cambio. Drawing 06 provides estimated water depths estimated for the 200-year return period design peak instantaneous flow event.

## 5.5. Flood Construction Level Mapping

FCL results for the 200-year design peak instantaneous flow water surface elevation plus 0.6 m freeboard are presented on Drawing 07. Note that elevations from the FCLs have not been surveyed in the field and should not be relied upon for accuracy of ground levels at the building lot scale.

# 6. SUMMARY AND RECOMMENDATIONS

This report provides a detailed flood hazard assessment of the Kaslo River floodplain. This river was chosen as a high priority site amongst hundreds in the RDCK due to its comparatively high risk. This report has resulted in digital hazard maps that provide a basis for quantitative risk assessment, if required. FCL maps are provided that can be used to support construction and community development planning. It also provides the basis to inform the conceptualization and potential design and construction of mitigation measures should those be found to be required for the Kaslo River. A variety of analytical desktop and field-based tools and techniques were combined to understand the Kaslo River geomorphological and hazard history, its hydrology and hydraulics.

## 6.1. Hazard Assessment

### 6.1.1. Channel Change Mapping and Bank Erosion Analysis

These analyses were completed to gain an understanding of historical geomorphic changes on the fan and how these changes relate to channel migration and flooding. Channel change and bank erosion results illustrate:

- The observable geomorphic features identified from the different sets of aerial photographs and imagery. These maps are useful to understand the geomorphic evolution of the channel in terms of sediment transport and erosion processes, and how these fluvial processes may influence flooding (Drawing 04). Delineating the interpreted channel thalweg from each set of photos was critical to find the major changes with the reviewed periods.
- The bank retreat rates identified between the analyzed set of imagery as summarized in Figure 5-1 (Drawing 05). The quantitative results indicate the rate of bank retreatment and the direction, but they do not explain the processes responsible for the change. There are some limitations related to these analyses when based on desktop mapping (See Section 4.2.3). Additional steps to understand bank erosion hazard should include a characterization of bank susceptibility (erodibility) and the critical shear stresses required to erode the banks at the identified reaches and for the different discharge events.
- Despite the identified limitations, the analysis identified a few key areas for future bank erosion hazard assessment. Both bank failures and fluvial erosion processes need to be considered within the following reaches (see Figure 5-1):
    - Within Reach-3, where the channel adopts a meandering pattern.
    - Within Reach-4 (left bank) where ongoing erosion have been identified.
    - Within Reach-5 to determine the integrity and stability of the dike and its potential susceptibility to erosion under different shear stresses scenarios.

Both maps guide the analysis of channel dynamics within the analyzed area and their possible influence on flood hazards. Further efforts to assess bank erosion should be intended to estimate the erosion hazard for the different return periods.

### 6.1.2. Peak Discharge Estimates

In recognition of the impacts of climate change, the clearwater flows estimated from a pro-rated FFA were adjusted. Key findings from estimating peak discharges suitable for modelling are:

- The climate change impact assessment results were difficult to synthesize to select climate-adjusted peak discharges on a site-specific basis. Consequently, a 20% increase in peak discharge was adopted (Appendix D).
- The climate-change adjusted peak discharges for Kaslo River range from 110 $m^3/s$ (2-year flood) to 320 $m^3/s$ (500-year flood). Other return period estimates are presented in Table 5-4.

### 6.1.3. Hydraulic Modelling

A 2D numerical model developed using HEC-RAS was employed to simulate the chosen hazard scenarios on Kaslo River. Table 5-5 provides key observations derived from the numerical modelling. The numerical modelling demonstrates that the key hazards and associated risks at Kaslo River stem from potential dike breaches.

### 6.1.4. Flood Hazard Mapping

Model results are cartographically expressed in two ways:

- The individual hazard scenarios are captured through hazard maps that display estimated flow velocity, flow depth and flood intensity. These maps are useful for assessments of development and emergency planning.
- An FCL map that combines the estimated water surface elevation for 200-year return period event plus a 0.6 m freeboard. This map is useful to assist development proposals.

Both the individual scenario hazard and FCL maps serve as decision-making tools to guide subdivision and other development permit approvals.

## 6.2. Limitations and Uncertainties

While systematic engineering and geoscience methods were applied in this study, some uncertainties prevail. As with all hazard assessment and concordant maps, the hazard maps prepared at Kaslo River represent a snapshot in time. Future changes to the Kaslo River watershed or fan including the following may warrant re-assessment and/or re-modelling:

- Future land use (urbanization) or landcover (deforestation, forest fire) changes in the floodplain or fan
- Substantial flood events
- Major changes in the channel planform or aggradation
- Bridge re-design
- Alteration to the existing dikes or construction of new dikes or flood control structures
- Substantial changes to Kaslo River flood levels.

The assumptions made on changes in runoff due to climate change reflect the current state of knowledge and will likely need to be updated occasionally as scientific understanding of such

processes evolves. This assessment does not include a dike condition assessment or determination of whether the dike is geotechnically and hydraulically sound to withstand the modelled flood events. Despite these limitations and uncertainties, BGC believes that a credible hazard assessment has been achieved on which land use decisions can be made.

### 6.3. Considerations for Hazard Management

Recommendations are provided in the Summary Report as they pertain to all studied RDCK creeks. This section notes Kaslo River-specific issues that could be considered in the short term given the findings of this report. They are purposely not named “recommendations” as those would come out of a more in-depth discussion with the District.

Key considerations are:

- Predicated floodplain extents are generally similar to results presented in historical floodplain mapping for Kaslo River (MFLNRO, 2016), although the area on the right (south) bank upstream of the Highway 31 bridge is no longer in the floodplain. Flooding may occur outside the defined floodplain boundary and floodplain limits were not established on the ground by legal survey.
- Numerical modelling indicates that the surveyed dike crest elevation is typically greater than 1 m higher than the 200-year return period flood elevation.
- An assessment of the geotechnical stability of the dikes was not conducted, although condition assessments have been conducted by others (e.g., Austin Engineering, 2016). Dike stability assessments could be completed in future as part of a separate scope of work for the clearwater assessment areas. This work would inform if failure may occur due to reasons other than flood overtopping or approaches to manage large woody debris.
- Hydraulic modelling results indicate that the Highway 31 and Kaslo River Trail pedestrian bridges are not predicted to overtop during a 200-year return period. However, the piers may trap and collect large woody debris during a flood event. This assessment does not explicitly consider the potential for the bridge to be blocked with large woody debris or due to accumulation of gravel, although these may be processes that contribute to a dike breach. It is noted that the Highway 31 bridge is currently scheduled for replacement in 2021.
- The hazard mapping conducted for a range of return periods provides an improved hazard basis to apply for funding for additional risk assessment, emergency response planning and mitigation projects. Results of the hazard mapping are provided on Drawing 06 for the 200-year return period water depth, assuming a breach in the dike downstream of the Highway 31 bridge. A range of scenarios (e.g., 20-year, 50-year, 500-year) and hazards (e.g. depth, velocity, flow intensity) are presented on Cambio.
- The FCLs presented in Drawing 07 for the 200-year return period flood event plus 0.6 m freeboard provides an improved basis for community planning, bylaw development, and emergency response planning in areas subject to flood hazards, with consideration of climate change. The application of the FCL map requires discussions and regulatory decisions for both existing and proposed development. Building and floodproofing elevations should be established from legal survey and benchmarks. Setback distances

from the natural boundaries of watercourses are not shown on maps. FCLs provide a standards-based approach which are simple to apply and interpret. In some cases, the FCL may be impossible or impractical to implement for several reasons. Allowances should be permitted for stakeholders to apply for a site-specific reduction in the FCLs contingent on a report by a suitably qualified Professional Engineer, preferably using a risk-based approach.

## 6.4. Recommendations

Recommendations are provided in the Summary Report (BGC, 2020) as they pertain to all studied RDCK creeks.

## 7. CLOSURE

We trust the above satisfies your requirements at this time. Should you have any questions or comments, please do not hesitate to contact us.

Yours sincerely,

**BGC ENGINEERING INC.**
**per:**

Toby Perkins, M.A.Sc., P.Eng.
Senior Hydrotechnical Engineer

Elisa Scordo, M.Sc., P.Geo.
Senior Hydrologist

Melissa Hairabedian, M.Sc., P.Geo.
Senior Hydrologist

Patrick Grover, M.A.Sc., P.Eng.
Senior Hydrotechnical Engineer

Reviewed by:

Rob Millar, PhD., P.Eng., P.Geo.
Principal Hydrotechnical Engineer

Hamish Weatherly, M.Sc., P.Geo.
Principal Hydrologist

ES/RM/HW/mp/mm

**Final stamp and signature version to follow once COVID-19 restrictions are lifted**

# REFERENCES

Austin Engineering. (2016, October). *Kaslo River Dike and Bank Remediation Plan* [Report]. Prepared for the Village of Kaslo.

BGC Engineering Inc. (2019, March 31). *Flood and Steep Creek Geohazard Risk Prioritization* [Report]. Prepared for Regional District of Central Kootenay.

BGC Engineering Inc. (2019, May 24). *NDMP Stream 2 Application: Flood Mapping* [Work Plan (Revised)]. Prepared for Regional District of Central Kootenay.

BGC Engineering Inc. (2019, July 5). *Kaslo River Bridge Replacement* (Draft) [Report]. Prepared for BC Ministry of Transportation and Infrastructure.

BGC Engineering Inc. (2019, November 15). *NDMP Stream 2 Project Deliverables* (Revised). Prepared for Regional District of Central Kootenay.

BGC Engineering Inc. (2020, January 15). *Kootenay Lake Flood Impact Analysis* [Draft Report]. Prepared for Regional District of Central Kootenay.

Boyer, D. (2000). *Kaslo River 1999 Channel Shift Below Keen Creek*. Report number 1104. Water Management Branch, Nelson.

British Columbia Ministry of Forests, Lands and Natural Resource Operations, Water Management Branch (BC MFLNRO). (2016). Floodplain maps [Web page.] Retrieved from https://www2.gov.bc.ca/gov/content/environment/air-land-water/water/drought-flooding-dikes-dams/integrated-flood-hazard-management/flood-hazard-land-use-management/floodplain-mapping/floodplain-maps-by-region.

British Columbia Ministry of Transportation and Infrastructure. (2016). *Bridge Standards & Procedures Manual (Volume 1 – Supplement to CHBDC S6-14)*.

Charlton, R. (2007). *Fundamentals of fluvial geomorphology.* Routledge.

Demarchi, D.A. (2011, March). *An introduction to the ecoregions of British Columbia* (3rd ed.). Victoria, BC: British Columbia Ministry of Environment, Ecosystem Information Section. Retrieved from https://www2.gov.bc.ca/assets/gov/environment/plants-animals-and-ecosystems/ecosystems/broad-ecosystem/an_introduction_to_the_ecoregions_of_british_columbia.pdf

Engineers and Geoscientists of British Columbia (EGBC). (2017, January). *Professional practice guidelines: Flood mapping in BC*. Retrieved from https://www.egbc.ca/getmedia/8748e1cf-3a80-458d-8f73-94d6460f310f/APEGBC-Guidelines-for-Flood-Mapping-in-BC.pdf.aspx.

Engineers and Geoscientists of British Columbia (EGBC). (2018, July). *Professional practice guidelines: Legislated flood assessments in a changing climate in BC*. Retrieved from https://www.egbc.ca/getmedia/f5c2d7e9-26ad-4cb3-b528-940b3aaa9069/Legislated-Flood-Assessments-in-BC.pdf.aspx.

Farjad, B., Gupta, A., & Marceau, D.J. (2016). Annual and seasonal variations of hydrological processes under climate change scenarios in two sub-catchments of a complex watershed. *Water Resources Management, 30*(8), 2851-2865. https://doi.org/10.1007/s11269-016-1329-3

Fearon Environmental (Fearon). (2002). *Confirmation of Existing Bank Stabilization Works, Kaslo River, Kaslo, British Columbia*. Report number 1239.

Fulton, R.J., Shetsen, I., & Rutter, N.W. (1984). *Surficial Geology, Kootenay Lake, British Columbia-Alberta*. Geological Survey of Canada, Open File 1084, 2 sheets.

Harder, P., Pomeroy, J.W., & Westbrook, C.J. (2015). Hydrological resilience of a Canadian Rockies headwaters basin subject to changing climate, extreme weather, and forest management. *Hydrological Processes, 29*, 3905-3924. https://doi.org/10.1002/hyp.10596

Kaslo Now (n.d.). Indigenous Nations a Local Presence for Millennia - Kaslo 125. Retrieved from https://www.kaslonow.ca/2018/07/30/indigenous-nations-a-local-presence-for-millennia/

KWL Associates Ltd. (2014). Creek Hydrology, Floodplain Mapping and Bridge Hydraulic Assessment – Floodplain Development Permit Area, Flood Construction Level Development and Use [Report]. Prepared for the City of North Vancouver and the District of North Vancouver.

KWL Associates Ltd. (2017). Wildlife Enhancement Program at Burton Flats Design Feasibility Final Report. Prepared for BC Hydro. Ref: CLBWORKS-30B

Lawler, D.M. (2006). The measurement of river bank erosion and lateral channel change: a review. *Earth Surface Processes and Landforms, 18*(9), 777-821. https://doi.org/10.1002/esp.3290180905

Loukas, A. & Quick, M.C. (1999). The effect of climate change on floods in British Columbia. *Nordic Hydrology, 30*(3), 231-256. https://doi.org/10.2166/nh.1999.0013.

Marcus, W.A. (2012). Remote sensing of the hydraulic environment in gravel-bed rivers. In M. Church, P. Biron, and A. Roy (Eds.), *Gravel-bed rivers: Processes, tools, environments* (pp. 259-285). Wiley-Blackwell.

Masse Environmental Consultants Ltd. (Masse Environmental). (2012, June). *Kaslo River Flood Works Environmental Monitoring Report*.

Ministry of Environment (MoE). (1981, November). *Kaslo River Flood Protection*. Victoria, B.C., File P77-23.

Natural Resources Canada. (2017). *Federal Floodplain Mapping Framework*. Version 1.0, General Information Product 112e. 20 pp.

Northwest Hydraulic Consultants (NHC). (October 2008a). Comprehensive Review of Fraser River at Hope Flood Hydrology and Flows – Scoping Study: Final Report. Prepared for BC Ministry of Environment.

Northwest Hydraulic Consultants. (2008b). *Flood Risk Evaluation and Flood Control Solutions, Phase 1* [Report]. Prepared for the City of Prince George.

Northwest Hydraulic Consultants. (2014). *Simulating the Effects of Sea Level Rise and Climate Change on Fraser River Flood Scenarios (GS14LMN-035)* [Report]. Prepared for BC Ministry of Forests Lands and Natural Resource Operations.

Northwest Hydraulic Consultants. (2016). North Alouette and South Alouette Rivers Additional Floodplain Analysis: Phase 2 – Technical Investigations Completion Report. Prepared for the City of Maple Ridge.

Northwest Hydraulic Consultants. (2018). *Lillooet River Floodplain Mapping, Phase 1* [Report]. Prepared for the Pemberton Valley Dyking District Office.Schnorbus, M., Werner, A., & Bennett, K. (2014). Impacts of climate change in three hydrologic regimes in British Columbia, Canada. *Hydrological Processes, 28*, 1170-1189. https://doi.org/10.1002/hyp.9661

Statistics Canada. (2016). Census Profile, 2016 Census [Webpage]. Retrieved from https://www12.statcan.gc.ca/census-recensement/2016/dp-pd/prof/details/page.cfm?Lang=E&Geo1=DPL&Code1=590126&Geo2=PR&Code2=24&Data=Count&SearchText=Edgewood&SearchType=Begins&SearchPR=01&B1=All&TABID=1.

Trimble, S.W. & Cooke, R.U. (1991). Historical sources for geomorphological research in the United States. *The Professional Geographer*, 43(2), 212-228. https://doi.org/10.1111/j.0033-0124.1991.00212.x

Turner, R.J.W., Anderson, R.G., Franklin, R., & Fowler, F. (2009). *Geotour guide for the West Kootenay, British Columbia. Geology, landscapes, mines ghost towns, caves and hot springs*. Geological Survey of Canada Open file 6135, British Columbia Geological Survey Geofile 2009-06.

Wahba, G. (1990). Spline models for Observational data. Paper presented at CBMS-NSF Regional Conference Series in Applied Mathematics. Philadelphia: Soc. Ind. Appl. Maths.

Wang, T., Hamann, A., Spittlehouse, D.L & Carroll, C. (2016). Locally downscaled and spatially customizable climate data for historical and future periods for North America. *PLoS One 11*: e0156720. https://doi.org/10.1371/journal.pone.0156720

Water Management Consultants Inc. (2004, March 19). *Floodplain Mapping: Guidelines and Specifications* [Report]. Prepared for Fraser Basin Council.

Watt, W.E. (Editor-in Chief). (1989). *Hydrology of Floods in Canada: a Guide to Planning and Design*. N.R.C., Ottawa, Canada. 245 p.

Wolman, M. G. (1954). A method of sampling coarse river-bed material. Transactions of the American Geophysical Union, 35(6), 951-956.

# APPENDIX A
# TERMINOLOGY

Table A-1 provides defines terms that are commonly used in geohazard assessments. BGC notes that the definitions provided are commonly used, but international consensus on geohazard terminology does not fully exist. **Bolded terms** within a definition are defined in other rows of Table A-1.

**Table A-1. Geohazard terminology.**

| Term | Definition | Source |
|---|---|---|
| Active Alluvial Fan | The portion of the fan surface which may be exposed to contemporary hydrogeomorphic or avulsion hazards. | BGC |
| Aggradation | Deposition of sediment by a (river or stream). | BGC |
| Alluvial fan | A low, outspread, relatively flat to gently sloping mass of loose rock material, shaped like an open fan or a segment of a cone, deposited by a stream at the place where it issues from a narrow mountain valley upon a plain or broad valley, or where a tributary stream is near or at its junction with the main stream, or wherever a constriction in a valley abruptly ceases or the gradient of stream suddenly decreases | Bates and Jackson (1995) |
| Annual Exceedance Probability ($P_H$) (AEP) | The Annual Exceedance Probability (AEP) is the estimated **probability** that an event will occur exceeding a specified magnitude in any year. For example, a flood with a 0.5% AEP has a one in two hundred chance of being reached or exceeded in any year. AEP is increasingly replacing the use of the term **'return period'** to describe flood recurrence intervals. | Fell et al. (2005) |
| Avulsion | Lateral displacement of a stream from its main channel into a new course across its fan or floodplain. An "avulsion channel" is a channel that is being activated during channel avulsions. An avulsion channel is not the same as a paleochannel. | Oxford University Press (2008) |
| Bank Erosion | Erosion and removal of material along the banks of a river resulting in either a shift in the river position, or an increase in the river width. | BGC |
| Clear–water flood | Riverine and lake flooding resulting from inundation due to an excess of clear-water discharge in a watercourse or body of water such that land outside the natural or artificial banks which is not normally under water is submerged. | BGC |
| Climate normal | Long term (typically 30 years) averages used to summarize average climate conditions at a particular location. | BGC |
| Consequence (C) | In relation to risk analysis, the outcome or result of a **geohazard** being realised. Consequence is a product of **vulnerability** (V) and a measure of the **elements at risk** (E) | Fell et al. (2005); Fell et al. (2007), BGC |

| Term | Definition | Source |
|---|---|---|
| Consultation Zone | The Consultation Zone (CZ) includes all proposed and existing development in a geographic zone defined by the approving authority that contains the largest credible area affected by specified **geohazards**, and where damage or loss arising from one or more simultaneously occurring specific **geohazards** would be viewed as a single catastrophic loss. | Adapted from Porter et al. (2009) |
| Debris Flow | Very rapid to extremely rapid surging flow of saturated, non-plastic debris in a steep channel (Hungr, Leroueil & Picarelli, 2014). Debris generally consists of a mixture of poorly sorted sediments, organic material and water (see Appendix B of this report for detailed definition). | BGC |
| Debris Flood | A very rapid flow of water with a sediment concentration of 3-10% in a steep channel. It can be pictured as a flood that also transports a large volume of sediment that rapidly fills in the channel during an event (see Appendix B of this report for detailed definition). | BGC |
| Design Peak Daily Flow | The design flow (e.g. 200-year flood) based on the analysis of annual maximum daily average discharge records. | BGC |
| Design Peak Instantaneous Flow | The design flow (e.g. 200-year flood) based on the analysis of annual maximum instantaneous discharge records. | BGC |
| Elements at Risk (E) | This term is used in two ways:<br>a) To describe things of value (e.g., people, infrastructure, environment) that could potentially suffer damage or loss due to a **geohazard**.<br>b) For risk analysis, as a measure of the value of the elements that could potentially suffer damage or loss (e.g., number of persons, value of infrastructure, value of loss of function, or level of environmental loss). | BGC |

| Term | Definition | Source |
|---|---|---|
| Encounter Probability | This term is used in two ways:<br>a) **Probability** that an event will occur and impact an element at risk when the element at risk is present in the **geohazard** zone. It is sometimes termed **"partial risk"**<br>b) For quantitative analyses, the **probability** of facilities or vehicles being hit at least once when exposed for a finite time period L, with events having a **return period** T at a location. In this usage, it is assumed that the events are rare, independent, and discrete, with arrival according to a statistical distribution (e.g., binomial or Bernoulli distribution or a Poisson process). | BGC |
| Erosion | The part of the overall process of denudation that includes the physical breaking down, chemical solution and transportation of material. | Oxford University Press (2008) |
| Flood | A rising body of water that overtops its confines and covers land not normally under water. | American Geosciences Institute (2011) |
| Flood Construction Level (FCL) | A designated flood level plus freeboard, or where a designated flood level cannot be determined, a specified height above a natural boundary, natural ground elevation, or any obstruction that could cause flooding. | BGC |
| Flood mapping | Delineation of flood lines and elevations on a base map, typically taking the form of flood lines on a map that show the area that will be covered by water, or the elevation that water would reach during a flood event. The data shown on the maps, for more complex scenarios, may also include flow velocities, depth, or other hazard parameters. | BGC |
| Floodplain | The part of the river valley that is made of unconsolidated river-borne sediment, and periodically flooded. | Oxford University Press (2008) |
| Flood setback | The required minimum distance from the natural boundary of a watercourse or waterbody to maintain a floodway and allow for potential bank erosion. | BGC |

| Term | Definition | Source |
|---|---|---|
| Freeboard | Freeboard is a depth allowance that is commonly applied on top of modelled flood depths. There is no consistent definition, either within Canada or around the world, for freeboard. Overall, freeboard is used to account for uncertainties in the calculation of a base flood elevation, and to compensate for quantifiable physical effects (e.g., local wave conditions or dike settlement). Freeboard in BC is commonly applied as defined in the BC Dike Design and Construction manual (BC Ministry of Water, Land and Air Protection [BC MWLAP], 2004): a fixed amount of 0.6 m (2 feet) where mean daily flow records are used to develop the design discharge or 0.3 m (1 foot) for instantaneous flow records. | BC Ministry of Water, Land and Air Protection [BC MWLAP] (2004) |
| Frequency (f) | Estimate of the number of events per time interval (e.g., a year) or in a given number of trials. Inverse of the **recurrence interval** (**return period**) of the **geohazard** per unit time. Recurring **geohazards** typically follow a **frequency**-magnitude (F-M) relationship, which describes a spectrum of possible **geohazard magnitudes** where larger (more severe) events are less likely. For example, annual **frequency** is an estimate of the number of events per year, for a given **geohazard event magnitude**.<br>In contrast, annual **probability** of exceedance is an estimate of the **likelihood** of one or more events in a specified time interval (e.g., a year). When the expected **frequency** of an event is much lower than the interval used to measure **probability** (e.g., **frequency** much less than annual), **frequency** and **probability** take on similar numerical values and can be used interchangeably. When **frequency** approaches or exceeds 1, defining a relationship between **probability** and **frequency** is needed to convert between the two. The main document provides a longer discussion on **frequency** versus **probability**. | Adapted from Fell et al. (2005) |
| Hazard | Process with the potential to result in some type of undesirable outcome. Hazards are described in terms of scenarios, which are specific events of a particular frequency and magnitude. | BGC |
| Hazardous flood | A flood that is a source of potential harm. | BGC |

| Term | Definition | Source |
|---|---|---|
| Geohazard | Geophysical process that is the source of potential harm, or that represents a situation with a potential for causing harm.<br>Note that this definition is equivalent to Fell et al. (2005)'s definition of Danger (threat), defined as an existing or potential natural phenomenon that could lead to damage, described in terms of its geometry, mechanical and other characteristics. Fell et al. (2005)'s definition of danger or threat does not include forecasting, and they differentiate Danger from Hazard. The latter is defined as the **probability** that a particular danger (threat) occurs within a given period of time. | Adapted from CSA (1997), Fell et al. (2005). |
| Geohazard Assessment | Combination of **geohazard analysis** and evaluation of results against a **hazard tolerance standard** (if existing). Geohazard assessment includes the following steps:<br>a. **Geohazard analysis**: identify the **geohazard** process, characterize the geohazard in terms of factors such as mechanism, causal factors, and trigger factors; estimate **frequency** and magnitude; develop **geohazard scenarios**; and estimate extent and intensity of **geohazard scenarios**.<br>b. Comparison of estimated hazards with a hazard tolerance standard (if existing) | Adapted from Fell et al. (2007) |
| Geohazard Event | Occurrence of a **geohazard**. May also be defined in reverse as a non- occurrence of a **geohazard** (when something doesn't happen that could have happened). | Adapted from ISO (2018) |
| Geohazard Intensity | A set of parameters related to the destructive power of a **geohazard** (e.g. depth, velocity, discharge, impact pressure, etc.) | BGC |
| Geohazard Inventory | Recognition of existing **geohazards.** These may be identified in geospatial (GIS) format, in a list or table of attributes, and/or listed in a **risk register**. | Adapted from CSA (1997) |
| Geohazard Magnitude | Size-related characteristics of a **geohazard**. May be described quantitatively or qualitatively. Parameters may include volume, discharge, distance (e.g., displacement, encroachment, scour depth), or acceleration. In general, it is recommended to use specific terms describing various size-related characteristics rather than the general term magnitude. Snow avalanche magnitude is defined differently, in classes that define destructive potential. | Adapted from CAA (2016) |

| Term | Definition | Source |
|---|---|---|
| Geohazard Risk | Measure of the **probability** and severity of an adverse effect to health, property the environment, or other things of value, resulting from a geophysical process. Estimated by the product of **geohazard probability** and **consequence**. | Adapted from CSA (1997) |
| Geohazard Scenario | Defined sequences of events describing a **geohazard** occurrence. Geohazard scenarios characterize parameters required to estimate risk such **geohazard extent** or **runout exceedance probability,** and **intensity.** Geohazard scenarios (as opposed to **geohazard risk scenarios**) typically consider the chain of events up to the point of impact with an element at risk, but do not include the chain of events following impact (the **consequences**). | Adapted from Fell et al. (2005) |
| Hazard | Process with the potential to result in some type of undesirable outcome. Hazards are described in terms of scenarios, which are specific events of a particular frequency and magnitude. | BGC |
| Inactive Alluvial Fan | Portions of the fan that are removed from active hydrogeomorphic or avulsion processes by severe fan erosion, also termed fan entrenchment. | BGC |
| LiDAR | Stands for Light Detection and Ranging, is a remote sensing method that uses light in the form of a pulsed laser to measure ranges (variable distances) to the Earth. These light pulses - combined with other data recorded by the airborne system - generate precise, three-dimensional information about the shape of the Earth and its surface characteristics. | National Oceanic and Atmospheric Administration, (n.d.). |
| Likelihood | Conditional **probability** of an outcome given a set of data, assumptions and information. Also used as a qualitative description of **probability** and **frequency**. | Fell et al. (2005) |
| Melton Ratio | Watershed relief divided by square root of watershed area. A parameter to assist in the determination of whether a creek is susceptible to flood, debris flood, or debris flow processes. | BGC |
| Nival | Hydrologic regime driven by melting snow. | Whitfield, Cannon and Reynolds (2002) |
| Orphaned | Without a party that is legally responsible for the maintenance and integrity of the structure. | BGC |
| Paleofan | Portion of a fan that developed during a different climate, base level or sediment transport regime and which will not be affected by contemporary geomorphic processes (debris flows, debris floods, floods) affecting the active fan surface | BGC |

| Term | Definition | Source |
|---|---|---|
| Paleochannel | An inactive channel that has partially been infilled with sediment. It was presumably formed at a time with different climate, base level or sediment transport regime. | BGC |
| Pluvial – hybrid | Hydrologic regime driven by rain in combination with something else. | BGC |
| Probability | A measure of the degree of certainty. This measure has a value between zero (impossibility) and 1.0 (certainty) and must refer to a set like occurrence of an event in a certain period of time, or the outcome of a specific event. It is an estimate of the **likelihood** of the magnitude of the uncertain quantity, or the **likelihood** of the occurrence of the uncertain future event.<br>There are two main interpretations:<br>i) Statistical – **frequency** or fraction – The outcome of a repetitive experiment of some kind like flipping coins. It includes also the idea of population variability. Such a number is called an "objective" or relative frequentist probability because it exists in the real world and is in principle measurable by doing the experiment.<br>ii) Subjective (or Bayesian) probability (degree of belief) – Quantified measure of belief, judgement, or confidence in the **likelihood** of an outcome, obtained by considering all available information honestly, fairly, and with a minimum of bias. Subjective probability is affected by the state of understanding of a process, judgement regarding an evaluation, or the quality and quantity of information. It may change over time as the state of knowledge changes. | Fell et al. (2005) |
| Return Period (Recurrence Interval) | Estimated time interval between events of a similar size or **intensity**. Return period and **recurrence interval** are equivalent terms. Inverse of **frequency**. | BGC |
| Risk | Likelihood of a geohazard scenario occurring and resulting in a particular severity of consequence. In this report, risk is defined in terms of safety or damage level. | BGC |
| Rock (and debris) Slides | Sliding of a mass of rock (and debris). | BGC |
| Rock Fall | Detachment, fall, rolling, and bouncing of rock fragments. | BGC |

| Term | Definition | Source |
|---|---|---|
| Scour | The powerful and concentrated clearing and digging action of flowing air or water, especially the downward erosion by stream water in sweeping away mud and silt on the outside curve of a bend, or during a time of flood. | American Geological Institute (1972) |
| Steep-creek flood | Rapid flow of water and debris in a steep channel, often associated with avulsions and bank erosion and referred to as debris floods and debris flows. | BGC |
| Steep Creek Hazard | Earth-surface process involving water and varying concentrations of sediment or large woody debris. (see Appendix B of this report for detailed definition). | BGC |
| Uncertainty | Indeterminacy of possible outcomes. Two types of uncertainty are commonly defined:<br>a) Aleatory uncertainty includes natural variability and is the result of the variability observed in known populations. It can be measured by statistical methods, and reflects uncertainties in the data resulting from factors such as random nature in space and time, small sample size, inconsistency, low representativeness (in samples), or poor data management.<br>b) Epistemic uncertainty is model or parameter uncertainty reflecting a lack of knowledge or a subjective or internal uncertainty. It includes uncertainty regarding the veracity of a used scientific theory, or a belief about the occurrence of an event. It is subjective and may vary from one person to another. | BGC |
| Waterbody | Ponds, lakes and reservoirs | BGC |
| Watercourse | Creeks, streams and rivers | BGC |

# REFERENCES

American Geological Institute. (1972). *Glossary of Geology*. Washington, DC.: Author.

American Geosciences Institute. (2011). *Glossary of Geology* (5th ed.). Virginia: Author.

Bates, R.L. & Jackson, J.A. (1995). *Glossary of Geology* (2nd ed.). Virginia: American Geological Institute.

Canadian Avalanche Association (CAA). (2016). Technical Aspects of Snow Avalanche Risk Management – Resources and Guidelines for Avalanche Practitioners in Canada (C. Campbell, S. Conger, B. Gould, P. Haegeli, B. Jamieson, & G. Statham Eds.). Revelstoke, BC, Canada: Canadian Avalanche Association.

Canadian Standards Association (CSA). (1997). *CAN/CSA – Q859-97 Risk Management: Guideline for Decision Makers*. CSA Group, Toronto, ON, pp. 55.

Fell, R., Ho., K.K.S., LaCasse, S., & Leroi, E. (2005). A framework for landslide risk assessment and management. In Hungr, O., Fell, R., Couture, R. (Eds.) *Landslide Risk Management:* Proceedings *of the International Conference on Landslide Risk Management.* Vancouver, BC.

Fell, R., Whitt, G. Miner, A., & Flentje, P.N. (2007). Guideline for Landslide Susceptibility, Hazard and Risk Zoning for Land Use Planning. *Australian Geomechanics Journal* 42: 13-36.

International Organization for Standardization (ISO). (2018). *ISO 31000:2018 Risk Management – Guidelines*. Retrieved from https://www.iso.org/standard/65694.html

Ministry of Water, Land and Air Protection. (MWLAP) (2004). *Flood Hazard Area Land Use Management Guidelines*.

National Oceanic and Atmospheric Administration. (n.d.) What is LIDAR? [Web page]. Retrieved from https://oceanservice.noaa.gov/facts/lidar.html

Oxford University Press. (2008). *A dictionary of Earth Sciences* (3rd ed.). Oxford, England: Author.

Porter, M., Jakob, M., & Holm, K. (2009, September). Proposed Landslide Risk Tolerance Criteria. *GeoHalifax 2009*. Paper presented at the meeting of the Canadian Geotechnical Society, Halifax, Canada.

Whitfield, P.H., Cannon, A.J., & Reynolds, C.J. (2002). Modelling Streamflow in Present and Future Climates: Examples from the Georgia Basin, British Columbia. *Canadian Water Resources Journal, 27(*4), 427 – 456. https://doi.org/10.4296/cwrj2704427.

# APPENDIX B
# SITE PHOTOGRAPHS

**Photo 1.**

**Kaslo River and fan looking upstream. Photo: BGC, July 6, 2019**

**Photo 2.**

**Kaslo River and fan looking downstream showing the primary study area. Photo: BGC, July 6, 2019**

**Photo 3.**

**Standing on the Kaslo River Trail pedestrian bridge looking upstream. Photo: BGC, July 4, 2019**

**Photo 4.**

**Standing on the Kaslo River Trail pedestrian bridge looking downstream. The Highway 31 bridge is visable in the distance. Photo: BGC, July 4, 2019**

**Photo 5.**

**Standing on the Kaslo River dike looking upstream to the Highway 31 bridge Photo: BGC, July 4, 2019**

**Photo 6.**

**Standing on the Kootenay Lake shoreline looking upstream to Kaslo River and the contemporary river fan. Photo: BGC, July 4, 2019**

**Photo 7.**

**Standing on the Kaslo River dike looking towards Kaslo fan. Photo: BGC, July 4, 2019**

**Photo 8.**

**Example of bank erosion. In this location the right (far) bank is eroding causing the leaning tree (arrow) to be undermined. Photo: BGC, July 4, 2019**

# APPENDIX C
# REGIONAL FLOOD FREQUENCY ANALYSIS

## C.1. INTRODUCTION

Estimating flood magnitude is of fundamental importance to reliable floodplain mapping. As most watercourses are not gauged, flood magnitude is commonly estimated for an ungauged catchment using a Regional Flood Frequency Analysis (Regional FFA). There are several methods to complete a Regional FFA. This appendix documents the methodology followed by BGC Engineering Inc. (BGC) for the regionalization of floods in British Columbia using the index-flood method (Dalrymple 1960).

This appendix begins with a description of Regional FFA and the index-flood method (Section C1.0). The study area over which the index-flood is developed is discussed in Section C2.0. The data acquisition and compilation to support the analysis is described in Section C3.0. A description of the methods and assumptions for the regionalization of floods is included in Section C4.0. Results for the different hydrologic regions that cover the Regional District of Central Kootenay (RDCK) are presented in Section C5.0, while the application of the index-flood method to ungauged catchments in the RDCK is presented in Section C6.0. Finally, the limitations of the study are discussed in Section C7.0.

### C.1.1. Regional FFA

Extreme events are rare by definition and record lengths at hydrometric stations are often short. Regional FFA accounts for short record lengths by trading space for time where flood events at several hydrometric stations are pooled to estimate flood magnitude in a homogeneous region. Homogeneous regions can be defined as geographically contiguous regions, geographically non-contiguous regions, or as hydrological neighbourhoods. Grouping catchment areas of similar catchment characteristics into homogeneous regions is a critical part of Regional FFA because hydrologic information can be transferred accurately only within a region that is homogeneous. The more homogeneous a region is, the more reliable the flood quantile estimates. Some heterogeneity may be deemed acceptable in some cases. Studies show that even moderately heterogeneous regions can yield more accurate flood quantile estimates than a single-station FFA (Hosking & Wallis, 1997).

### C.1.2. Index-flood Method

Several methods have been developed to conduct a Regional FFA in homogeneous regions. Among the quantile estimation methods, the index-flood is considered superior to other models (Ouarda et al., 2008). The index-flood is a method of regionalization with a long history in FFA (Dalrymple, 1960). The index-flood method involves the development of a dimensionless regional growth curve assumed to be constant within a homogenous region. The index-flood method also requires the selection of an index-flood which can be the mean annual flood, the median annual flood, or another quantile of choice calculated at each hydrometric station in the region.

The probability distribution of flood events at hydrometric stations in a homogeneous region are identical apart from a site-specific scaling factor, the index-flood. The parameters of the probability

distribution are estimated at each hydrometric station. These at-site estimates are combined using a weighted average to generate a regional estimate. The regional growth curve is thus a dimensionless quantile function common to every hydrometric station in the region and takes on the following form (Eq. C-1):

$$X_T = Q_T / Q_m \quad \text{[Eq. C-1]}$$

where $X_T$ is the growth factor for return period $_T$, $Q_T$ is the flood magnitude at return period $_T$, and $Q_m$ is the index-flood magnitude. The flood magnitude at any return period is calculated using this relationship given the index-flood estimate.

### C.1.3. Application to Ungauged Catchments

The index-flood method can be applied to an ungauged catchment by developing a regional relationship between the index-flood and catchment characteristics at hydrometric stations in the region. The relationship can be expressed in many forms including a multivariate linear regression. Flood events can be assumed to depend on the characteristics of individual catchments such as area, elevation, percent lake, forest coverage, mean annual precipitation, mean annual temperature, etc. Once the catchment characteristics are extracted at the ungauged site, the index-flood can be estimated. The flood magnitude of any annual exceedance probability (AEP) can be estimated for an ungauged catchment using the index-flood estimate and the regional growth curve by re-organizing equation Eq. C1-1.

## C.2. STUDY AREA

A Regional FFA for British Columbia represents a considerable challenge given its regional variations in precipitation caused by sharp changes in topography as well as diverse geology. The proportion of annual precipitation that falls as snow as opposed to rain increases with latitude, elevation, and distance from the Pacific Ocean. Significant regional variations in precipitation are observed in British Columbia, influenced by the various mountain ranges. Storms approaching the West Coast are lifted rapidly along the windward mountain slopes, resulting in widespread precipitation. A rain shadow is created on the lee side of the mountains. For example, Tofino receives an average of 3,160 mm of annual precipitation while Nanaimo, on the east coast of Vancouver Island, receives 1,060 mm.

This climate pattern is repeated several times from east to west. As the weather systems approach the Coast Mountains, orographic effects result in twice as much precipitation in North Vancouver compared to Vancouver proper. Moving to the east, the Okanagan Valley is located on the lee side of the Coast Mountains resulting in an arid to semi-arid climate with annual precipitation on the order of 350 mm. The cycle is repeated over the Monashees, the Columbia Trench, and the Rocky Mountains. These orographic effects impact flood events and complicate regionalization efforts due to significant areal variations in precipitation, even for small catchments. These significant variations in precipitation suggest that a multivariate approach to regionalization is practical for British Columbia.

Similar to precipitation, surficial geology in the province demonstrates significant spatial variability. This variability is important in that while two catchments may be located in a similar precipitation zone, the hydrologic response can be significantly different. Catchments dominated by colluvial veneers and bedrock will tend to have larger unit peak flows, than those mantled by coarse morainal sediment, with the latter tending to attenuate peak flows through available soil moisture storage. To avoid introducing boundary effects at the border with the Unites States and Alberta, the study area was extended to include the northern portion of Washington, Idaho, and Montana as well as the eastern Slopes of the Rocky Mountains. A map of the study area is presented in Figure C-1.


**Figure C-1. Study area where the red outline defines the boundary.**

## C.3. DATA ACQUISITION AND COMPILATION

A large component of this study consisted of acquiring the data and compiling it in a format that was usable for analysis. Suitable hydrometric stations in the study area were identified and the flood records were acquired from the appropriate monitoring agency. The catchment polygons upstream from the hydrometric stations were then delineated and the area calculated using

methods specific to the scale of the catchment. Lastly, a suite of catchment characteristics was selected based on potential to influence flood events. These catchment characteristics were extracted for each polygon. The acquisition and the compilation of this rich dataset was the most time-consuming portion of the procedure. The following sections include a detailed description of how the data were acquired and how the dataset was compiled for analysis.

### C.3.1. Hydrometric Stations

A total of 3,309 hydrometric stations are located within the study area. Of these, 2115 are managed by the Water Survey of Canada (WSC) and the remaining 1194 are managed by the United States Geological Survey (USGS).

### C.3.2. Flood Records

As an initial step, all flood events recorded at the hydrometric stations were extracted. This extraction was challenging as records are stored differently by the WSC and USGS. In Canada, flood events are stored in the HYDAT database, which includes the annual maximum peak instantaneous streamflow, the maximum average daily streamflow, as well as the date and time of each event. The catchment area and the number of years on record are also available in the HYDAT database. The flood records were acquired directly from the HYDAT database for hydrometric stations in Canada. In the US, flood events are stored online on websites specific to each hydrometric station. The annual maximum peak instantaneous streamflow, the catchment area, and the number of years on record are also stored in this way. This information was extracted from the online storage space using a programming script for each USGS hydrometric station.

### C.3.3. Maximum Peak Instantaneous Streamflow

The preferred metric for analysis is the annual maximum peak instantaneous streamflow. However, it is not uncommon for flood records to have more annual maximum average daily streamflow records than peak instantaneous values, which are greater in magnitude. The ratio (I/D) between maximum peak instantaneous and maximum average daily streamflow is typically greater for small catchments than for very large catchments. Therefore, where only a maximum daily streamflow is reported for some years, maximum peak instantaneous streamflow values can be estimated from available maximum average daily streamflow records using regression analysis.

The reliability of the regression analysis was judged based on the coefficient of determination ($R^2$) in combination with the Cook distance (D). The $R^2$ is the proportion of the variance in the peak instantaneous streamflow that is predictable from the average daily streamflow. The D value is used to assess the influence of outliers present in the dataset. The regression analysis was deemed acceptable by BGC if the $R^2$ is above 0.95 and the D value is above 25. In this case, the maximum peak instantaneous streamflow record was extended using the regression analysis for a longer record length. Alternatively, maximum peak instantaneous streamflow record remained as-is where the regression analysis was deemed unacceptable.

### C.3.4. Catchment Polygons

The catchment polygons at hydrometric stations within the study area were estimated using two different approaches.

1. River Networks Tools™[1] (RNT).
2. Using an Environmental Systems Research Institute (ESRI) process (i.e., GIS-based).

The RNT-based approach is dependent on the delineation of a stream network, while the ESRI-based process is dependent on topographic data. Catchment polygons were defined for all hydrometric stations located within the study area. Catchment delineation based on a stream network was observed to be more reliable for small catchments, especially where topographic relief is low. The catchment polygons defined by the ESRI process were selected for larger catchments (>1,000 km$^2$), while the RNT-based approaches were selected for smaller catchment areas (<1,000 km$^2$). The selection of the best catchment polygon for analysis could not be checked directly as the monitoring agencies (WSC and USGS) do not publish polygon shape information.

### C.3.5. Catchment Areas

The catchment area was estimated for each catchment polygon (RNT, modification based on RNT, and ESRI) at each hydrometric station. The catchment area for each polygon was then compared with the value published by the respective monitoring agency. The catchment area published by monitoring agencies is generally considered most reliable (although recognizing many of the catchment areas for the WSC stations were calculated with 1:50,000 scale mapping and may not reflect more recent topographic mapping) and was used to quality check the calculated areas.

The estimated value of the catchment area was deemed acceptable if it was within ±15% of the published value. If more than 1 catchment area estimate (of the 3) was within ±15% of the published value, the catchment area with the smallest difference relative to the published value was selected as the best estimate for analysis. Approximately 90% of catchment polygons were within ±15% of the published value.

Published values are not available for all hydrometric stations. In those cases, the catchment area was deemed acceptable if the 3 estimates were within ±15% of each other. Catchment areas that did not meet the ± 15% criteria were not included in the analysis. A total of 2269 hydrometric stations were removed from the analysis because either the catchment area was deemed unreliable or water level data only was recorded at the station. Manual quality checks were not completed for these catchments due to the time-consuming nature of this effort. The number of hydrometric stations lost that could have been considered useful is considered negligible. The

[1] The RNT is a proprietary software developed by BGC. RNT is based on publicly available 1:24,000-scale or better topographic and hydrographic datasets throughout North America that BGC has compiled and systematically developed to support a wide range of hydrotechnical calculations (e.g., catchment area) and site-specific precipitation and flood monitoring.

number of hydrometric stations in the study area is summarized in Table C-1. The ESRI catchment polygons were used for the hydrometric stations at the border between Canada and the United States because the polygons based on the two RNT approaches are observed to be poorly delineated due to differences in data resolution available between both countries.

**Table C-1. Number of hydrometric stations in the study area.**

| Criteria | Number |
|---|---|
| Hydrometric Stations in Study Area | 3284 |
| Station with Unacceptable Catchment Area Estimates | 2269 |
| Stations with Acceptable Catchment Area Estimates | 1015 |

### C.3.6. Catchment Characteristics

Catchment characteristics were selected based on potential to influence flood events. A suite of 18 catchment characteristics was ultimately selected and estimated for each hydrometric station, as summarized in Table C-2. Several data sources were used to compile the catchment characteristics which are described in the following sections.

#### C.3.6.1. Catchment Statistics

The Shuttle Radar Topography Mission (STRM) dataset (Farr et al., 2007) was used to extract the catchment elevation statistics. The catchment elevation statistics were averaged over the catchment area. This dataset was used to calculate the catchment area (just for catchments over 1000 $km^2$), relief, length, and slope. The centroid statistics were also extracted from this dataset.

#### C.3.6.2. Climate Variables

The Climate North America (ClimateNA) dataset was used to estimate the climate variables for each catchment polygon (Wang et al., 2016). The climate variables were averaged over the catchment area and were based on the average for the period 1961 to 1990.

**Table C-2. List of selected catchment characteristics.**

| Type | No. | Acronym | Characteristic | Units | Dataset |
|---|---|---|---|---|---|
| Catchment | 1 | Centroid_Lat | Latitude at the centroid location in the catchment polygon | degrees | STRM |
| | 2 | Centroid_Long | Longitude at the centroid location in the catchment polygon | degrees | |
| | 3 | Centroid_Elev | Elevation at the centroid location in the catchment polygon | m | |
| | 4 | Area | Area of the catchment polygon | $km^2$ | |
| | 5 | Relief | Maximum minus minimum catchment elevation | m | |
| | 6 | Length | Area divided by perimeter | km | |
| | 7 | Slope | Catchment length divided by relief times 100 | % | |
| Climate | 8 | MAP | Mean annual precipitation | mm | Climate NA |
| | 9 | MAT | Mean annual temperature | °C | |
| | 10 | PAS | Precipitation as snow | mm | |
| | 11 | PPT_wt | Winter precipitation (Dec, Jan, Feb) | mm | |
| | 12 | PPT_sp | Spring precipitation (Mar, Apr, May) | mm | |
| | 13 | PPT_sm | Summer precipitation (Jun, Jul, Aug) | mm | |
| | 14 | PPT_fl | Fall precipitation (Sep, Oct, Nov) | mm | |
| Physiographic | 15 | Forest | Forest cover in the catchment | % | NALCMS |
| | 16 | Water_Wetland | Wetland and open water cover in the catchment | % | |
| | 17 | Urban | Urban cover in the catchment | % | |
| | 18 | CN | Inferred based on integrating land cover and soils cover | unitless | NALCMS and HYSOGs250m |

### C.3.6.3. Land cover

The North American Land Change Monitoring System (NALCMS) land cover products include the 2005 land cover map of North America. This dataset includes 19 land cover classes derived from 250 m Moderate Resolution Spectroradiometer (MODIS) image composites (Latifovic et al., 2012). This dataset was used to calculate the percent forest, percent wetland and lake, and the urban portion of the catchment.

### C.3.6.4. Curve Number

The curve number (CN) is an empirical parameter used for predicting runoff from rainfall. BGC integrated the land cover (NALCMS) and the hydrologic soils group (HYSOGs250m) datasets to

infer the average CN over each catchment. The NALCMS dataset is described in Section C.3.6.3. The HYSOGs250m dataset represents typical soil runoff potential at a 250 m spatial resolution (Ross et al., 2018). Hydrologic soils groups are defined based on soil texture, depth to bedrock or depth to groundwater. There are four basic groups: A, B, C, D. Four additional groups are included where the depth to bedrock is considered to be less than 60 cm: AD, BD, CD, and DD. The area covered by each hydrologic soils group is summed for a total area over the catchment for each hydrologic soils group.

The CN was assigned following guidance from the USGS (1986). The CN values for soils where the depth to bedrock or depth to groundwater.is expected to be less than 0.6 m from the surface (i.e., D soils) were assumed to be the same as the case where it is not expected to be close to the ground surface. The CN value assignment for the combinations of land cover and hydrologic soils groups identified in the catchments is presented in Table C-3. The CN values were averaged over the catchment area using a weighted mean. The weight reflects the percentage of the area covered by a given CN value.

**Table C-3. CN values based on the integration between the land cover and soils datasets.**

| Land Cover (NALCMS 2005) | Cover Type (USGS 1986) | Soils | | | |
|---|---|---|---|---|---|
| | | HSG-A | HSG-B | HSG-C | HSG-D |
| Temperate or sub-polar needleleaf forest | Woods - Good | 30 | 55 | 70 | 77 |
| Temperate or sub-polar broadleaf deciduous forest | Woods - Good | 30 | 55 | 70 | 77 |
| Mixed forest | Woods - Good | 30 | 55 | 70 | 77 |
| Temperate or sub-polar shrubland | Brush - brush-weed-grass mixture with brush the major element - Fair | 35 | 56 | 70 | 77 |
| Temperate or sub-polar grassland | Pasture, grassland, or range—continuous for grazing - Good | 39 | 61 | 74 | 80 |
| Sub-polar or polar grassland-lichen-moss | Pasture, grassland, or range—continuous for grazing - Good | 39 | 61 | 74 | 80 |
| Sub-polar or polar barren-lichen-moss | Desert shrub - major plants include saltbrush. Greasewood, creosotebush, blackbrish, bursage, palo verde, mesquite, and cactus - good | 49 | 68 | 79 | 84 |
| Sub-polar taiga needleleaf forest | Woods - Good | 30 | 55 | 70 | 77 |
| Cropland | Row crops - straight row (SR) | 63 | 74 | 81 | 85 |
| Barren land | Desert shrub - major plants include saltbrush. Greasewood, creosotebush, blackbrish, bursage, palo verde, mesquite, and cactus - good | 49 | 68 | 79 | 84 |
| Urban and built-up | Urban districts - commercial and business | 89 | 92 | 94 | 95 |
| Snow and ice | NA | 0 | 0 | 0 | 0 |
| Wetland | NA | 0 | 0 | 0 | 0 |
| Water | NA | 0 | 0 | 0 | 0 |

## C.4. METHODS AND ASSUMPTIONS

Once the dataset is compiled for analysis, the regionalization of floods procedure can begin. A description of the methods and assumptions for the index-flood method is included in this section.

### C.4.1. Flood Statistics Calculations

Flood statistics were calculated using the flood record at each of the selected hydrometric stations (2101) in the study area. Flood statistics include L-moments and flood quantile estimates.

#### C.4.1.1. L-moments

The L-moment approach in the index-flood procedure was used by BGC for the regionalization of floods in British Columbia. The shape of a probability distribution has traditionally been described by the moments of the distribution including the mean, standard deviation, skewness, and kurtosis. However, moment estimators have some undesirable properties where the skewness and kurtosis can be severely biased. Both have algebraic bounds that depend on the sample size (Hosking & Wallis, 1997).

L-moments are an alternative system for describing the shape of probability distributions. Studies have shown that L-moments are unbiased, less sensitive to outliers, and are better estimators of distribution parameters especially for short to moderate record length (Hosking, 1990). Furthermore, L-moments allow for the efficient computation of parameter estimates and flood quantile estimates.

L-moments evolved as modifications to the probability weighted moments (Greenwood et al., 1979). In terms of probability weighted moments, L-moments are defined as $\lambda_1$, $\lambda_2$, $\lambda_3$, and $\lambda_4$ with their mathematical expressions published for a range of probability distributions in Hosking and Wallis (1997, Appendix).

Dimensionless versions of L-moments are defined as L-moment ratios by dividing the higher order L-moments by $\lambda_2$. L-moment ratios are defined by Eq. C-2:

$$\tau_r = \lambda_r / \lambda_2 \qquad \text{[Eq. C-2]}$$

L-moment ratios depict the shape of a distribution independently of its scale measurement. Refer to Table C-4 for L-moment terminology.

**Table C-4. L-moment terminology.**

| Symbol (population) | Symbol (sample) | Definition |
|---|---|---|
| $\lambda_1$ | $\iota_1$ | L-location or the mean of the distribution |
| $\lambda_2$ | $\iota_2$ | L-scale |
| $\tau$ | $t$ | L-CV |
| $\tau_3$ | $t_3$ | L-skewness |
| $\tau_4$ | $t_4$ | L-kurtosis |

### C.4.1.2. At-site Flood Quantile Estimates

The flood quantile estimates at hydrometric stations are referred to as 'at-site' estimates and are used to compare with the modeled quantile estimates to assess the validity of the model. Flood quantile estimates were calculated using the flood data by means of a single-station FFA. A popular approach in FFA is the Annual Maximum Series (AMS) where the maximum peak instantaneous streamflow for each year on record is used for analysis. The basic assumption is that the flood events are independent and identically distributed from a single population of flood events.

A probability distribution is selected to describe the flood events in the record. The true form of the underlying probability distribution is not known and there is no standard distribution appropriate in all cases. The goal is to select a probability distribution that fits the observed data well but also generates robust quantile estimates that are not sensitive to physical deviations of the true probability distribution (Hosking & Wallis, 1997). In extreme value statistics, data follow one of three extremal types of distributions: Gumbel, Fréchet, or Weibull (Coles, 2001). These three distributions can be expressed as a single formula and are considered a family of distributions known as the Generalized Extreme Value (GEV) distribution. The GEV distribution is shown to arise as an asymptotic model for maximum values in a sample and hence can be viewed as a natural model for observed flood events. For these reasons, the GEV distribution was used to describe the recorded flood events. No statistical tests were used to assess this choice because the GEV distribution is considered flexible to account for the variability captured at a single hydrometric station.

The parameters of the GEV distribution were estimated using the L-moments. The flood quantiles were calculated for a range of return periods (Table C-5). The reliability of the quantile estimates depends on a range of factors including the record length and the range of flood event magnitudes captured in the record. The longer the record length, the more reliable the quantile estimates.

**Table C-5. Return period and associated AEP.**

| Return Period (Years) | AEP |
|---|---|
| 2 | 0.5 |
| 5 | 0.2 |
| 10 | 0.1 |
| 20 | 0.05 |
| 50 | 0.02 |
| 100 | 0.001 |
| 200 | 0.005 |
| 500 | 0.002 |

## C.4.2. Formation of Hydrological Regions

The catchment characteristics extracted over the catchment polygons were used to group the hydrometric stations into hydrological regions using a cluster analysis. Cluster analysis is an objective method for creating regions (Tasker, 1982) which historically were based subjectively using geographical, political, administrative or physiographic boundaries. The essence of cluster analysis is to identify clusters (groups) of hydrometric stations such that the stations within a cluster are similar while there is dissimilarity between the clusters. Hosking and Wallis (1997) suggest that cluster analysis is the most practical method of forming regions for large datasets and provides several opportunities for subjective adjustments to the regions. The algorithm used by BGC to group hydrometric stations is Agglomerative Hierarchal Clustering.

### C.4.2.1. Data Preparation

The catchment characteristics at each hydrometric station were normalized so that the average is zero and the standard deviation is approximately 1. The distance metric used is the Euclidian distance between the catchment characteristics. The suite of catchment characteristics at all hydrometric stations were compared to one another and organised using Ward's Distance measure (d) (Ward, 1963).

### C.4.2.2. Number of Hydrological Regions

Several statistical measures were used to guide the number of clusters to partition the hydrometric stations. The statistical measures include the Elbow Method, the Silhouette Score, and review of the dendrogram. The selection of the number of clusters was also subjectively assessed by reviewing the physical basis of the cluster distribution (e.g., is there a physical meaning behind the number and distribution of the clusters?).

The Elbow Method accounts for the percentage of variance explained as a function of the number of clusters. The percentage of the variance explained decreases with increasing number of

clusters. The minimum number of clusters that provides the most gain in the variance explained was selected for analysis.

The Silhouette Score is a measure of how similar the catchment of a hydrometric station is to its own cluster compared to other clusters. The Silhouette Score was calculated for each hydrometric gauge station and averaged over each cluster. The Silhouette Score ranges from -1 to +1 where a high value indicates that the hydrometric stations are well matched to their own clusters and poorly matched to neighboring clusters.

The dendrogram represents how the clustering algorithm (i.e., agglomerative hierarchal clustering) groups the catchments and depicts a road map of the merging procedure showing which catchments were merged and when in order of increasing cluster distance.

The spatial distribution of the clusters was then reviewed to verify that they are physically plausible. This review was done by superimposing the clusters on a map of British Columbia to see whether there is a physical meaning supporting the cluster distributions.

#### C.4.2.3. Manual Adjustments of Hydrologic Regions

The clusters identified using the clustering algorithm were adjusted manually to increase homogeneity. The manual adjustments were completed by considering the topography, spatial patterns in hydrological processes, and ecozones in Canada. The clusters were further separated based on the scale of catchment area to respect the statistical requirement for constancy in the coefficient of variation (CV) for homogeneous regions.

#### C.4.2.4. Refinement of the Hydrometric Station Selection

The hydrometric station selection was refined to increase the homogeneity of the clusters by reducing the variability introduced by many hydrometric stations. The refinement process was guided by the following 5 criteria.

1. Catchments upstream of hydrometric stations with a regulation level greater than 25% were not included for analysis. The level of regulation is inferred by proportion of the catchment area upstream of the dams to the total catchment area upstream of the hydrometric station.
2. The catchment area range considered in the regionalization extends up to 5,000 $km^2$. Catchments with a greater catchment area size are most likely well gauged and studied that a regionalization of flood is not required.
3. Nested hydrometric stations along the same watercourse were also removed from the region to reduce cross-correlation.
4. A minimum of 6 years of maximum peak instantaneous streamflow data was set as a minimum for analysis. While this threshold is low, it is considered adequate since the influence of each hydrometric stations on the model reflects the record length.
5. Hydrometric stations recording water level only were excluded from the analysis at the onset. Hydrometric stations recording water level and streamflow measurements but located within or immediately at the outlet of lakes were also removed from the analysis.

The flow regime at these locations is considered heavily regulated precluding the use of frequency analysis to estimate peak flows.

In addition to these criteria, discordancy (*Di*) was considered to refine the selection. The discordancy is measured in term of the L-moments of the data at the hydrometric stations within a cluster. The formal definition for *Di* is found in Hosking and Wallis (1997, equation 3.3, page 46). A hydrometric station is considered discordant if *Di* is "large". The definition of "large" depends on the number of hydrometric stations in the cluster. If the cluster includes more than 15 hydrometric stations, the critical value for the discordancy statistic is 3. Discordancy was calculated for each hydrometric station within each hydrologic region. Hydrometric stations with *Di* values greater than 3 were removed from the cluster. This process was re-iterated until no more hydrometric stations showed *Di* values greater than 3.

#### C.4.2.5. Testing for Homogeneity

The hypothesis for homogeneity is that the probability distribution of the flood events at the hydrometric stations within a cluster is the same except for a site-specific scale factor. The goal is to have clusters that are sufficiently homogenous that the regionalization of floods is advantageous to a single station FFA. Testing for homogeneity is done using the H-Test. The H-Test result helps assess whether the hydrometric stations in a cluster may reasonably be considered homogeneous. The formal definition for the H-Test is found in Hosking and Wallis (1997, equation 4.5, page 63). Of note, some level of heterogeneity is expected in these clusters due to the natural variability of hydrological processes that control flood events. The H-Test is not intended to be used as a significance test but rather as a guideline to inform whether the re-definition of a region could lead to a meaningful increase in the accuracy of the flood quantile estimates (Hosking and Wallis 1993).

### C.4.3. Regionalization

Once the clusters were considered sufficiently homogeneous, they were considered "hydrologic regions". The regionalization of floods was then completed for each region. The L-moment approach in the index-flood procedure was used by BGC for the regionalization exercise. The procedure for each hydrologic region included: averaging the L-moments, selecting a distribution, estimating the parameters, developing the growth curve, and estimating the index-flood. The mean annual flood (MAF) was selected as the index-flood for this study. The following sections describe the methods and assumptions for the regionalization of floods for a given hydrologic region.

#### C.4.3.1. Regional L-moments

The L-moment ratios were averaged over each hydrologic region. A weighted average was used where the weight reflected the number of observations at each hydrometric station. The weighted average was used to put more weight on hydrometric stations with a longer record length. The weighted average helps take advantage of all available data as it is often limited in many areas of the province. The regional average L-moment ratios are defined in Table C-6. The L-moment

ratios are used rather than the L-moments because they yield slightly more accurate quantile estimates.

**Table C-6. Definition for regional average L-moment ratios.**

| Symbol (sample) | Definition |
|---|---|
| $\iota_1^R$ | L-location or the mean of the distribution |
| $\iota_2^R$ | L-scale |
| $t^R$ | L-CV |
| $t_3^R$ | L-skewness |
| $t_4^R$ | L-kurtosis |

### C.4.3.2. Distribution Selection for Growth Curves

The selection of an appropriate probability distribution for the growth curves was done using a goodness-of-fit test and review of L-moment ratio diagrams. These tests were completed to assess the variability imposed compiling the results of many hydrometric stations into a single growth curve. The goodness-of-fit test was based on 1,000 simulations and looked at a suite of candidate distributions. The candidate probability distributions included Generalised Logistic (GLO), Generalised Extreme Value (GEV), Generalised Pareto (GPA), Generalised Normal (GNO), and Pearson Type III (PE3). Probability distributions with Z statistics $\leq$1.64 were deemed acceptable (Hosking & Wallis, 1997). The regional L-moments were also plotted with the L-skewness and L-kurtosis relationships for two (Exponential (E), Gumbel (G), Logistic (L), Normal (N), and Uniform (U)) and three-parameter (GLO, GEV, GPA, GNP, PE3) candidate distributions in L-moment ratio diagrams. The plotting position of the regional L-moments was reviewed for the distribution selection that provided an acceptably close visual fit.

### C.4.3.3. Parameter Estimation

The regional L-moments were used to estimate the parameters of the selected probability distribution. The equations used to estimate the parameters for the GEV distribution are found in Hosking and Wallis (1997, A.52, A.55, and A.56, page 196) in addition to other select probability distributions.

### C.4.3.4. Growth Curves and Error Bounds

The index-flood was selected to be the MAF. As a result, the regional mean was set to 1 ($\iota_1^R = 1$). The probability distribution was fit by equating the L-moment ratios of the population ($\lambda_1, \tau, \tau_3, \tau_4$) to the regional average L-moment ratios ($\iota_1^R, t^R, t_3^R, t_4^R$).

One of the strengths of the Regional FFA completed using the regional L-moments is that the procedure is useful even when the assumptions are not all satisfied (e.g., possibility of heterogeneity, misspecification of the probability distribution, and statistical dependence between observations at different sites). An approach to estimate the accuracy of the estimated flood

quantiles is by Monte Carlo simulation. A Monte Carlo simulation was therefore run to estimate the variability in the quantile estimates from the regional GEV distribution. This variability was used to set the error bounds on the regional growth curve.

### C.4.3.5. Index-flood Estimation

The index-flood was estimated using a multiple linear regression. Regression is a classic statistical method to describe the relationship between a dependent variable (index-flood) and independent variables (catchment characteristics). The multiple linear regression model is expressed as follows:

$$Q_T = aA^b B^c \ldots N^n \quad \text{[Eq. C-3]}$$

where $Q_T$ is the flood magnitude at return period $_T$, A, B, …, N are the catchment characteristics, a is the regression constant, and b, c, …, n are the regression coefficients. Base 10 logarithms are used to convert this equation to a linear form by transforming the variables to the following:

$$\log Q_T = \log a + b(\log A) + c\,(\log B) + \cdots + n\,(\log N) \quad \text{[Eq. C-4]}$$

These coefficients were estimated using the Weighted Least Squares method introduced by Tasker (1980), which accounts for the sampling error introduced by unequal record lengths. Unequal record lengths mean that the sampling errors of the observations (flood quantiles) are not equal (heteroscedastic) and the assumption of constant variance in Ordinary Least Squares method is not valid.

The top 5 models were selected using consideration for the adjusted $R^2$ and the Bayesian information criterion (BIC). The 5 models with the lowest BIC were selected and the index-flood estimate was averaged. Select diagnostic plots were reviewed to control the quality of the regressions. The diagnostic plots are listed in Table C-7. The index-flood model was developed over two scales: regional and provincial. These two scales were compared to assess the influence of the distribution of hydrometric stations on the reliability of the MAF estimate.

**Table C-7. Diagnostic plots.**

| Plot | Diagnostic |
|---|---|
| At-site vs. Modeled | Inspect for a one to one relationship as close to as possible |
| At-site Quantile vs. Modeled Quantile | Inspect whether the distribution of the fitted values match the distribution of the observed values |
| At-site Quantiles vs. Modeled Residuals | Inspect for constancy in residuals. Residuals are the differences between the at-site and the modeled estimates |

#### C.4.3.6. Regional Model

The first scale considered is the regional scale where the MAF was modeled over an area consistent with the hydrologic regions defined across the province. This scale is consistent with the scale used to do develop the regional growth curves.

#### C.4.3.7. Provincial Model

The second scale considered is the provincial scale where all hydrometric stations across the province, that meet the selection criteria, were used to model the MAF. The provincial model was developed to capture the range of hydrological processes that control flood events in British Columbia.

#### C.4.3.8. Flood Quantile Estimates

Flood quantile were than estimated using the regional growth curve and index-flood estimates (both scales) for all hydrometric stations in a given region. Quantile plots were generated to compare the at-site and modeled results over the range of AEPs.

#### C.4.3.9. Catchment Characteristic Transformations

The relationship between flood events and catchment characteristics need not be linear. Experience and judgement were used to guide the selection of independent variables and inform the relationship between flood events and catchment characteristics. An exhaustive comparison of correlations between flood magnitude and catchment characteristics showed that catchment area and catchment length are proportional to flood magnitude. For this analysis, the remaining catchment characteristics needed to be log transformed.

### C.4.4. Error Statistics

The quality of the flood quantile estimates was assessed using select error statistics including the Root Mean Square Error (SRMSE), the Percent Error (SPE), and the Bias (SBIAS) for the following AEPs: 0.5, 0.1, 0.02, 0.005. The standardized version of the error statistics is used to account for the different scales (Table C-8).

**Table C-8. Error statistics, definitions, and diagnostic.**

| Error Statistic (acronym) | Definition | Diagnostic |
|---|---|---|
| SRMSE | Standard deviation of the residuals. | Inspect how concentrated the modeled estimates are around the line of best fit. |
| SPE | The difference between the modeled and at-site estimate, divided by the at-site estimate, multiplied by 100%. | Inspect how close the modeled estimate is to the at-site estimate/ |
| SBIAS | The tendency to overestimate or underestimate the modeled variable. | Inspect for a consistent over or underestimate of the modeled variable |

The mathematical expressions for the SRMSE, SPE, and SBIAS are included below in Eq. C-5, Eq. C-6, and Eq. C-7.

$$SRMSE = \sqrt{\frac{\sum_{i=1}^{Np}\left(\frac{Qm_{mod}^{i} - Qm_{at-site}^{i}}{Qm_{at-site}^{i}}\right)}{Np}} \quad \text{[Eq. C-5]}$$

$$SPE = \frac{\sum_{i=1}^{Np} abs\left(\frac{Qm_{mod}^{i} - Qm_{at-site}^{i}}{Qm_{at-site}^{i}}\right)}{Np} * 100 \quad \text{[Eq. C-6]}$$

$$SBIAS = \frac{\sum_{i=1}^{Np}\left(\frac{Qm_{mod}^{i} - Qm_{at-site}^{i}}{Qm_{at-site}^{i}}\right)}{Np} \quad \text{[Eq. C-7]}$$

### C.4.5. Decision Tree

A decision tree model was used to assign hydrologic regions to ungauged catchments. A decision tree was built using the Random Forest classification algorithm. The decision tree model was based on the catchment characteristics at the hydrometric stations in the study area. A total of 500 random samples were pulled from the dataset (with replacement). From each random sample, a decision tree was generated by using 3 variables at each decision point. The hydrologic region assignment was based on majority votes. The out-of-bag (OBB) error rate was 7.2%. The OBB is a method of measuring the prediction error specific to random forest algorithms.

### C.4.6. Statistical Software

The statistical software used by BGC for the analysis was R (R Core Team, 2019). R is a free software environment for statistical computing. The analysis is completed with support from several packages. These packages are listed in Table C-9 for reference.

**Table C-9. Analysis and associated R package.**

| Analysis | R Packages | Authors |
|---|---|---|
| Flood Statistics | Lmom | J. R. M. Hosking |
| Clustering | stats | R Core Team |
| Discordancy, H-Test, Distribution Selection, Parameter Estimation, and Growth Curve Development | lmomRFA | J. R. M. Hosking |
| Index-flood Estimation | stats and leaps | R Core Team and Alan Miller |
| Random Forest decision tree | Rpart, randomForest | Andy Liaw and Matthew Wiener |

## C.5. RESULTS

### C.5.1. Hydrometric Station Selection

A total of 1015 hydrometric stations were included in the analysis. The hydrometric stations were distributed across the study area with a greater concentration in the south compared to the north, largely reflecting population density. There is also a greater concentration of hydrometric stations in the United States than Canada (Figure C-2).

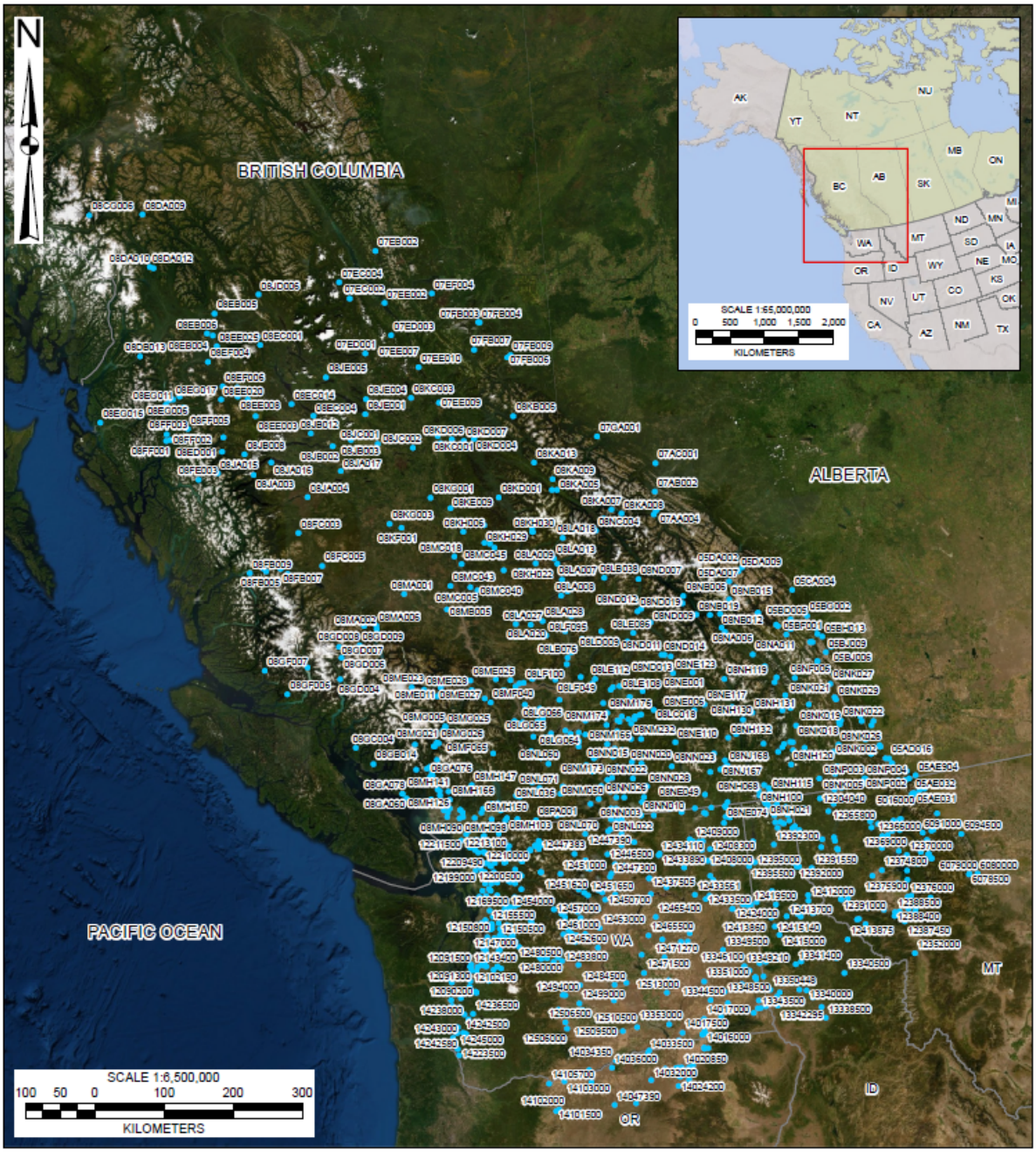


**Figure C-2. Distribution of hydrometric stations within the study area.**

The 18 catchment characteristics and their range in magnitude are summarized over the 1015 hydrometric stations in Table C-10. The climate catchment characteristics show a wide range in magnitude which is not surprising considering the sharp regional contrast imposed by the topography. The urban catchments are concentrated in coastal Washington.

**Table C-10. Summary of catchment characteristics, including the mean, maximum, and minimum values over all hydrometric stations considered for analysis (1,015).**

| Type | No. | Acronym | Mean | Min | Max | Standard Deviation |
|---|---|---|---|---|---|---|
| Catchment | 1 | Centroid_Lat | 49.3092758 | 43.75066 | 57.094597 | 2.3 |
| | 2 | Centroid_Long | -119.5562752 | -130.965466 | -112.917172 | 3.5 |
| | 3 | Centroid_Elev | 1,133 | 18 | 3,046 | 534 |
| | 4 | Area | 7,572 | 1.3 | 601,746 | 38,417 |
| | 5 | Relief | 1,639 | 19 | 4,355 | 791 |
| | 6 | Length | 5 | 0.2 | 71 | 7 |
| | 7 | Slope | 62 | 4 | 350 | 49 |
| Climate | 8 | MAP | 1,299 | 218 | 4,173 | 787 |
| | 9 | MAT | 4.1 | -3.0 | 10.9 | 3.0 |
| | 10 | PAS | 499 | 25 | 2191 | 323 |
| | 11 | PPT_wt | 476 | 71 | 1,683 | 328 |
| | 12 | PPT_sp | 283 | 56 | 955 | 173 |
| | 13 | PPT_sm | 185 | 31 | 522 | 77 |
| | 14 | PPT_fl | 355 | 58 | 1,329 | 249 |
| Physiographic | 15 | Forest | 61 | 0 | 100 | 25 |
| | 16 | Water_Wetland | 1 | 0 | 18 | 2 |
| | 17 | Urban | 2 | 0 | 100 | 12 |
| | 18 | CN | 68 | 55 | 94 | 6 |

### C.5.2. Formation of Hydrological Regions

Based on an interative selection process, the 1,015 hydrometric stations were ultimately organized into 10 clusters. The results of the Elbow Method showed that a selection of approximately 10 hydrological regions explained the most variance in the catchment characteristics (Figure C-3).

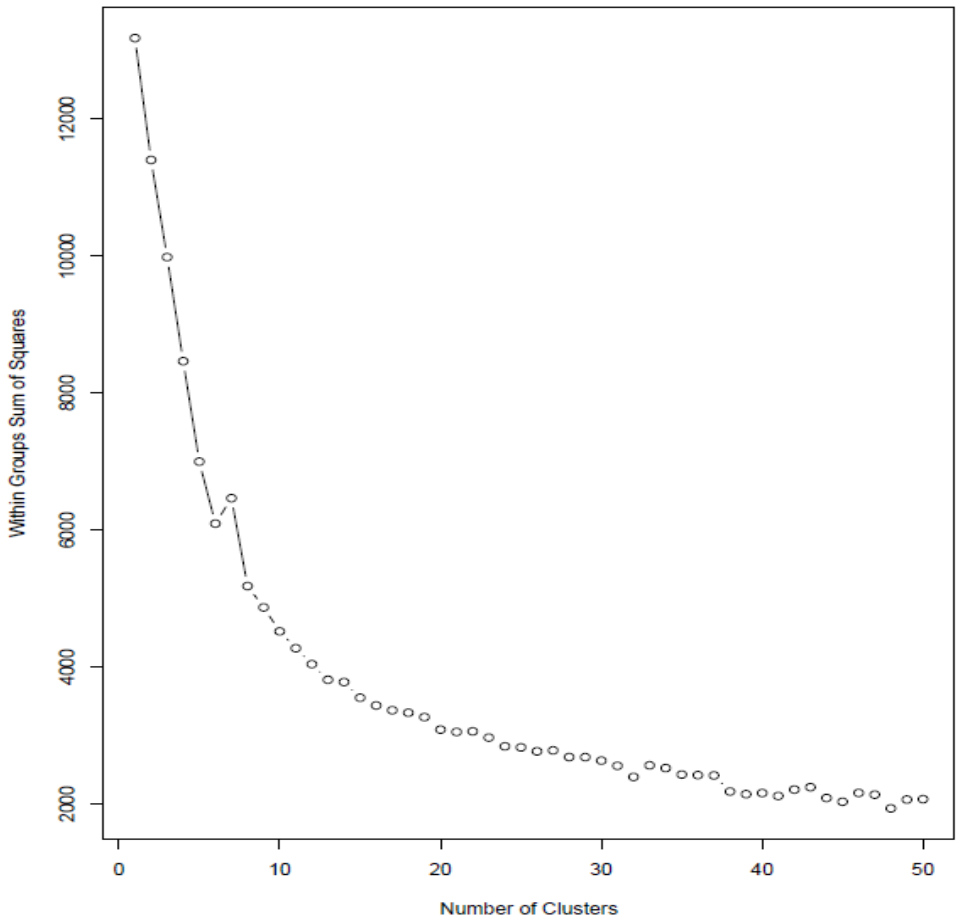


**Figure C-3. The Elbow Plot.**

The Silhouette Scores for the 10 clusters suggested some difficulty in organising the hydrometric stations based on catchment characteristics (Figure C-4). The average Silhouette Score is 0.2, suggesting that the hydrometric stations are poorly assigned to their hydrological regions. A low Silhouette Score is expected however, as it reflects the physical variability across the study area.

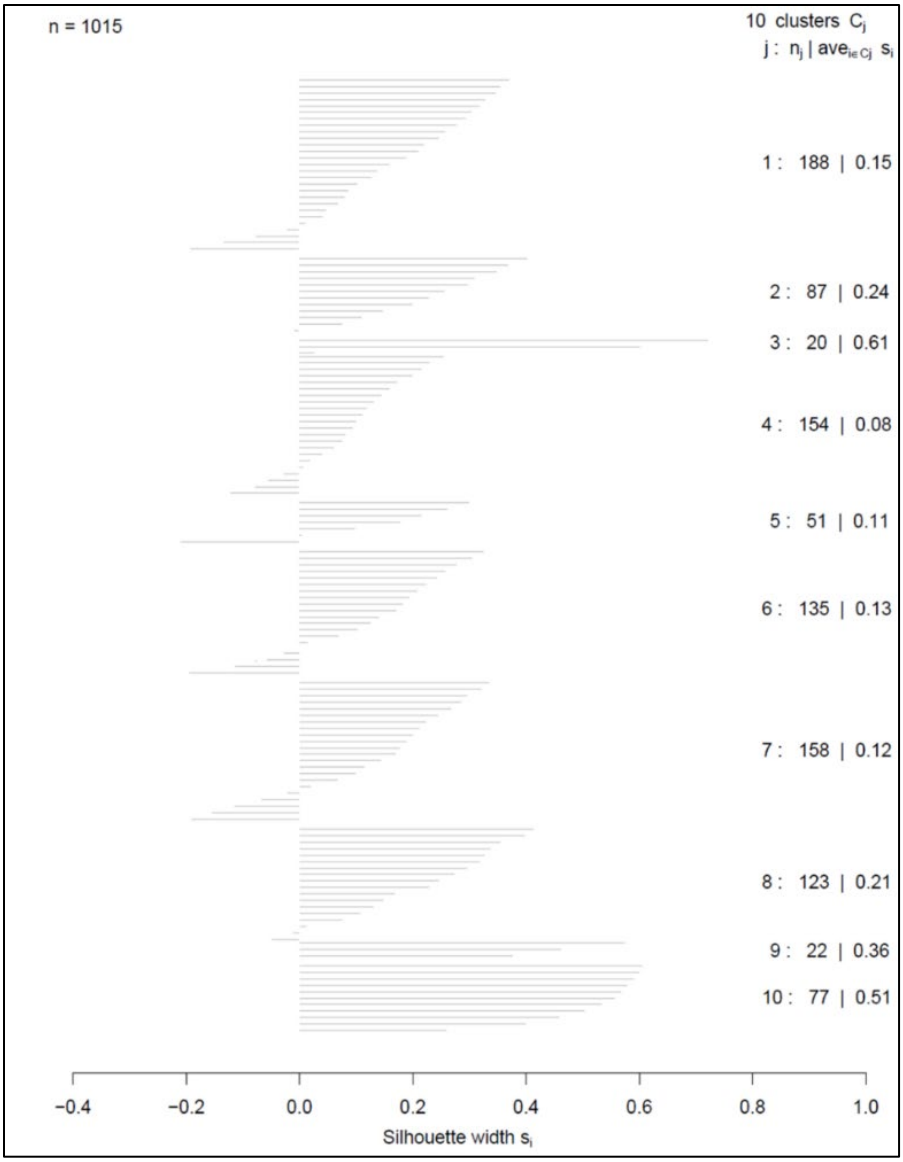


**Figure C-4. Silhouette score.**

The organization of the hydrometric stations into clusters is compiled in a dendrogram (Figure C-5). The y-axis is the dissimilarity index based on the distance metric. The horizontal axis represents the Ward's Distance (d). The green boxes separate the clusters. The 10 clusters are shown along the bottom of the dendrogram. Because we do not know how many clusters there should be in the landscape, the merging process was stopped once the clusters were more dissimilar than a threshold of approximately 90. The threshold was selected to generate a number of clusters consistent with the Elbow Plot.

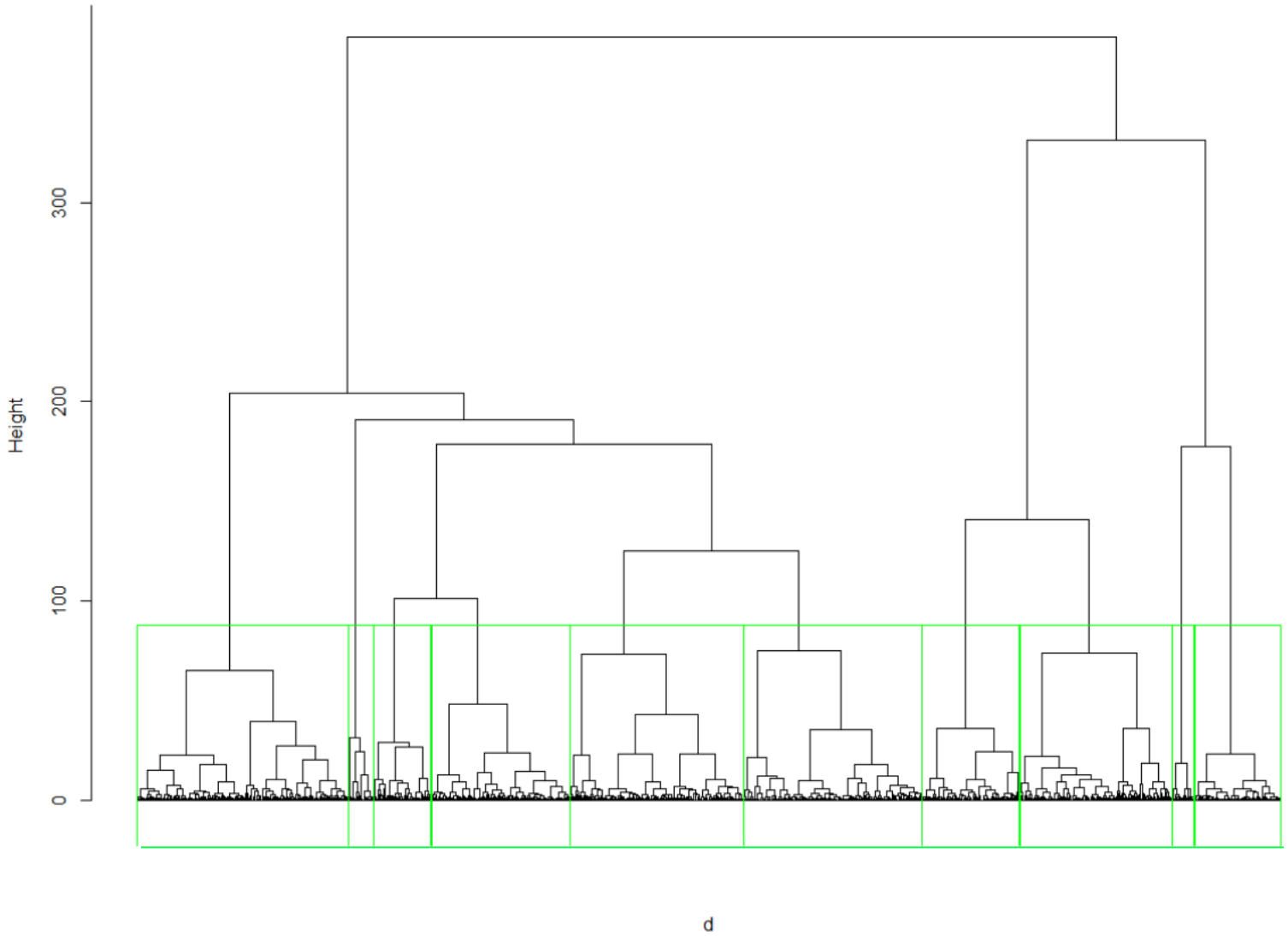


**Figure C-5. Dendrogram.**

### C.5.2.1. Physical Basis of Regions and Flood Characteristics

The spatial distribution of the clusters is considered physically plausible, considering the range in the climate catchment characteristics. Significant regional variations are expected due to the influence of the mountain ranges across the study area (e.g., Coast Mountains, Monashees, the Columbia Trench, and the Rocky Mountains). These orographic effects are expected to control, at least in part, the distribution clusters (Figure C-6).

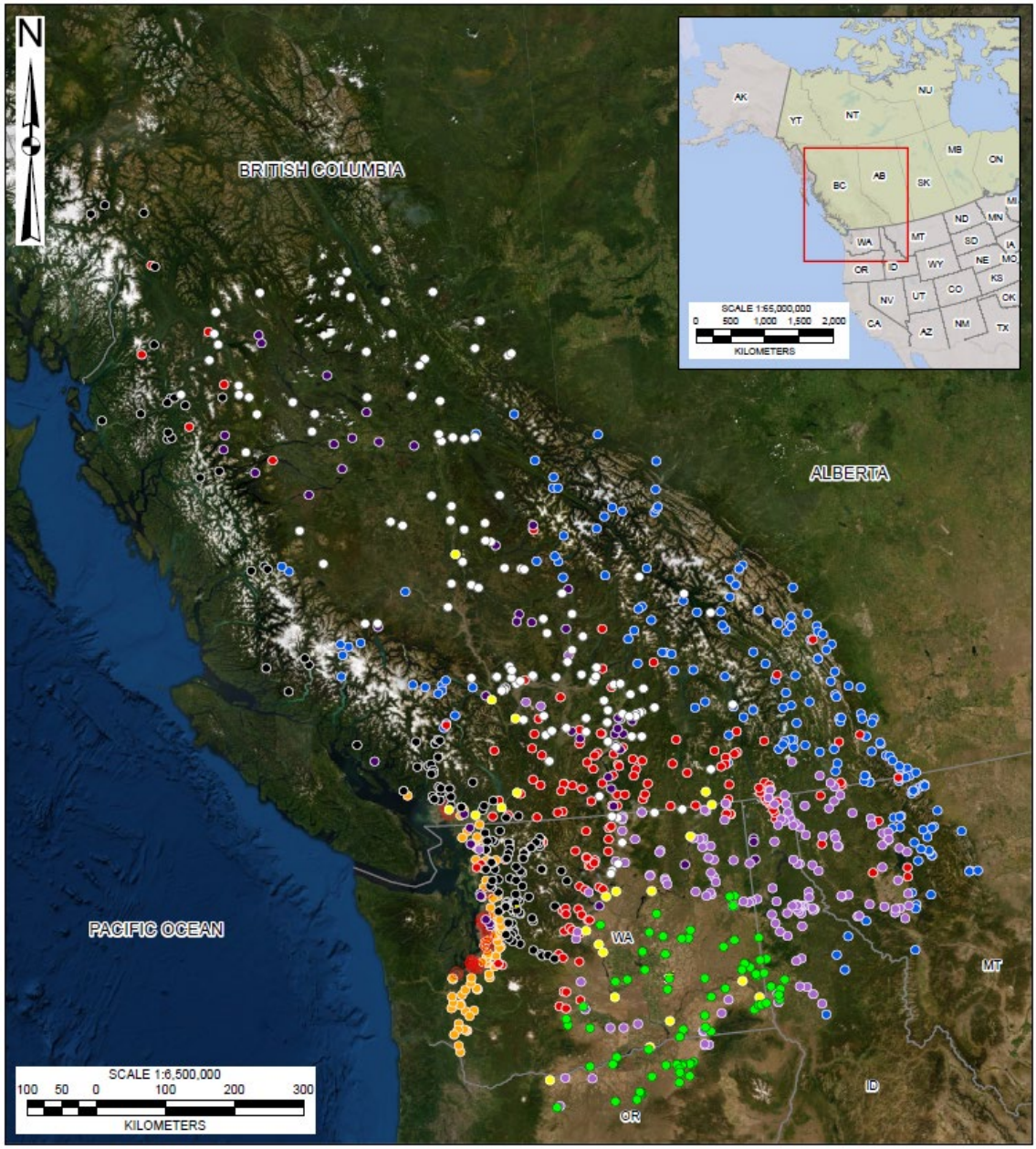


**Figure C-6. Spatial distribution of 10 clusters.**

The clusters that cover the RDCK region include 1 (blue), 4 (red), and 7 (lilac) with 188, 154, and 158 hydrometric stations, respectively. Cluster 1 is defined by the influence of the Rocky Mountains to the east forming the physiographic boundary with Alberta. Most flood events in this cluster are caused by snowmelt or rain-on-snow events in the spring. The eastern range of the Coastal mountains to the west also includes a small group of hydrometric station assigned to Cluster 1. Cluster 4 is defined generally by a climate characteristic of the semi-arid plateau between major mountain ranges. Most flood events are snowmelt dominated in the spring. In this drier climate, evaporation from water surfaces and from the land as well as transpiration from vegetation make up a large component of the regional water balance. Additional hydrometric stations assigned to Cluster 4 are in the montane cordillera to the east where flood events are often associated with rain-on-snow events during the spring freshet. Cluster 7 is defined by the southern edge of the Rocky Mountains in northwestern Montana. Significant floods in this region are caused by runoff from rain associated with moist air masses from the Gulf of Mexico, although most annual peak streamflow events are from snowmelt or rain-on-snow events in the spring.

#### C.5.2.2. Manual Adjustments

The clusters were further separated manually due to the large number of hydrometric stations in each cluster. Cluster 1 was separated into the eastern and western ranges of the Rocky Mountains. The small group of hydrometric stations located along the eastern range of the Coastal Mountains were also separated from Cluster 1. Cluster 4 was separated into the eastern portion in the montane cordillera and the western portion in the semi-arid plateau. Cluster 7 was not separated due to the limited geographic spread of the hydrometric stations. Based on these manual adjustments, Cluster 1 West, 4 East, and 7 cover the RDCK region (Figure C-7).

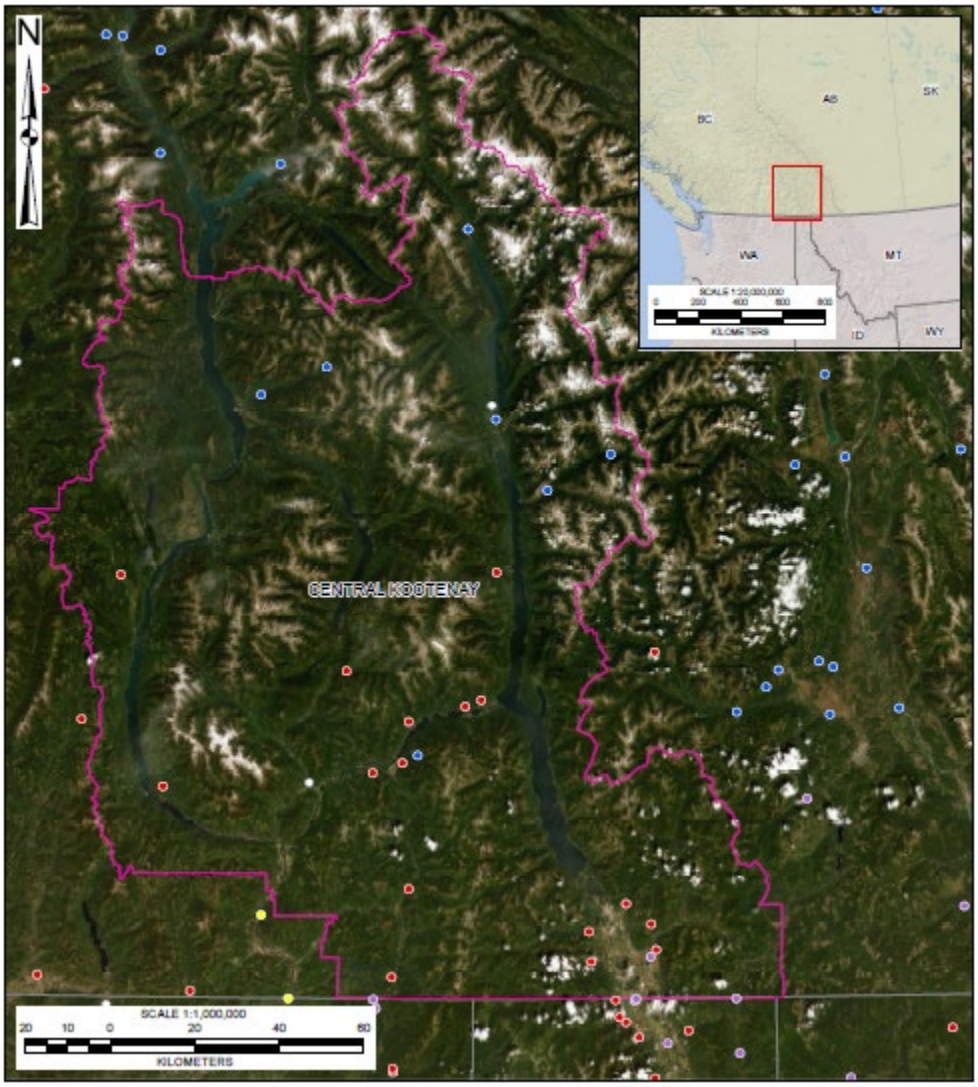


**Figure C-7. Clusters that cover the RDCK region.**

The clusters were further separated based on the scale of catchment area. The coefficient of variation (CV) is required to be constant for a given homogeneous region. A relationship between the catchment area and L-CV is observed in the clusters that cover the RDCK. However, the strength of the relationship varies considerably (Table C-11). In a flood regionalization study in British Columbia, Wang (2000) observed that in L-moment space, the L-CV varied with catchment area for the defined clusters making them heterogeneous. Wang (2000) demonstrated that the small catchments show an increase and the large catchments show a decrease in the L-CV.

**Table C-11. $R^2$ for regression between catchment area and L-CV**

| Cluster | Number of Hydrometric Stations | R2 for regression between catchment area and L-CV |
|---|---|---|
| 1 West | 88 | 0.01 |
| 4 East | 45 | 0.12 |
| 7 | 158 | 0.15 |

To account for the lack of constancy in the L-CV reported by Wang (2000) and observed in the clusters, the range in the catchment area considered in the study was modified to include two groups: 1) less than 500 km$^2$ and 2) more than 500 km$^2$ up to 5,000 km$^2$. The clusters that cover the RDCK region thus include the following which will be the focus of the results herein.

- Cluster 1 West < 500 km$^2$
- Cluster 1 West > 500 km$^2$
- Cluster 4 West < 500 km$^2$
- Cluster 4 West > 500 km$^2$
- Cluster 7 < 500 km$^2$
- Cluster 7 > 500 km$^2$.

### C.5.2.3. Refinement of the Hydrometric Station Selection

The final number of hydrometric stations, including the range of discordancy (*Di*) values, for each hydrologic region is presented in Table C-12. The number of hydrometric stations removed is based on the criteria presented in Section C.4.2.4.

**Table C-12. Final number of hydrometric stations and range in discordancy measure for each hydrologic region.**

| Cluster | Catchment Area Range | Initial Number of Hydrometric Stations | Number of Hydrometric Stations Removed | Final Number of Hydrometric Stations | Di (Min) | Di (Max) | Di (Mean) |
|---|---|---|---|---|---|---|---|
| 1 West | < 500 km$^2$ | 36 | 10 | 26 | 0.13 | 3.0 | 1 |
| | > 500 km$^2$ | 52 | 28 | 24 | 0.09 | 3.0 | 1 |
| 4 East | < 500 km$^2$ | 43 | 9 | 34 | 0.04 | 2.8 | 1 |
| | > 500 km$^2$ | 2 | Not enough data for regionalisation | | | | |
| 7 | < 500 km$^2$ | 75 | 35 | 40 | 0.09 | 2.6 | 1 |
| | > 500 km$^2$ | 83 | 65 | 18 | 0.11 | 2.9 | 1 |

### C.5.2.4. Homogeneity

The H-Test results are summarized in Table C-13. A cluster is declared heterogeneous if H is sufficiently “large”. Hosking and Wallis (1997) recommend a cluster be considered “definitely

heterogeneous" if $H \geq 2$. Increasing the threshold implies that more heterogeneous regions are included in the analysis. Guse, Thieken, Castellarin, & Merz (2010) assessed the effect of the H-Test threshold on the performance of probabilistic regional envelope curves in Germany. Increasing the H-Test threshold from 2 to 4 resulted in a larger number of regions considered for analysis. This increase is important as it can include hydrometric stations that would have been excluded otherwise.

The reality is that while removing hydrometric stations may improve the homogeneity of a region, there may be some important reasons why the H-Test score is high. For example, the site may include a hydrometric station where a very large flood occurred. A representative heterogeneous region is better than a region that has been forced to be homogeneous (Robson and Reed, 1999).

The physical variability of British Columbia was recognized by Wang (2000) where the average value for the H-Test was 6.85 based on 19 clusters. The physiographic regions in BC may be less distinct than other regions. As a result, the threshold for the H-Test was relaxed to what is practical for British Columbia.

**Table C-13. Number of hydrometric stations, Discordancy values, and H-Test results.**

| Hydrologic Region | Catchment Area Range | Number of Hydrometric Stations | H-Test |
|---|---|---|---|
| **1 West** | < 500 km$^2$ | 26 | 6.8 |
| | > 500 km$^2$ | 24 | 9.0 |
| **4 East** | < 500 km$^2$ | 34 | 13.1 |
| | > 500 km$^2$ | 2 | Not enough data |
| **7** | < 500 km$^2$ | 40 | 4.5 |
| | > 500 km$^2$ | 18 | 7.7 |

## C.5.3. Regionalization

### C.5.3.1. Regional Probability Distributions

The regionally averaged L-moments are presented in Table C-14 for hydrologic region 1 West, 4 East, and 7. For the index-flood procedure, $\iota_1$ is set to 1.

**Table C-14. Regionally averaged L-moments.**

| Hydrologic Region | Catchment Area Range | Number of Hydrometric Stations | $\iota_1$ | $\iota_2$ | $t_3$ | $t_4$ |
|---|---|---|---|---|---|---|
| 1 West | < 500 km$^2$ | 26 | 1 | 0.1796 | 0.2519 | 0.1879 |
| | > 500 km$^2$ | 24 | 1 | 0.1756 | 0.2411 | 0.2012 |
| 4 East | < 500 km$^2$ | 34 | 1 | 0.2364 | 0.2245 | 0.1624 |
| 7 | < 500 km$^2$ | 40 | 1 | 0.3014 | 0.2539 | 0.1904 |
| | > 500 km$^2$ | 18 | 1 | 0.2601 | 0.2138 | 0.1924 |

The Z-statistics for a range of candidate probability distributions is presented in Table C-15. The candidate probability distributions include GLO, GEV, GPA, GNO, and PE3. Probability distributions with Z statistics ≤1.64 are deemed acceptable (Hosking & Wallis 1997). All candidate distributions are deemed acceptable for the hydrologic regions that cover the RDCK based on the Z-statistic.

**Table C-15. Goodness of fit Z statistic for probability distribution selection.**

| Hydrological Region | Catchment Area Range | GLO | GEV | GNO | PE3 | GPA |
|---|---|---|---|---|---|---|
| 1 West | < 500 km$^2$ | 1.30 | -0.34 | -1.14 | -2.57 | -4.47 |
| | > 500 km$^2$ | 0.53 | -1.59 | -2.50 | -4.16 | -6.85 |
| 4 East | < 500 km$^2$ | 3.30 | 0.69 | -0.21 | -1.92 | -5.60 |
| 7 | < 500 km$^2$ | 1.41 | -0.59 | -1.59 | -3.38 | -5.66 |
| | > 500 km$^2$ | 0.62 | -1.79 | -2.55 | -4.01 | -7.54 |

To help make the decision on the most representative probability distribution, L-moment diagrams were plotted for each hydrologic region. The $t_3$ and $t_4$ position of the regional average relative to the relationships for five three-parameter (GLO, GEV, GPA, GNP, PE3) and five two-parameter (E, G, L, N, and U) candidate probability distributions are depicted in Figure C-8. The three-parameter probability distributions are depicted by the coloured lines while the two-parameter distributions are depicted by the black squares. The L-skewness and L-kurtosis ratio for each hydrologic region is depicted by the cross symbol on Figure C-8. The GEV probability distribution gives an acceptably close fit to the regional L-moments for the different hydrologic regions. As a result, the GEV probability distribution was deemed representative for all hydrologic regions.

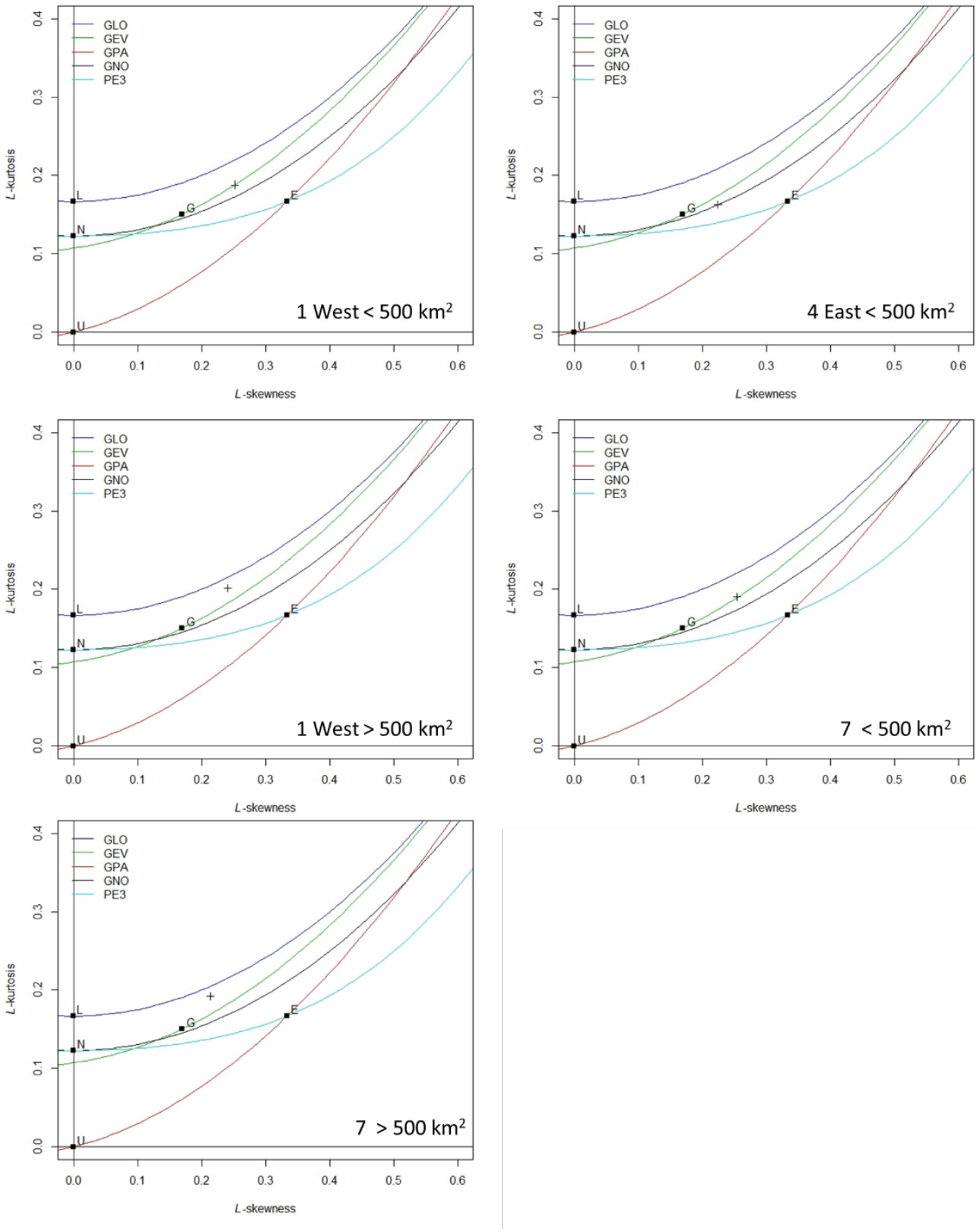


**Figure C-8. L-moment ratio diagram for each hydrologic region.**

### C.5.3.2. Parameter Estimation

The regionally weighted L-moments are used to estimate the parameters of the GEV probability distribution. The parameters for each hydrologic region are presented in Table C-16.

**Table C-16. Parameter estimates for the GEV distribution.**

| Hydrological Region | Catchment Area limit | $\xi$ | $\alpha$ | $\kappa$ |
|---|---|---|---|---|
| 1 West | < 500 km$^2$ | 0.8369 | 0.2280 | -0.1236 |
| | > 500 km$^2$ | 0.8421 | 0.2269 | -0.1078 |
| 4 East | < 500 km$^2$ | 0.7908 | 0.3139 | -0.0832 |
| 7 | < 500 km$^2$ | 0.7257 | 0.3814 | -0.1266 |
| | > 500 km$^2$ | 0.7724 | 0.3513 | -0.0671 |

### C.5.3.3. Growth Curves and Error Bounds

The regional growth curves and error bounds are presented for each region in Figure C-9.

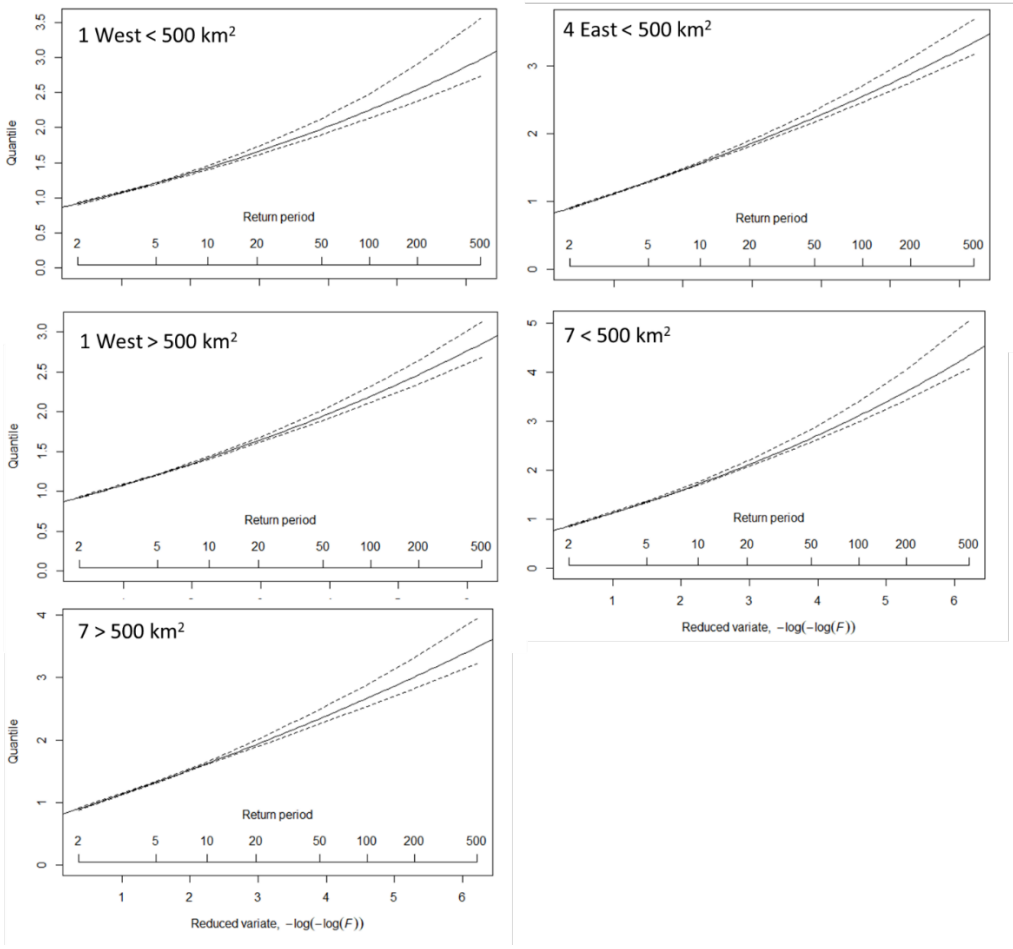


**Figure C-9. Growth curves for each hydrologic region.**

### C.5.3.4. Index Flood

The regional equations for the index-flood for each hydrologic region are presented in Table C-17. The provincial equations are also included at the end of Table C-17. The results are reported to 5 significant figures. However, a total of 5 equations are developed for each hydrologic region and across the province with the intention to average the index-flood estimates. Consequently, the results should be rounded to the nearest unit for flood magnitudes greater than 10 $m^3/s$. The adjusted $R^2$ is included for comparison of the models. Models with more catchment characteristics tend to have a lower adjusted $R^2$ as these models are penalized for increased number of independent variables.

**Table C-17. Regional and provincial equations for the index-flood including the adjusted $R^2$.**

| Hydrologic Region | Catchment Area Range | | Index-flood Equations | Adj. $R^2$ |
|---|---|---|---|---|
| **1 West < 500 km²** | 42 to 454 km² | 1 | $\log Q_m = 10.169 + 1.8553(\log Area) - 0.012434(Slope) + 0.098984\ (Cen\_Long) + 0.0055555(PPT_{fl}) + 0.34911(Water\_Wetland)$ | 0.91 |
| | | 2 | $\log Q_m = 12.127 + 1.9358(\log Area) - 0.013271(Slope) + 0.11264\ (Cen\_Long) - 0.00022260(Cen\_Elev) + 0.0053230(PPT_{fl}) + 0.40695(Water\_Wetland)$ | 0.92 |
| | | 3 | $\log Q_m = 6.951 + 1.8564(\log Area) - 0.011048(Slope) + 0.071361\ (Cen\_Long) + 0.0053236(PPT_{fl})$ | 0.90 |
| | | 4 | $\log Q_m = -0.96349 + 1.7509(\log Area) - 0.0095976(Slope) + 0.0043293(PPT_{fl})$ | 0.89 |
| | | 5 | $\log Q_m = -3.2303 + 2.1932(\log Area) + 0.0015075(MAP)$ | 0.88 |
| **1 West > 500 km²** | 586 to 4312 km² | 1 | $\log Q_m = -2.5781 + 2.0480(\log Area) + 0.0012740\ (MAP)$ | 0.83 |
| | | 2 | $\log Q_m = -2.3716 + 1.8939(\log Area) + 0.41806(\log Catch\_Length) + 0.0012775(MAP)$ | 0.82 |
| | | 3 | $\log Q_m = 1.3411 + 1.9306(\log Area) + 0.18827(\log Catch\_Length) + 0.0011046\ (MAP) - 0.04866(CN)$ | 0.82 |
| | | 4 | $\log Q_m = -0.70946 + 1.6015(\log Area) - 0.0081664(Slope) + 0.0013574\ (MAP) + 0.057906\ (MAT) - 0.0036032(Forest)$ | 0.83 |
| | | 5 | $\log Q_m = 0.40059 + 1.6514(\log Area) - 0.0082135(Slope) + 0.0010135\ (MAP) + 0.15045\ (MAT) - 0.016425(Forest) - 0.19361(Water\_Wetland)$ | 0.88 |

| Hydrologic Region | Catchment Area Range | | Index-flood Equations | Adj. $R^2$ |
|---|---|---|---|---|
| **4 East < 500 km²** | 6 to 441 km² | 1 | $\log Q_m = -3.5763 + 2.7620(\log Area) - 0.15167(MAT) + 0.0035040(PPT_{wt}) - 0.26513(Water\_Wetland)$ | 0.96 |
| | | 2 | $\log Q_m = -4.1636 + 2.7871(\log Area) + 0.0037150(PPT_{wt}) - 0.30562(Water\_Wetland)$ | 0.96 |
| | | 3 | $\log Q_m = -1.8437 + 2.6974(\log Area) + 0.0038(PPT_{wt}) - 0.18063(MAT) + 0.0030438(PPT_{wt}) - 0.28288(Water_{Wetland}) - 0.020392(CN)$ | 0.96 |
| | | 4 | $\log Q_m = -4.0189 + 2.7063(\log Area) + 0.0047397(PPT_{fl}) - 0.3056(Water\_Wetland)$ | 0.95 |
| | | 5 | $\log Q_m = -1.3176 + 2.6880(\log Area) - 0.00069570(MAP) - 0.19022(MAT) + 0.0044279(PPT_{wt})$ | 0.96 |
| **7 < 500 km²** | 8 to 471 km² | 1 | $\log Q_m = -3.8856 + 1.8844(\log Area) + 0.010435(PPT_{fl})$ | 0.74 |
| | | 2 | $\log Q_m = -3.9002 + 1.9484(\log Area) + 0.10058(PPT_{fl}) - 0.17007(Water\_Wetland)$ | 0.74 |
| | | 3 | $\log Q_m = -4.4499 + 2.0486(\log Area) + 0.0051660(PPT_{wt}) + 0.0062765(PPT_{sm}) - 0.21014(Water\_Wetland)$ | 0.74 |
| | | 4 | $\log Q_m = -20.730 + 1.7210(\log Area) + 0.36720(Cen\_Lat) - 0.00093400(Cen_{Elev}) + 0.13920(PPT_{sp}) - 0.30900(Water\_Wetland)$ | 0.75 |
| | | 5 | $\log Q_m = -1.9967 + 2.9199(\log Area) - 0.44581(\log Catch\ Length) + 0.22219(Cen\_Lat) + 0.11838(Cen\_Long) + 0.007305(PPT_{wt}) - 0.32687(Water\_Wetland)$ | 0.75 |

| Hydrologic Region | Catchment Area Range | | Index-flood Equations | Adj. $R^2$ |
|---|---|---|---|---|
| **7 >500 km²** | 529 to 4138 km² | 1 | $\log Q_m = -2.8251 + 2.0765(\log Area) - 0.65058(MAT) - 0.01087(PAS) + 0.15245(PPT_{wt}) + 0.014215(PPT_{sm}) + 0.14232(Forest)$ | 0.93 |
| | | 2 | $\log Q_m = 0.51542 + 1.4852(\log Area) - 0.024121(Slope) - 0.0078710(MAP) - 0.69867(MAT) - 0.010055(PAS)$ | 0.93 |
| | | 3 | $\log Q_m = -0.28887 + 2.1311(\log Area) - 0.00048080(Cen_{Elev}) - 0.59076(MAT) - 0.10256(PAS) + 0.14034(PPT_{wt}) + 0.14291(PPT_{sm}) + 0.018084(Forest)$ | 0.94 |
| | | 4 | $\log Q_m = -12.290 + 4.2860(\log Area) - 4.4640(\log Catch\_Length) + 0.54240(Cen\_Lat) + 0.19690(Cen\_Long) - 0.0066490(PAS) + 0.013790(PPT_{wt}) + 0.38640(Forest)$ | 0.94 |
| | | 5 | $\log Q_m = -6.0632 + 2.1265(\log Area) + 0.0053923(PPT_{wt}) + 0.030556(Forest)$ | 0.90 |
| **Provincial Model** | 1 to 4,888 km² | 1 | $\log Q_m = -10.280 + 2.0840(\log Area) - 0.052950(Cen\_Long) + 0.00078170(PAS) + 0.0045490(PPT_{sp}) - 0.077680(Water\_Wetland) + 0.015770(CN)$ | 0.88 |
| | | 2 | $\log Q_m = -10.990 + 2.0900(\log Area) - 0.054870(Cen\_Long) + 0.00079820(PAS) + 0.0045680(PPT_{sp}) + 0.0022550(Forest) - 0.079050(Water\_Wetland) + 0.020340(CN)$ | 0.88 |
| | | 3 | $\log Q_m = -9.7160 + 2.0890(\log Area) - 0.044870(Cen_{Long}) - 0.00015400(Cen\_Elev) + 0.00095000(PAS) + 0.0043910(PPT_{sp}) + 0.0027010(Forest) - 0.081050(Water\_Wetland) + 0.021030(CN)$ | 0.89 |
| | | 4 | $\log Q_m = -8.3390 + 2.0610(\log Area) - 0.047040(Cen_{Long}) + 0.00070070(PAS) + 0.0043090(PPT_{sp}) + 0.0027010(Forest)$ | 0.88 |
| | | 5 | $\log Q_m = -2.7860 + 2.0520(\log Area) - 0.0023640(PPT_{wt}) + 0.0028430(PPT_{sm}) - 0.063700(Water\_Wetland)$ | 0.88 |

### C.5.4. Error Statistics

The weighted standardized error statistics for the regional and provincial model over a range of flood quantiles for the different hydrologic regions are presented in Table C-18. The error statistics are not consistent across all hydrologic regions. The regional model may be selected for the 4 East < 500 $km^2$ hydrologic region. In the case of the 1 West region, either the regional or provincial model would be considered adequate. Lastly, the regional model is probably the model of choice for the 7 hydrologic region. As expected, the error statistics for the lower flood quantiles are lower than those for higher flood quantiles reflecting the increased uncertainty in higher quantile estimates.

**Table C-18. Weighted standardized error statistics for the regional and provincial models over a range of flood quantiles. Green highlighted cells depict a positive bias while the red highlighted cells depict a negative bias.**

| Error Stats | AEP | 1 West < 500 km² | | 1 West > 500 km² | | 4 East < 500 km² | | 7 < 500 km² | | 7 > 500 km² | |
|---|---|---|---|---|---|---|---|---|---|---|---|
| | | Regional Qm | Provincial Qm | Regional Qm | Provincial Qm | Regional Qm | Provincial Qm | Regional Qm | Provincial Qm | Regional Qm | Provincial Qm |
| SRMSE | 0.5 | 0.24 | 0.31 | 0.27 | 0.26 | 0.39 | 0.92 | 2.71 | 3.80 | 0.19 | 0.99 |
| | 0.1 | 0.28 | 0.31 | 0.26 | 0.28 | 0.33 | 0.69 | 3.08 | 4.10 | 0.21 | 0.96 |
| | 0.02 | 0.40 | 0.41 | 0.31 | 0.33 | 0.38 | 0.64 | 3.70 | 4.80 | 0.27 | 1.01 |
| | 0.005 | 0.54 | 0.53 | 0.38 | 0.39 | 0.45 | 0.66 | 4.37 | 5.59 | 0.36 | 1.09 |
| SPercent Error | 0.5 | 18 | 21 | 20 | 21 | 27 | 59 | 70 | 122 | 15 | 65 |
| | 0.1 | 22 | 24 | 20 | 24 | 22 | 45 | 74 | 128 | 14 | 65 |
| | 0.02 | 31 | 32 | 25 | 29 | 27 | 39 | 84 | 144 | 20 | 68 |
| | 0.005 | 42 | 40 | 30 | 33 | 34 | 38 | 97 | 165 | 29 | 74 |
| SBIAS | 0.5 | 0.03 | -0.08 | 0.04 | -0.09 | 0.07 | 0.30 | 0.39 | 1.03 | 0.03 | 0.39 |
| | 0.1 | 0.06 | -0.06 | 0.04 | -0.07 | 0.07 | 0.23 | 0.44 | 1.08 | 0.03 | 0.39 |
| | 0.02 | 0.09 | -0.03 | 0.06 | -0.06 | 0.08 | 0.20 | 0.52 | 1.21 | 0.04 | 0.42 |
| | 0.005 | 0.13 | 0.02 | 0.08 | -0.03 | 0.10 | 0.20 | 0.62 | 1.37 | 0.06 | 0.45 |

## C.6. APPLICATION TO UNGAUGED CATCHMENTS

The goal of the regionalization of floods is to estimate quantiles for ungauged catchments in the RDCK. A total of 12 catchments are modeled for clearwater floods. To begin, a catchment polygon was defined for each ungauged catchment, as shown in Figure C-10. The suite of 18 catchment characteristics were then extracted and averaged over the area for each ungauged catchment. The resulting catchment characteristics are presented in Table C-19.

The ungauged catchments were subsequently assigned to one of the hydrologic regions identified across the study area. The hydrologic region assignment was completed using the Random Forest classification algorithm. Once a hydrologic region was assigned to the ungauged catchment; the index-flood was estimated based on the appropriate model (regional and / or provincial). The flood quantiles were then estimated for a range of AEPs using the index-flood estimate and the appropriate regional growth curve. The hydrologic region assignment, index-flood estimate, and flood quantiles for each ungauged catchment are presented in Table C-20.

The magnitude of the flood quantiles is influenced by the catchment characteristics. This is because the index-flood is calculated using a multiple linear regression that depends on the catchment characteristics that define the best 5 models for a given region. Two catchments of similar area may have significantly different flood quantile estimates because of major differences in catchment characteristics. For example, Lost Creek and Porcupine Creek share comparable catchment areas of 62 $km^2$ and 68 $km^2$, respectively. However, flood quantiles for Porcupine Creek are 35% greater than Lost Creek, with the difference in magnitude attributed to difference in climate characteristics.

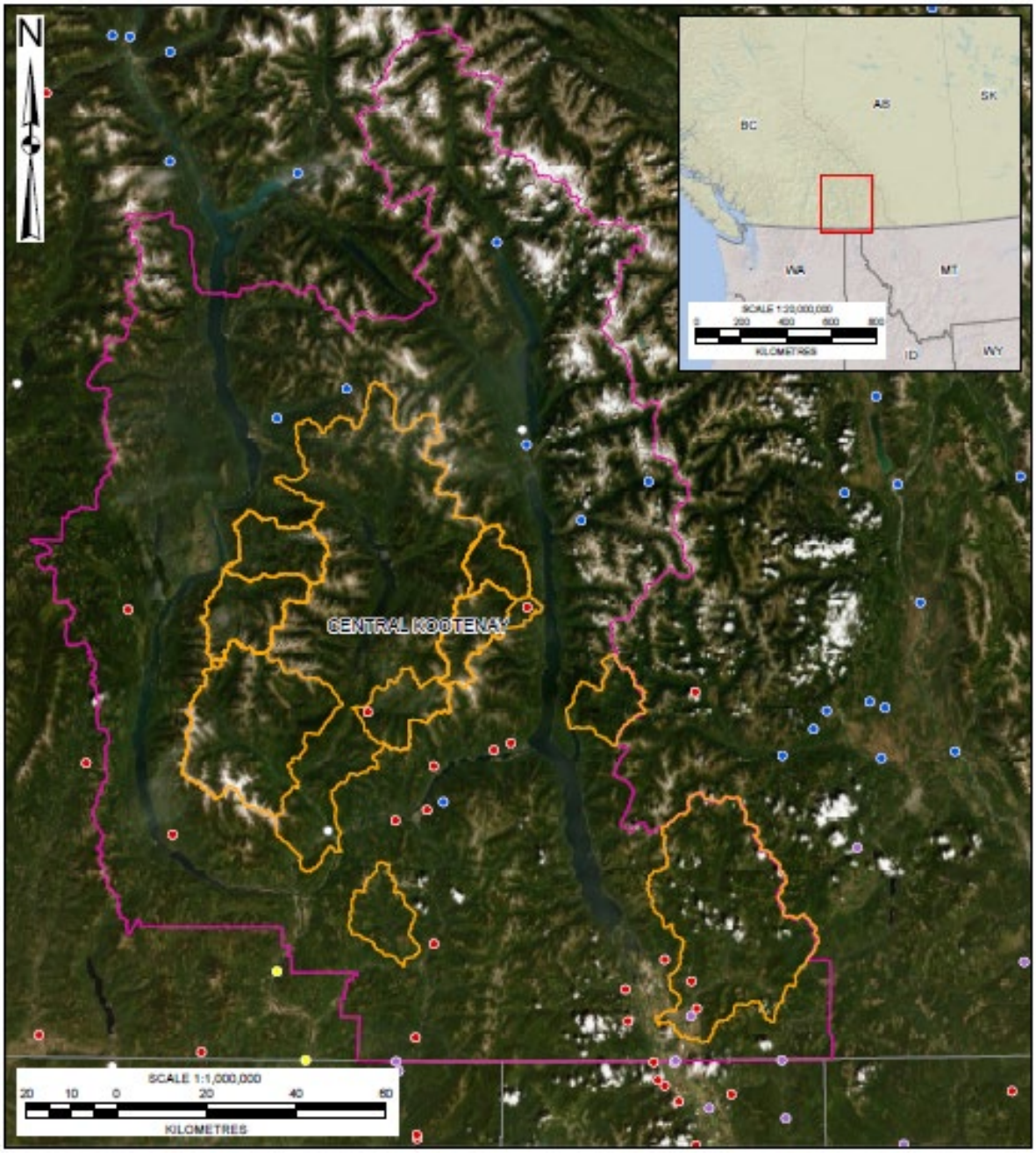


**Figure C-10. Catchment polygons for the ungauged catchments.**

**Table C-19. Catchment characteristics for the clearwater sites located in the RDCK region.**

| Catchment Name | Area ($km^2$) | Relief (m) | Catchment Length (km) | Slope (%) | Centroid Latitude (degrees) | Centroid Longitude (degrees) | Centroid Elevation (m) | MAP (mm) | MAT (ºC) | PAS (mm) | PPT_wt (mm) | PPT_sp (mm) | PPT_sm (mm) | PPT_fl (mm) | Forest (%) | Water and Wetland (%) | Urban (%) | CN |
|---|---|---|---|---|---|---|---|---|---|---|---|---|---|---|---|---|---|---|
| Crawford Creek | 186 | 2092 | 2.53 | 83 | 49.693818 | -116.700089 | 1181 | 1116 | 3.0 | 590 | 383 | 233 | 198 | 302 | 88 | 0.0 | 0.2 | 70 |
| Keen Creek | 202 | 2066 | 2.37 | 87 | 49.861962 | -117.119617 | 1584 | 1390 | 1.3 | 857 | 460 | 307 | 240 | 384 | 66 | 0.2 | 7.7 | 67 |
| Upper Kaslo Creek | 150 | 1927 | 2.35 | 82 | 49.990505 | -117.046683 | 1182 | 1244 | 2.7 | 668 | 416 | 265 | 223 | 340 | 90 | 0.0 | 0.8 | 70 |
| Kalso Creek at Kootenay Lake | 386 | 2228 | 3.09 | 72 | 49.914818 | -117.077853 | 1280 | 1312 | 2.1 | 756 | 438 | 284 | 230 | 360 | 78 | 0.2 | 4.3 | 68 |
| Lemon Creek | 206 | 2046 | 2.58 | 79 | 49.717145 | -117.338618 | 1956 | 1322 | 2.7 | 754 | 461 | 284 | 206 | 370 | 90 | 0.1 | 0.7 | 65 |
| Burton at Arrow Lake | 530 | 2323 | 4.13 | 56 | 49.952644 | -117.773748 | 1300 | 1242 | 2.4 | 704 | 4280 | 258 | 220 | 336 | 85 | 0.3 | 1.2 | 64 |
| Caribou Creek | 238 | 2235 | 2.97 | 75 | 50.019565 | -117.726695 | 1213 | 1260 | 2.4 | 709 | 432 | 261 | 226 | 341 | 92 | 0.1 | 0.3 | 67 |
| Snow Creek | 291 | 2314 | 3.05 | 76 | 49.897831 | -117.811685 | 1742 | 1227 | 2.3 | 700 | 425 | 255 | 216 | 331 | 80 | 0.3 | 1.8 | 63 |
| Little Slocan River | 818 | 2281 | 5.40 | 42 | 49.664986 | -117.79715 | 1612 | 1161 | 2.8 | 643 | 416 | 245 | 188 | 313 | 82 | 0.5 | 1.7 | 63 |
| Slocan River | 3475 | 2544 | 8.13 | 31 | 49.85497 | -117.525816 | 1196 | 1224 | 3.0 | 666 | 431 | 256 | 206 | 332 | 81 | 2.9 | 2.1 | 66 |
| Goat River | 1259 | 2111 | 6.01 | 35 | 49.28428 | -116.347233 | 1050 | 857 | 3.2 | 433 | 284 | 194 | 163 | 217 | 88 | 0.1 | 0.2 | 69 |
| Erie Creek Upstream End | 201 | 1575 | 2.71 | 58 | 49.288665 | -117.392234 | 1010 | 1265 | 3.8 | 617 | 435 | 286 | 210 | 333 | 95 | 0.0 | 0.0 | 62 |

**Table C-20. Hydrologic region assignment for the ungauged catchments.**

| Catchment Name | Hydrometric Station | Catchment Area ($km^2$) | Hydrologic Region[1] | Qm ($m^3/s$) | Flood Quantiles | | |
|---|---|---|---|---|---|---|---|
| | | | | | 0.05 AEP ($m^3/s$) | 0.02 AEP ($m^3/s$) | 0.005 AEP ($m^3/s$) |
| Crawford Creek | - | 186 | 7 | 27 | 50 | 61 | 80 |
| Keen Creek | 08NH132 | 202 | pro-rated | - | 78 | 94 | 125 |
| Upper Kaslo Creek | 08NH005 | 150 | pro-rated | - | 99 | 120 | 160 |
| Kaslo Creek at Kootenay Lake | 08NH005 | 386 | pro-rated | - | 160 | 200 | 260 |
| Lemon Creek | 08NJ160 | 206 | pro-rated | - | 72 | 84 | 105 |
| Burton at Arrow Lake | - | 530 | 4 | 80 | 150 | 180 | 230 |
| Caribou Creek | - | 238 | 4 | 42 | 78 | 94 | 120 |
| Snow Creek | - | 291 | 4 | 45 | 83 | 100 | 130 |
| Little Slocan River | | 818 | 4 | 103 | 190 | 230 | 290 |
| Slocan River | 08NJ013 | 3475 | pro-rated | - | 685 | 770 | 880 |
| Goat River | 8NH004 | 1259 | 7 | - | 387 | 430 | 500 |
| Erie Upstream End | - | 201 | 4 | 35 | 65 | 79 | 102 |

Note:

1. A pro-rated calculation is completed when a representative hydrometric station is located upstream or downstream from the ungauged site and has a record length considered long enough for reliable frequency analysis. Flood quantile estimates calculated at the hydrometric station are transferred to the ungauged site by relating the annual maximum peak instantaneous streamflow at the hydrometric station to the ungauged site using catchment area size.

## C.7. UNCERTAINTY

The process of flood regionalization is inherently uncertain because of the several limitations. The probability distribution of flood events is unknown. While there are statistical tools to help reach a ‘best estimate’, it is not possible to know what the probability distribution is in practice. As a result, the flood quantile estimates are supported by a mathematical model that is considered reliable based on the available flood data.

The regionalisation of floods tends to underestimate peak flows for small catchments and overestimate peak flows for larger catchments. This is in part due to differences in hydrological processes that control peak flows. For example, maximum annual peak instantaneous flows in small catchments within the study area are more likely controlled by rainfall compared to larger catchment that tend to be more snowmelt-dominated in the spring. The rainfall control in small catchments reflects the greater likelihood that a rainfall event, like a convective storm, covers the entire catchment area. In the case for larger catchments, it is more likely for snowmelt to occur across the entire area in the spring.

While hydrometric stations with catchment areas starting from approximately 6 $km^2$ up to 5,000 $km^2$ are included in the analysis, it is not likely that the equations apply to catchments if they are either too small or too large. The regional models are only reliable if applied within the range of catchment areas used to build the models in the first place. Extrapolation beyond the limit of the model may yield poor or unreliable results.

The regional models are as reliable as the data that is used to support them. There is inherent measurement error in flood events, especially for larger flood events. Furthermore, the data record may simply be incorrect due to a transcription error. In addition, the measuring device may have been moved to a new location or trends over time may come about from changes in the monitoring device. It is not possible to inspect every record at every hydrometric station to control for these sources of error because so much data are pooled across such a large area.

The same applies to the catchment polygon delineation. Much of the catchment delineation was automated using tools that were developed to speed up this process (RNT and ESRI tools). Manual spot checks were completed in conjunction with quality control of the area by means of comparison with published values. Nevertheless, it was not possible to inspect every catchment polygon to control for delineation errors due to the high number of polygons that were generated for this study. It is expected that these sources of error are negligible next to the quantity of data that is processed across the study area.

Trends in the flood record imposed by climate change, land use change, wildfires, insect infestations, or urban development generally precludes the use of frequency analysis. Trend analyses were completed on the flood record to account for some level of trend. However, the flood record often captures a small window of the flood history at a given location. The limited record makes it difficult to identify a real trend from an artifact of the data record. Therefore, no hydrometric stations were discarded from the analysis due to the presence of a trend in the flood record.

# REFERENCES

Coles, S. (2001). *An Introduction to Statistical Modeling of Extreme Values*. Springer Verlag London Limited. 208 p.

Dalrymple, T. (1960). *Flood Frequency Analysis*. US Geological Survey. Water Supply Paper, 1543 A.

Farr, T.G., et al. (2007), The Shuttle Radar Topography Mission. *Reviews of Geophysics, 45*, RG2004, https://doi.org/10.1029/2005RG000183.

Greenwood, J.A., Lanswehr, J.M., Matalas, N.C., & Wallis, J.R. (1979). Probability weighted moments: Definition and relation to parameters of several distributions expressible in reserve form. *Water Resources Research, 15*, 1049-54.

Guse, B., Thieken, A.H., Castellarin, A., & Merz, B. (2010). Deriving probabilistic regional envelope curves with two pooling methods. *Journal of Hydrology, 380(1-2)*, 14-26. https://doi.org/10.1016/j.jhydrol.2009.10.010

Hosking, J.R.M. (1990). L-moments: Analysis and estimation of distributions using linear combinations of order statistics. *Journal of the Royal Statistical Society, Series B, 52*, 105-24.

Hosking, J.R.M. & Wallis, J.R. (1993). Some statistics useful in regional frequency analysis. *Water Resources Research*, 29, 271-81.

Hosking, J.R.M. & Wallis, J.R. (1997) *Regional Frequency Analysis: An Approach Based on L-moments*. Cambridge University Press, UK. http://dx.doi.org/10.1017/cbo9780511529443

Ouarda, T.B.M.J., St-Hilaire, A., & Bobée, B. (2008). Synthèse des développements récents en analyse régionale des extrêmes hydrologiques. *Journal of Water Sciences, 21*, 219–232. https://doi.org/10.7202/018467ar.

R Core Team. (2019). R: A language and environment for statistical computing. R Foundation for Statistical Computing, Vienna, Austria. https://www.R-project.org/.

Robson, A.J. & Reed, D.J. (1999). Statistical Procedures for Flood Frequency Estimation. Flood Estimation Handbook, vol. 3. Institute of Hydrology, Wallingford, UK.

Ross, C.W., Prihodko, L., Anchang, J., Kumar, S., Ji, W., & Hanan, N.P. (2018). HYSOGs250m, global gridded hydrologic soil groups for curve-number-based runoff modeling. ORNL Distributed Active Archive Center. https://doi.org/10.3334/ORNLDAAC/1566.

rvic, R., Homer, C., Ressl, R., Pouliot, D. Hossain, S.N., Colditz, R.R., Olthof, I., Giri, C., & Victoria, A. (2012). North American Land Change Monitoring System. In C. Giri (Ed) *Remote Sensing of Land and Land Cover: Principles and Applications* (p. 303-324). CRC Press.

Tasker, G.D. (1980). Hydrologic regression and weighted least squares. *Water Resources Research, 16(6)*, 1107–1113.

Tasker, G.D. (1982). Comparing methods of hydrologic regionalization. *Water Resources Bulletin, 18*(6), 965-970.

United States Geological Survey (USGS). (1986). *Urban hydrology for small watersheds*. Technical report 55.

Wang, Y. (2000). Development of methods for regional flood estimates in the province of British Columbia (Doctoral dissertation). Retrieved from University of British Columbia. 200 pp.

Wang, T., Hamann, A., Spittlehouse, D., & Carroll, C. (2016). Locally Downscaled and Spatially Customizable Climate Data for Historical and Future Periods for North America. *PLoS ONE 11(6)*: e0156720. https://doi.org/10.1371/journal.pone.0156720

Ward, J.H., Jr. (1963). Hierarchical Grouping to Optimize an Objective Function. *Journal of the American Statistical Association, 58*, 236–244.

# APPENDIX D
# CLIMATE CHANGE IMPACTS ON HYDROLOGY

## D.1. INTRODUCTION

The hydroclimate of British Columbia (BC) is complex because of proximity to the Pacific Ocean, mountainous terrain, and extent in latitude. The hydrologic regime is either freshet-dominated (nival regime) or snow-influenced (hybrid nival-pluvial or nival-glacial regimes) throughout most of BC (Eaton & Moore, 2010). Hydrologic trends over recent decades generally include a warming and decreasing snowpack (Kang, Shi, Gao, & Déry, 2014) and earlier onset of spring melt (Déry et al., 2009). The hydrologic response to climate change in BC is expected to be influenced by the regional variability in projected temperature and precipitation changes and by regional variations in physical geography. For example, snow dynamics are strongly influenced by elevation-based temperature gradients resulting in large spatial variations in regions of diverse topography (Schnorbus, Werner, & Bennett, 2014). Also, warmer hybrid nival-pluvial regimes may be more sensitive to changes in regional temperature, precipitation, and rainfall trends (Whitfield, Cannon, & Reynolds, 2002).

Climate change impacts were assessed by BGC for the clearwater watersheds using statistically- and process-based methods. This appendix presents a description of these methodologies and their results. This appendix begins with a description of the anticipated climate change impacts on the hydroclimate within the RDCK (Section D.2). The climate change sensitivity of clearwater watersheds within the region is examined in Section D.3. Finally, an evaluation of the climate change impacts using statistically- and process-based methods for the clearwater watersheds is presented in Section D.4. This appendix ends with a summary of the method that was used to account for the climate change impacts on the hydrology of clearwater watersheds in the RDCK region.

## D.2. CLIMATE CHANGE IMPACTS

### D.2.1. Hydroclimate

Historical changes to climate have been documented in BC (Barnett et al., 2008). While there is a natural variability component to the changes in climate, such as El Niño Southern Oscillation (ENSO) and the Pacific Decadal Oscillation (PDO), historical trends in western North America have been attributed to climate change in the form of increased regional warming (Barnett et al., 2008).

Climate change is projected to impact the overall mean as well as the extremes for a range of climate variables including temperature, precipitation, snow, and rainfall intensities. Projected change in mean annual precipitation (MAP), temperature (MAT), and precipitation as snow (PAS) from historical conditions (1961 to 1990) for clearwater watersheds across the RDCK region for 2050 (average of years 2041 to 2070) are presented in Table D-1.

The climate-adjusted variables are calculated using projections based on the Representative Carbon Pathway (RCP) 8.5 which are averaged across 15 fifth phase Coupled Model Intercomparison project (CMIP5) models (CanESM2, ACCESS1.0, IPSL-CM5A-MR,MIROC5,

MPI-ESM-LR, CCSM4, HadGEM2-ES, CNRM-CM5, CSIRO Mk 3.6, GFDL-CM3, INM-CM4, MRI-CGCM3, MIROC-ESM, CESM1-CAM5, GISS-E2R) that were chosen to represent all major clusters of similar atmosphere-ocean general circulation models (AOGCMs) (Knutti, Massin, & Gettleman, 2013), and that had high validation statistics in their CMIP3 equivalents.

**Table D-1. Projected change (RCP 8.5, 2050) from 1961 to 1990 historical conditions (Wang et al., 2016).**

| Watershed | Change in MAP (mm) | Change in MAT (ºC) | Change in PAS (Snow Water Equivalent, mm) |
|---|---|---|---|
| Crawford Creek | 59 | 3.5 | -206 |
| Keen Creek | 82 | 3.6 | -239 |
| Upper Kaslo Creek | 72 | 3.6 | -231 |
| Kalso Creek at Kootenay Lake | 76 | 3.6 | -233 |
| Lemon Creek | 82 | 3.5 | -252 |
| Burton at Arrow Lake | 73 | 3.5 | -221 |
| Caribou Creek | 75 | 3.5 | -225 |
| Snow Creek | 72 | 3.6 | -217 |
| Little Slocan River | 69 | 3.5 | -215 |
| Slocan River | 74 | 3.5 | -220 |
| Goat River | 40 | 3.5 | -151 |
| Erie Creek Upstream End | 69 | 3.6 | -247 |

Projected changes in average climate variables across the RDCK by 2050 show that there is likely to be:

- A net increase in MAP ranging from 40 mm to 82 mm
- A net increase in MAT ranging from 3.5 ºC to 3.6 ºC
- A net decrease in PAS ranging from 151 mm to 252 mm.

In addition, short-term precipitation extremes (sub-daily) are expected to increase in most of North America with a warming atmosphere. The frequency of extremes increases 5-fold in large parts of Canada in December, January, and February (Figure D-1a). The frequency of extremes decreases to approximately a 2-fold increase in southeast BC in June, July, and August (Figure D-1b). This shift in frequency covers the period January 2001 to September 2013. The increase is due to a shift towards moister and warmer climatic conditions (Prein et al., 2017). Extremes in short-term precipitation contributes to the frequency and magnitude of flood events, especially for small watersheds where soil storage is either low or full (i.e., < 250 $km^2$).

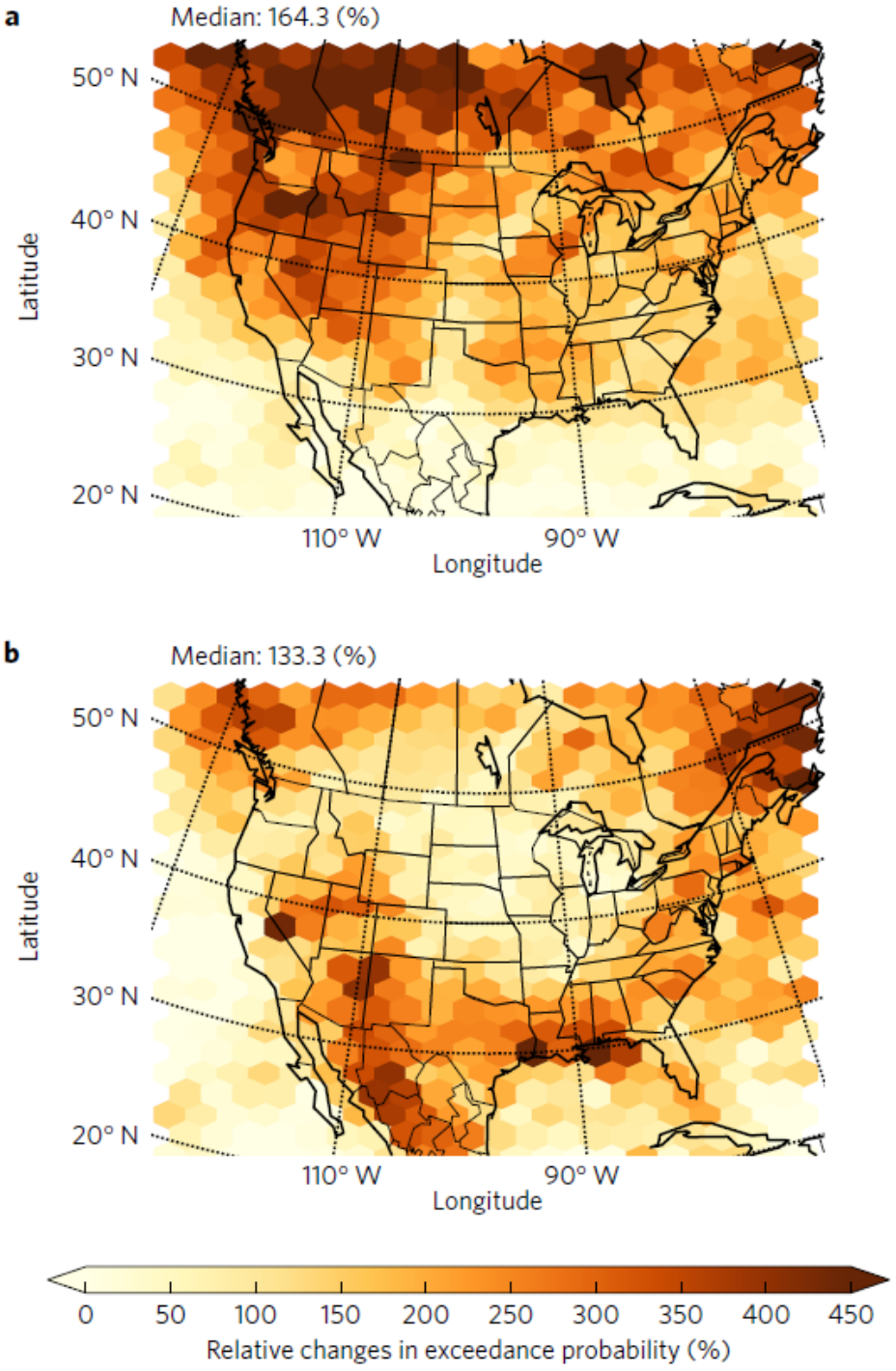


**Figure D-1. Change in the exceedance probability of hourly precipitation intensities for (a) December, January, and February, and (b) June, July, and August (Prein et al., 2017).**

### D.2.2. Peak discharges

The RDCK is situated within the Montane Cordillera ecozone which covers most of southern BC. Extreme flood events in this area are often associated with rain-on-snow events in the spring (Harder et al., 2015). A hydrograph example where the regime is freshet-dominated is shown in Figure D-2. Although the effects of climate change on precipitation are not clear, projected increases in temperature are expected to have the largest impact on annual minimum temperatures occurring in the winter months (Harder et al., 2015).

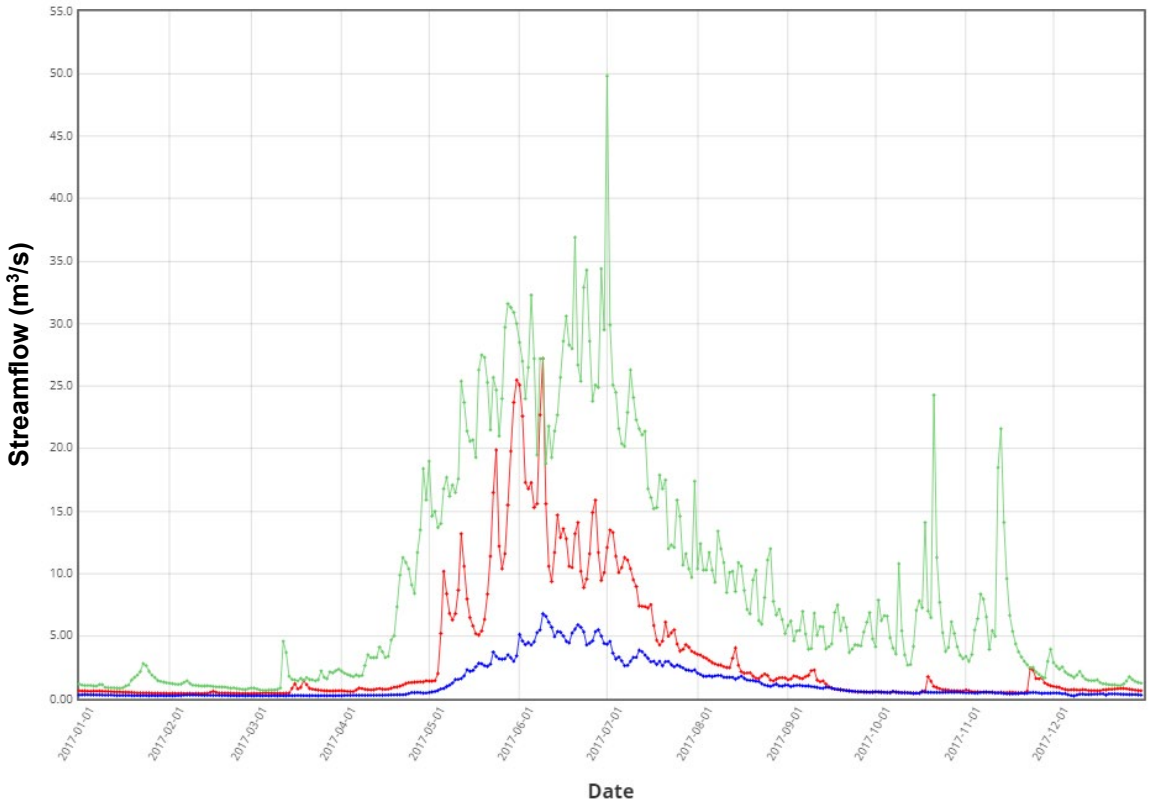


**Figure D-2. Example freshet-driven hydrologic regime for Keen Creek below Kyawats Creek (08NH132). Green line is the maximum streamflow, the blue line is the minimum streamflow, and the red line is the 2017 streamflow.**

The effects of temperature change differ throughout the region. High elevation regions throughout parts of the Montane Cordillera (e.g., Upper Columbia watershed) are projected to experience increases in snowpack, limiting the response in high elevation watersheds while lower elevations are projected to experience a decrease in snow water equivalent (Loukas & Quick, 1999; Schnorbus et al., 2014).

Projected changes in streamflow vary spatially and seasonally based on snow and precipitation changes and topography-based temperature gradients. Researchers anticipate that streamflow will increase in the winter and spring in the RDCK due to earlier snowmelt and more frequent rain-on-snow events, while earlier peak flow timing is expected in many rivers (Schnorbus et al., 2014; Farjad, Gupta, & Marceau, 2016).

## D.3. WATERSHED SENSITIVITY

The RDCK includes 6 detailed clearwater study areas (Crawford Creek, Kaslo Creek, Slocan River, Burton Creek, Goat River, and Salmo River). Each study area includes one or more clearwater watersheds that were assessed to inform the floodplain delineation. All clearwater watersheds in the RDCK are characterized by a freshet-dominated regime. Freshet-dominant regimes are characterized by a maximum annual streamflow in the spring

In a warmer climate, hydrologic regime shifts are likely to intensify although regional responses are expected due to each watershed's unique characteristics like elevation range and proximity to the 0$^{o}$C air temperature threshold during the cold season. The largest changes in the timing of peak floods would be expected for those areas with a hydrologic regime that shifts from a freshet-dominated to rainfall dominated regime. Therefore, those watersheds with the thinnest snowpacks would be the most sensitive.

The RDCK can be sub-divided into five regions, each with a relatively different, typical snowpack depth (Figure D-3). Two of those five regions cover the clearwater watersheds. The typical snow depths for the clearwater watersheds ranges from moderate snowpack at high elevations for Goat River and Crawford Creek to moderate to deep snowpack for the remaining sites (Table D-2). The elevation range for each clearwater watershed is included in Table D-2 for reference. The clearwater watershed with largest projected change in precipitation as snow by 2050 is Lemon Creek (decrease of 252 mm) followed by Erie Creek Upstream End (decrease of 247 mm) and Keen Creek (decrease of 239 mm) as listed in Table D-1. Hydrographs based on representative hydrometric stations for each study area are presented at the end of the appendix for reference (Figure D-8 to Figure D-11).

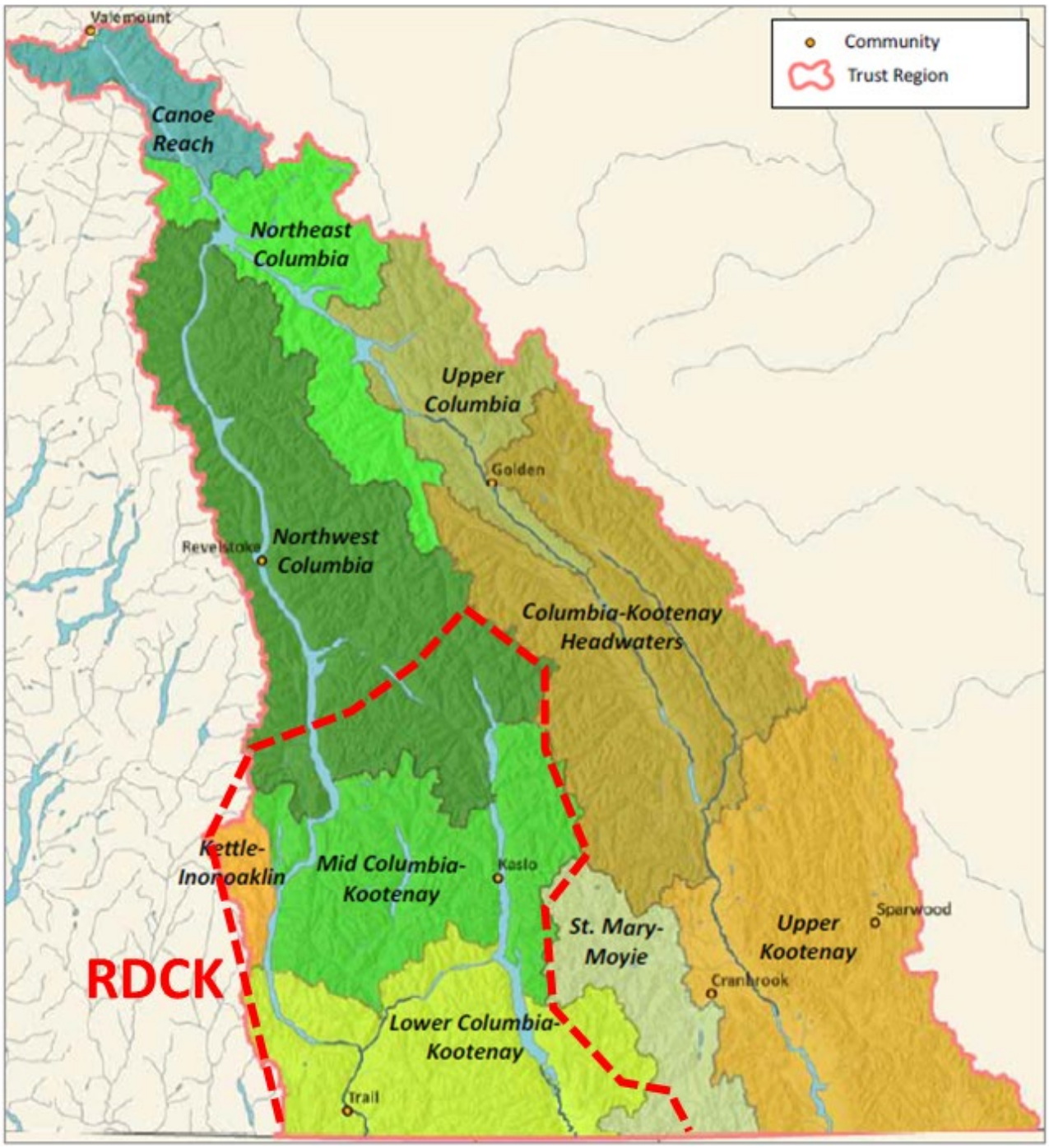


**Figure D-3. Regions of the Columbia Basin as defined by patterns of climate and surface runoff. The RDCK contains 5 of these regions, 2 of which cover the clearwater watersheds (CBT, 2017)**

**Table D-2. Regions of the Columbia Basin covering the RDCK and their current relative snowpack depth (CBT, 2017).**

| Region | Existing Relative Snowpack Depth | Study Area | Representative Hydrometric Station | Clearwater Watersheds | Elevation Range (m) |
|---|---|---|---|---|---|
| Lower Columbia-Kootenay | Moderate snowpack at higher elevations | Goat River | 08NH004 | Goat River | 532 to 2622 |
| | | Salmo River | 08NE074 | Erie Creek Upstream End | 712 to 2287 |
| Mid Columbia-Kootenay | Moderate to deep snowpack | Crawford Creek | ungauged watershed | Crawford Creek | 530 to 2627 |
| | | Kaslo Creek | 08NH005 | Keen Creek | 704 to 2797 |
| | | | | Upper Kaslo Creek | 699 to 2670 |
| | | | | Kalso Creek at Kootenay Lake | 549 to 2785 |
| | | Burton Creek | Ungauged watershed | Snow Creek | 465 to 2731 |
| | | | | Burton at Arrow Lake | 439 to 2785 |
| | | | | Caribou Creek | 1117 to 2630 |
| | | Slocan River | 08NJ013 | Lemon Creek | 538 to 2604 |
| | | | | Little Slocan River | 498 to 2803 |
| | | | | Slocan River | 450 to 2973 |

## D.4. CLIMATE CHANGE IMPACT ASSESSMENT

Assessments of climate change impacts for all clearwater watersheds were performed to quantify the anticipated changes in the annual maximum streamflow by 2050 under the RCP 8.5 emission scenario. Four different approaches were used which can be classified into statistically-based and process-based assessments.

### D.4.1. Statistically-based Assessment

Two statistically-based methods were developed to assess the effect of climate change on flood quantiles. The first method was based on an examination of the historical annual maximum flood series data to identify statistically significant trends (positive or negative). The second method was based on the index-flood model developed as part of the Regional Flood Frequency Analysis (Regional FFA) (see Appendix C) to estimate the climate-adjusted index flood using climate-adjusted variables derived from downscaled global circulation model (GCM) predictions (Wang et al., 2016). The two methods are described in more detail and results are presented in the following sections.

#### D.4.1.1. Streamflow Trend Analysis

Statistical streamflow trend analysis on the annual maximum series (AMS)[1] was performed on suitable gauges (e.g., sufficient period of record, not regulated) located within the watersheds of clearwater study areas and within the hydrological regions formed as part of the Regional FFA.

The presence of a trend (positive or negative) in the AMS was inferred to be caused, at least in part, by climate change. The Mann-Kendall (M-K) statistical test was used to conduct the trend analyses. The M-K test was preferred over alternative statistical tests because it is non-parametric, and therefore does not assume a functional relationship between time and streamflow magnitude. The M-K test detects consistently increasing or decreasing trends in time series. The M-K test examines for an absence of trend in the time series (the null hypothesis) and returns the probability that the null hypothesis (that there is no monotonic trend in the series) is true. Failing the null hypothesis would in turn suggest that there is a statistically significant temporal trend in the time series. The M-K test was applied only to hydrometric stations with periods of records which spanned the year 2000 to ensure the time series included the most current climate.

Although it was assumed that statistically significant trends were at least in part caused by climate change, changes to the watershed's land cover (e.g., wildfire, insect infestations, changes in land use) were considered as possible causes to trends in peak discharges. Furthermore, the peak flow records often capture a small window of the flood history at a given location. The limited record lengths make it difficult to differentiate between a long-term trend cause by climate change and the intrinsic climate variability captured in the time series. Consequently, the presence of a statistically significant trend in the peak flow time series could not be solely attributed to climate change.

##### D.4.1.1.1 Assessment of Streamflow Gauges within Study Areas

One or more suitable streamflow gauges were identified on the Slocan, Kaslo and Salmo Rivers for trend analysis. A streamflow gauge with historical streamflow data is available on the Goat River (*Goat River Near Erickson* (08NH004)); however, this gauge cannot be used for assessment of trends as the Goat River is regulated. Of the six streamflow gauges assessed for the three rivers, none were found to show strong or even weak evidence of a trend in the AMS.

[1] The Annual Maximum Series (AMS) is a time series of the largest peak discharge for each year.

**Table D-3. Trend results for streamflow gauges within the clearwater study areas (where suitable hydrometric station exist).**

| Hydrometric Station | Name | Start Year | End Year | p-value | Trend Direction | Sen's Slope[1] |
|---|---|---|---|---|---|---|
| **Slocan River** | | | | | | |
| 08NJ013 | Slocan River Near Crescent Valley | 1914 | 2018 | 0.18 | - | 0.48 |
| 08NJ160 | Lemon Creek Above South Lemon Creek | 1973 | 2017 | 0.23 | - | 0.17 |
| **Kaslo River** | | | | | | |
| 08NH005 | Kaslo River Below Kemp Creek | 1972 | 2017 | 0.32 | - | -0.21 |
| 08NH132 | Keen Creek Below Kyawats Creek | 1974 | 2016 | 0.79 | - | 0.04 |
| **Salmo River** | | | | | | |
| 08NE074 | Salmo River Near Salmo | 1949 | 2018 | 0.47 | - | -0.29 |
| 08NE114 | Hidden Creek Near the Mouth | 1973 | 2016 | 0.73 | - | 0.02 |

#### D.4.1.1.2 Assessment of Streamflow Trends within Homogenous Regions

Each clearwater watershed was assigned to a homogeneous region as part of the Regional FFA formed using cluster analysis. (see Section 4.5 in Appendix C). A trend analysis was performed on the annual peak streamflow time series recorded at the hydrometric stations located within the homogeneous region assigned to the clearwater watersheds

##### *D.4.1.1.2.1 1 West – for Watersheds < 500 km²*

Within the "1 West – for watersheds less than 500 km²" hydrological region, one hydrometric station out of 15 reported a statistically significant trend ($p < 0.05$ - less than a 5% chance of rejecting the null hypothesis) in the flood series: *Kuskanax near Nakusp* (08NE006). The trend in the magnitude of the flood series for that station was in the decreasing direction (Table D-4).

**Table D-4. Trend results for the hydrometric stations in the 1 West – for watersheds < 500 km$^2$ hydrologic region.**

| Hydrometric Station Code | Start Year | End Year | p-value | Trend Direction | Sen's Slope[1] |
|---|---|---|---|---|---|
| 08LB038 | 1985 | 2016 | 0.246 | - | 0.33 |
| 08NP004 | 1995 | 2017 | 0.239 | - | 0.13 |
| 08NH131 | 1973 | 2004 | 0.444 | - | 0.19 |
| 08KA001 | 1969 | 2013 | 0.738 | - | 0.06 |
| 08NJ168 | 1983 | 2014 | 0.475 | - | 0.04 |
| 08NB014 | 1973 | 2017 | 0.431 | - | -0.25 |
| 08NH132 | 1974 | 2016 | 0.795 | - | 0.04 |
| 08ND019 | 1973 | 2005 | 0.650 | - | 0.13 |
| 08NE006 | 1968 | 2011 | 0.006 | Decreasing* | -1.33 |
| 08NK022 | 1977 | 2015 | 0.143 | - | -0.19 |
| 08NG076 | 1973 | 2017 | 0.314 | - | 0.07 |
| 08KA009 | 1967 | 2018 | 0.881 | - | -0.04 |
| 08KB006 | 1978 | 2015 | 0.386 | - | 0.20 |
| 08LE086 | 1997 | 2016 | 1.000 | - | 0.00 |
| 08KA010 | 1908 | 2015 | 0.118 | - | -0.25 |

Notes:

1. The Sen's slope is a robust estimate of the magnitude of a trend and commonly used to identify the slope of a trend line in hydrological time series (Yue et al. 2002). It is considered robust because it is sensitive to outliers.

* Strong evidence of trend ($p < 5\%$) – less than 5% chance that the null hypothesis – that there is no trend – is true.

** Weak evidence of trend ($p < 10\%$)– less than 10% chance that the null hypothesis – that there is no trend – is true.

#### *D.4.1.1.2.2 1 West – for Watersheds > 500 km$^2$*

Within the "1 West – for watersheds greater than 500 km$^2$" hydrological region, one out of 15 hydrometric stations reporting a statistically significant trend in the flood series (*Fraser River at Red Pass*, 08KA007) with a trend in the decreasing direction (Table D-5).

**Table D-5. Trend results for the hydrometric stations in the 1 West – for watersheds > 500 km$^2$ hydrologic region.**

| Hydrometric Station Code | Start Year | End Year | p-value | Trend Direction | Sen's Slope[1] |
|---|---|---|---|---|---|
| 08NB019 | 1985 | 2018 | 0.836 | - | 0.20 |
| 08NB012 | 1970 | 2017 | 0.818 | - | 0.11 |
| 08LE024 | 1973 | 2017 | 0.143 | - | -1.07 |
| 08NP001 | 1929 | 2017 | 0.845 | - | -0.06 |
| 08NK018 | 1973 | 2015 | 0.530 | - | -0.23 |
| 08KA007 | 1955 | 2016 | 0.016 | Decreasing* | -0.81 |
| 08NH130 | 1973 | 2012 | 0.990 | - | 0.00 |
| 08ND012 | 1964 | 2018 | 0.670 | - | -0.11 |
| 08ND013 | 1964 | 2017 | 0.228 | - | 0.72 |
| 08NA006 | 1912 | 2017 | 0.317 | - | -0.61 |
| 12358500 | 1940 | 2017 | 0.623 | - | -0.45 |
| 08KA013 | 1998 | 2017 | 0.576 | - | 3.25 |
| 12355500 | 1911 | 2017 | 0.857 | - | -0.11 |
| 08LE027 | 1915 | 2017 | 0.598 | - | 0.15 |
| 08NA011 | 1949 | 2018 | 0.319 | - | -0.36 |

Notes:

1. The Sen's slope is a robust estimate of the magnitude of a trend and commonly used to identify the slope of a trend line in hydrological time series (Yue et al. 2002). It is considered robust because it is sensitive to outliers.

* Strong evidence of trend ($p < 5\%$) – less than 5% chance that the null hypothesis – that there is no trend – is true.

** Weak evidence of trend ($p < 10\%$)– less than 10% chance that the null hypothesis – that there is no trend – is true.

#### *D.4.1.1.2.3 4 East – for Watersheds < 500 km$^2$*

Within the "4 East – for watersheds less than 500 km$^2$" hydrological region, 19 hydrometric stations were analysed for presence of a trend (Table D-6). The M-K test identified two stations as having statistically significant trends in their time series with the first showing an increasing trend (*Boundary Creek near Porthill Idaho,* 12321500) and the second showing a decreasing trend (*Arrow Creek near Erickson*, 08NH084). Two other stations, *Redfish Creek near Harrop* (08NJ061) and *Outlet Creek near Metaline Falls* (12397100), were found to have marginally statistically significant decreasing trends ($p < 0.1$ - less than a 10% chance of rejecting the null hypothesis), while *St-Mary River below Morris Creek* (08NG077) was found to have a marginally statistically significant increasing trend ($p < 0.1$).

**Table D-6. Trend results for the hydrometric stations in the 4 East – for Watersheds > 500 km$^2$ hydrologic region.**

| Hydrometric Station Code | Start Year | End Year | p-value | Trend Direction | Sen's Slope[1] |
|---|---|---|---|---|---|
| 08NK026 | 1986 | 2018 | 0.332 | - | -0.01 |
| 08NJ130 | 1945 | 2017 | 0.177 | - | 0.01 |
| 12321500 | 1929 | 2017 | 0.002 | Increasing** | 0.23 |
| 08NH084 | 1980 | 2015 | 0.009 | Decreasing** | -0.30 |
| 08NH005 | 1972 | 2017 | 0.322 | - | -0.21 |
| 08NE110 | 1971 | 2015 | 0.567 | - | 0.14 |
| 08NJ061 | 1968 | 2017 | 0.052 | Decreasing** | -0.06 |
| 08NG077 | 1973 | 2017 | 0.083 | Increasing* | 0.50 |
| 08NN023 | 1974 | 2015 | 0.555 | - | -0.12 |
| 08NE087 | 2001 | 2017 | 0.964 | - | -0.01 |
| 08NH016 | 1947 | 2017 | 0.504 | - | -0.02 |
| 08NJ160 | 1973 | 2017 | 0.229 | - | 0.17 |
| 12313000 | 1928 | 2002 | 0.386 | - | 1.58 |
| 08NJ026 | 1995 | 2017 | 0.239 | - | 0.13 |
| 12397100 | 1959 | 2015 | 0.065 | Decreasing* | -0.07 |
| 08NE114 | 1973 | 2016 | 0.727 | - | 0.02 |
| 08NE039 | 1930 | 2017 | 0.507 | - | -0.06 |
| 12304040 | 1990 | 2000 | 0.533 | - | 0.43 |
| 08NH115 | 1964 | 2017 | 0.303 | - | 0.00 |

Notes:

1 The Sen's slope is a robust estimate of the magnitude of a trend and commonly used to identify the slope of a trend line in hydrological time series (Yue et al. 2002). It is considered robust because it is sensitive to outliers.

* Strong evidence of trend ($p < 5\%$) – less than 5% chance that the null hypothesis – that there is no trend – is true.

** Weak evidence of trend ($p < 10\%$)– less than 10% chance that the null hypothesis – that there is no trend – is true.

#### *D.4.1.1.2.4 7 – for Watersheds > 500 km$^2$*

Within the "7 – for watersheds greater than 500 km$^2$" hydrological region, 17 hydrometric stations were analysed for presence of a trend (Table D-7). The M-K test identified three USGS stations as having statistically significant decreasing trends in their time series: *Thompson River near Thompson Falls MT* (12389500), *Yaak River near Troy MT* (12304500), and *Yakima River at Umtanum, WA* (12484500). One other station, *Colville River at Kettle Falls, WA* (12409000), was found to have a marginally statistically significant increasing trend ($p < 0.1$).

**Table D-7. Trend results for the hydrometric stations in the 7 – for Watersheds > 500 km$^2$ hydrologic region.**

| Hydrometric Station Code | Start Year | End Year | p-value | Trend Direction | Sen's Slope[1] |
|---|---|---|---|---|---|
| 13339500 | 1980 | 2017 | 0.237 | - | 0.61 |
| 12414900 | 1966 | 2017 | 0.185 | - | 0.67 |
| 12433890 | 1972 | 2012 | 0.553 | - | 0.43 |
| 12354000 | 1911 | 2017 | 0.129 | - | -0.98 |
| 12388200 | 1990 | 2010 | 0.124 | - | 0.77 |
| 12301300 | 1948 | 2016 | 0.189 | - | -0.15 |
| 12365000 | 1931 | 2006 | 0.528 | - | -0.08 |
| 12306500 | 1930 | 2017 | 0.983 | - | 0.00 |
| 12389500 | 1948 | 2017 | 0.044 | Decreasing* | -0.55 |
| 12370000 | 1922 | 2017 | 0.290 | - | -0.15 |
| 12304500 | 1948 | 2017 | 0.006 | Decreasing* | -1.37 |
| 12302055 | 1948 | 2017 | 0.408 | - | -0.35 |
| 12413000 | 1912 | 2017 | 0.542 | - | 0.75 |
| 12409000 | 1923 | 2017 | 0.076 | Increasing** | 0.13 |
| 12414500 | 1911 | 2017 | 0.935 | - | 0.00 |
| 12413500 | 1911 | 2017 | 0.125 | - | 1.67 |
| 12484500 | 1906 | 2017 | 0.021 | Decreasing* | -0.70 |

Notes:

1 The Sen's slope is a robust estimate of the magnitude of a trend and commonly used to identify the slope of a trend line in hydrological time series (Yue et al. 2002). It is considered robust because it is sensitive to outliers.

* Strong evidence of trend ($p < 5\%$) – less than 5% chance that the null hypothesis – that there is no trend – is true.

** Weak evidence of trend ($p < 10\%$)– less than 10% chance that the null hypothesis – that there is no trend – is true.

### D.4.1.2. Statistical Flood Frequency Modelling

A statistical approach to estimating flood quantiles for the clearwater watersheds was performed using the Regional FFA model. The multivariate regression model to estimate the index-flood (mean annual peak flow) included three climatic variables as predictors: MAP, MAT, and PAS. This regression model was calibrated using historical values of climatic variables, thus representing current conditions.

To estimate the climate-adjusted index flood for 2050, projected values of the climatic variables were input to the regression model. These projected values were estimated from model ensemble results for the RCP 8.5 emissions scenario using the ClimateNA v5.10 software package, available at http://tinyurl.com/ClimateNA, and based on the methodology described by Wang et al. (2016). The historical and climate-adjusted MAP, MAT, and PAS for the clearwater watersheds in the RDCK region are presented in Table D-8.

**Table D-8. Climate variables used in the index flood quantile regression model with historical and climate-adjusted values for the clearwater watersheds in the RDCK.**

| Study Area | Watershed | MAP | | MAT | | PAS | |
|---|---|---|---|---|---|---|---|
| | | Historical Value | Climate-adjusted | Historical Value | Climate-adjusted | Historical Value | Climate-adjusted |
| Crawford Creek | Crawford Creek | 1116 | 1175 | 3.0 | 6.4 | 590 | 384 |
| Kaslo Creek | Keen Creek | 1390 | 1472 | 1.3 | 4.9 | 857 | 618 |
| | Upper Kaslo Creek | 1244 | 1316 | 2.7 | 6.3 | 668 | 437 |
| | Kalso Creek at Kootenay Lake | 1312 | 1389 | 2.1 | 5.7 | 756 | 523 |
| Burton Creek | Burton at Arrow Lake | 1242 | 1315 | 2.4 | 5.9 | 704 | 483 |
| | Caribou Creek | 1259 | 1334 | 2.4 | 6.0 | 709 | 484 |
| | Snow Creek | 1227 | 1299 | 2.3 | 5.8 | 700 | 483 |
| Slocan River | Little Slocan River | 1161 | 1230 | 2.8 | 6.3 | 643 | 428 |
| | Lemon Creek | 1322 | 1404 | 2.7 | 6.3 | 754 | 503 |
| | Slocan River | 1224 | 1297 | 3.0 | 6.6 | 666 | 446 |
| Goat River | Goat River | 857 | 897 | 3.2 | 6.7 | 433 | 282 |
| Salmo River | Erie Creek Upstream End | 1265 | 1334 | 3.8 | 7.4 | 617 | 371 |

Note:
1. The ensemble model projections are averages across 15 CMIP5 models (CanESM2, ACCESS1.0, IPSL-CM5A-MR, MIROC5, MPI-ESM-LR, CCSM4, HadGEM2-ES, CNRM-CM5, CSIRO Mk 3.6, GFDL-CM3, INM-CM4, MRI-CGCM3, MIROC-ESM, CESM1-CAM5, GISS-E2R).

Climate-adjusted flood quantiles were calculated using the climate-adjusted index flood and the regional growth curves. The regional growth curves are assumed to be stationary. The ratio between the magnitude of the index-flood and the other flood quantiles was assumed to be the same in a climate-adjusted context. The regional growth curves are presented in the Regional FFA (Appendix C). Historical and climate-adjusted flood quantiles are summarized in Table D-9. Results show a small decrease in magnitude between the historical and climate-adjusted flood quantiles. Examination of the regression model for the index flood revealed that both the MAP and PAS were dominant predictors. The increase in the MAP was found to offset the decrease in the PAS resulting in little change in the estimate of the climate-adjusted index flood.

**Table D-9. Historical and climate-adjusted flood quantiles for clearwater watersheds in the RDCK.**

| Study Area | Clearwater Watershed | Index-flood | | 2-year return period (0.5 AEP) | | 20-year return period (0.05 AEP) | | 200-year return period (0.005 AEP) | |
|---|---|---|---|---|---|---|---|---|---|
| | | Historical ($m^3/s$) | Climate-adjusted ($m^3/s$) | Historical ($m^3/s$) | Climate-adjusted ($m^3/s$) | Historical ($m^3/s$) | Climate-adjusted ($m^3/s$) | Historical ($m^3/s$) | Climate-adjusted ($m^3/s$) |
| Crawford Creek | Crawford Creek | 27 | 27 | 25 | 24 | 50 | 49 | 78 | 76 |
| Kaslo Creek | Keen Creek | 45 | 45 | 42 | 41 | 75 | 74 | 115 | 114 |
| | Upper Kaslo Creek | 38 | 37 | 34 | 34 | 70 | 68 | 109 | 106 |
| | Kalso Creek at Kootenay Lake | 81 | 80 | 74 | 73 | 150 | 148 | 234 | 230 |
| Burton Creek | Burton at Arrow Lake | 81 | 79 | 73 | 71 | 149 | 145 | 232 | 227 |
| | Caribou Creek | 42 | 41 | 38 | 37 | 78 | 76 | 121 | 119 |
| | Snow Creek | 45 | 44 | 41 | 40 | 83 | 81 | 129 | 126 |
| Slocan River | Little Slocan River | 103 | 100 | 94 | 91 | 191 | 186 | 297 | 289 |
| | Lemon Creek | 39 | 38 | 35 | 34 | 72 | 69 | 111 | 108 |
| | Slocan River | 347 | 339 | 315 | 308 | 642 | 627 | 1000 | 977 |
| Goat River | Goat River | 110 | 109 | 100 | 98 | 172 | 170 | 317 | 312 |
| Salmo River | Erie Creek Upstream End | 35 | 34 | 32 | 31 | 65 | 63 | 102 | 97 |

Note:
1. Final flood quantiles for Upper Kaslo Creek, Kaslo Creek at Kootenay Lake, Lemon Creek, Little Slocan River, Slocan River, and Goat River were estimated using a pro-rated calculation because they are gauged by a hydrometric station.

### D.4.2. Process-based Assessment

To complement the statistical assessment, results from process-based modelling were examined. Process-based models involve the direct application of the downscaled GCM model forecasts into hydrological models. Process-based assessments are better suited for situations where a threshold change in process is likely e.g., a transition from nival (snowmelt dominated) runoff regime to pluvial-hybrid (snow influenced) runoff regime streamflow.

#### D.4.2.1. Climate-adjusted Streamflow

PCIC provides simulated daily streamflow time series for over 120 sites located in the Peace, upper Columbia, Fraser, and Campbell River watersheds. The time series are simulated at Water Survey of Canada (WSC) hydrometric stations and BC Hydro project sites. The simulated time series represent naturalized flow conditions (i.e., with effects of upstream regulation removed) for those sites affected by storage regulation. The hydrologic projections were forced with GCM data downscaled to a 1/16-degree resolution using Bias-Correction Spatial Disaggregation (BCSD) (Wood et al., 2004) following Werner (2011). Application of the Variable Infiltration Capacity (VIC) model and the generation of hydrologic projections for the Peace, Fraser, upper Columbia, and Campbell River watersheds are described in Shrestha et al. (2012) and Schnorbus et al. (2011, 2014).

An ensemble of 8 models forecasting daily streamflow time series for locations near the study area was accessed from PCIC's website. This included forecasted time series on the Slocan and Salmo Rivers, specifically:

- Slocan River Near Crescent Valley (08NJ013)
- Salmo River Near Salmo (08NE074).

The RCP 8.5 emissions scenario was not available for this dataset so the IPCC A2 Emission Scenario (business as usual) was selected as the most similar. The 200-year flood quantile was assessed for three periods between 2009-2038, 2039-2068 and 2069-2098 and compared to the 200-year flood quantile based on the historical modelling (1955-2009). Maps showing the trend in the 200-year flood for the PCIC assessed sites and the location of the clearwater watersheds in the study for the three periods are shown in Figures D-4 to D-6 for the three periods assessed.

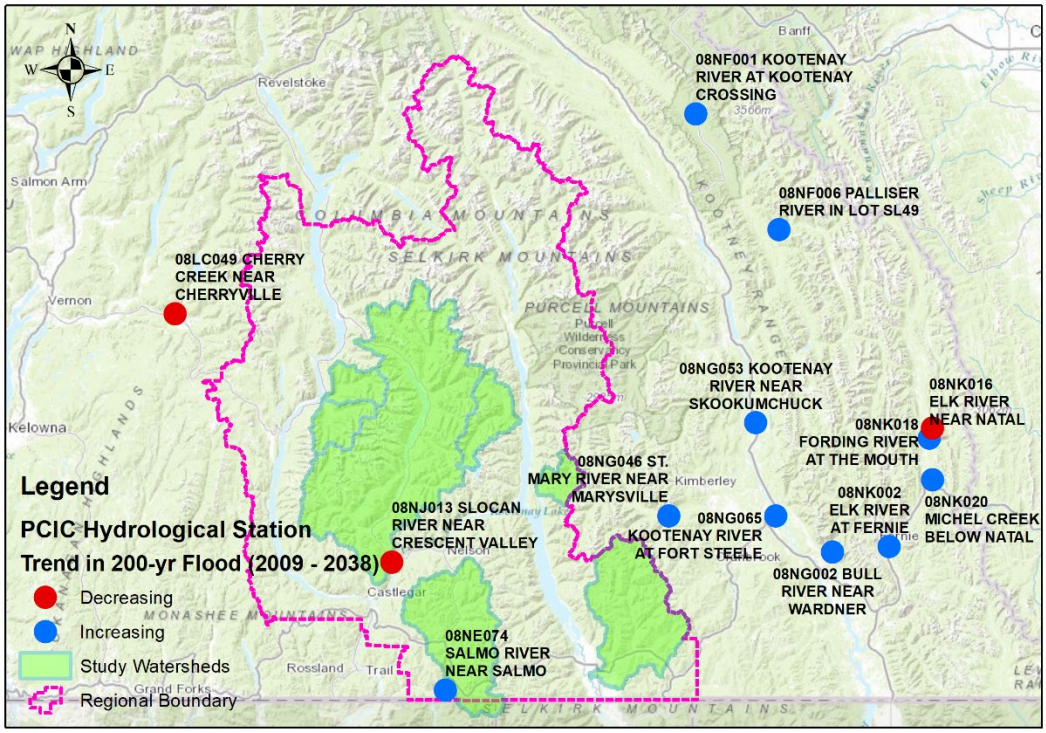


**Figure D-4. Map showing nearby the PCIC hydrometric stations examined and their trend in the 200-year flood (period between 2009-2038).**

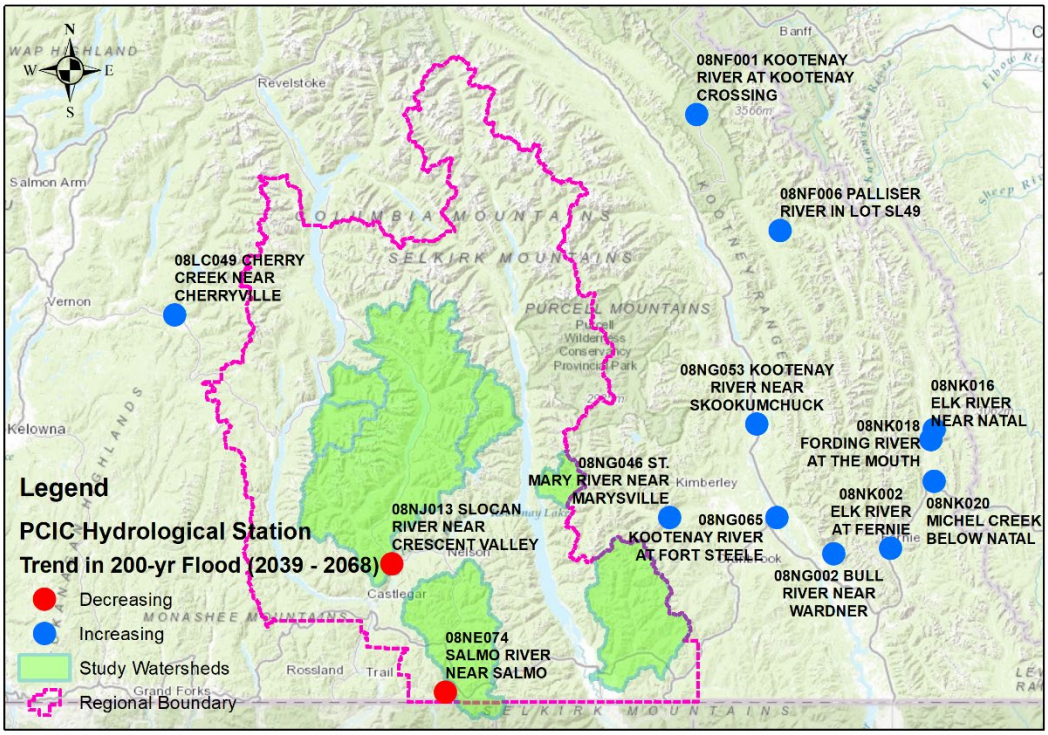


**Figure D-5. Map showing nearby the PCIC hydrometric stations examined and their trend in the 200-year flood (period between 2039-2068).**

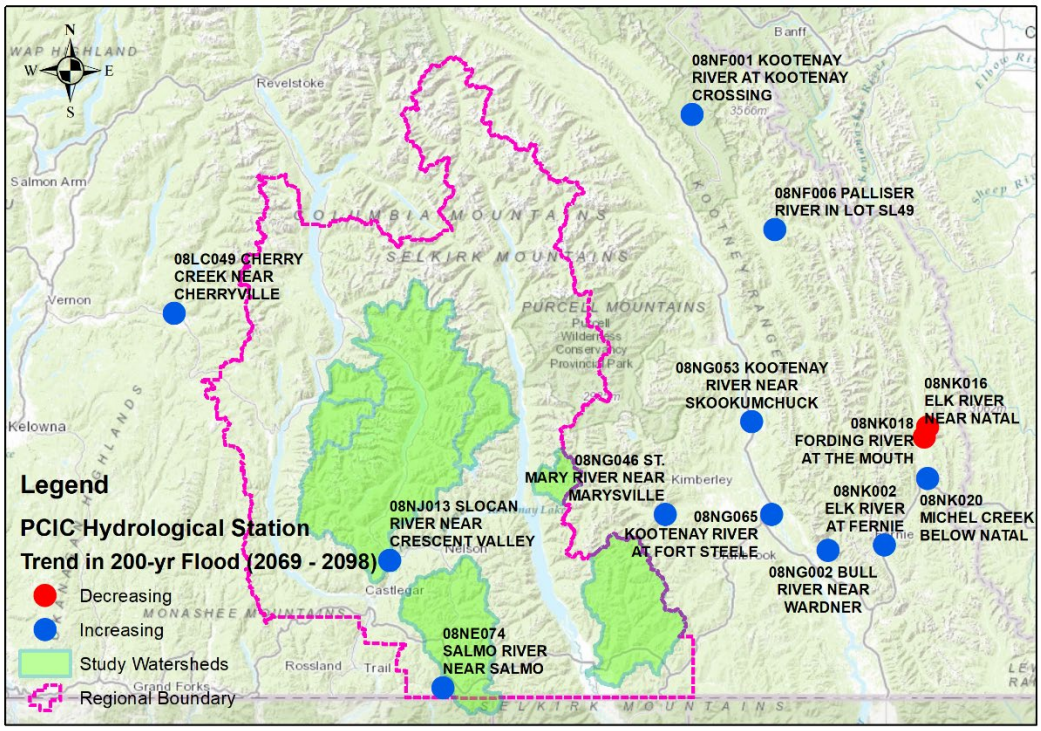


**Figure D-6. Map showing nearby the PCIC hydrometric stations examined and their trend in the 200-year flood (period between 2069-2098).**

The maps show that, in general, most of the thirteen stations examined show an increase in the magnitude of the 200-year flood over time with some exceptions based on an assessment of the mean of the eight models. A bar chart of the results for the individual hydrometric stations is shown in Figure D-7. The expected change in 200-year flood for the 2039-2068 period varies between –9% and +28% from the 1955-2009 period. For the 2069-2098 period, the range in the change of the 200-year flood magnitude increases from -7% and +60% from the 1955-2009 period. The mean of the predicted changes in the 200-year flood for Slocan River Near Crescent Valley (08NJ013) show virtually no change for the 2009-2038 period (-0.1%) followed by a small decrease and small increase for the 2039-2068 (-5%) and 2069-2098 (+16%) periods respectively. The mean of the predicted changes in the 200-year flood for Salmo River Near Salmo (08NE074) show a small increase for the 2009-2038 period (+8%) followed by small decrease for the 2039-2068 period (-97%) followed by a large increase for the 2069-2098 period (+60%).

Boxplots of the results for the three periods for the eight model runs are provided in Figure D-12a and Figure D-12b. The boxplots provide a sense of the uncertainty in the analysis by the considerable range in the estimated 200-year flood quantile. Of note, the PCIC hydrologic model output was found by BGC to poorly predict historical flood quantiles.

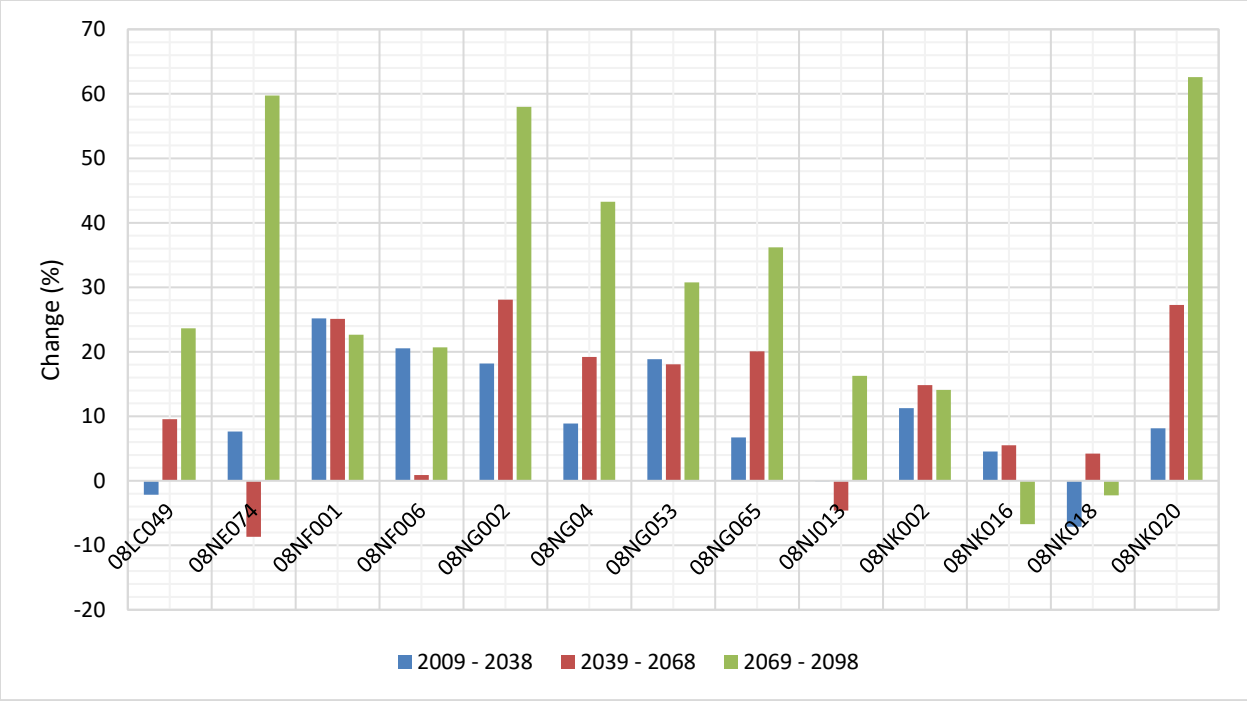


**Figure D-7. Bar-graph of the PCIC hydrometric stations and their change in the magnitude of the 200-year flood for the three periods examined compared to the 1955-2009 historical period. *Note that Station 08NJ013 and 08NE074 are stations located on the Slocan and Salmo Rivers respectively*.**

### D.4.3. Legislated Guidelines

The Engineers and Geoscientists British Columbia (EGBC, 2018) guidelines state that when a historical trend is not detectable, a 10% adjustment can be applied to the design flood to account for likely future change in water input from precipitation. In cases where the information of future local conditions is inadequate to make an informed decision on the impacts of climate on hydrology, the EGBC guidelines suggest “adjusting expected flood magnitude and frequency according to the projected change in runoff during the life of the project, or by 20% in small watersheds (<50 $km^2$) for which information of future local conditions is inadequate to provide reliable guidance.” These guidelines also include consideration of potential effects of land use change.

## D.5. SUMMARY

The impacts of climate change on flood quantile estimates were assessed using statistical and processed-based methods. The statistical methods included a trend assessment on historical flood events using the Mann-Kendall test as well as the application of climate-adjusted variables (mean annual precipitation, mean annual temperature, and precipitation as snow) to the Regional FFA model. The process-based methods included a trend analysis for climate-adjusted flood and precipitation data offered by PCIC.

The results of the statistical and process-based methods were found to be inconsistent across the RDCK. The results of the statistical flood frequency modelling generally show a small decrease in the flood magnitude, while the results of the process-based modelling generally show an increase with a wide range in magnitude. Although general trends for the region are predicted by GCMs and downscaled models, there is a wide range of predictions and estimation of future local conditions. The wide range in magnitude can be a function of many variables including watershed characteristics (e.g., proportion of watershed elevation above a given threshold) which were not explicitly addressed in this assessment.

## D.6. CONCLUSION

The guidance offered by the climate changes impact assessment results is considered unreliable for estimating climate-adjusted flood quantiles on a site-specific basis. As a result, flood quantile estimates were adjusted by 20% for all catchments to account for the uncertainty in the impacts of climate change as per the EGBC (2018) guidelines.

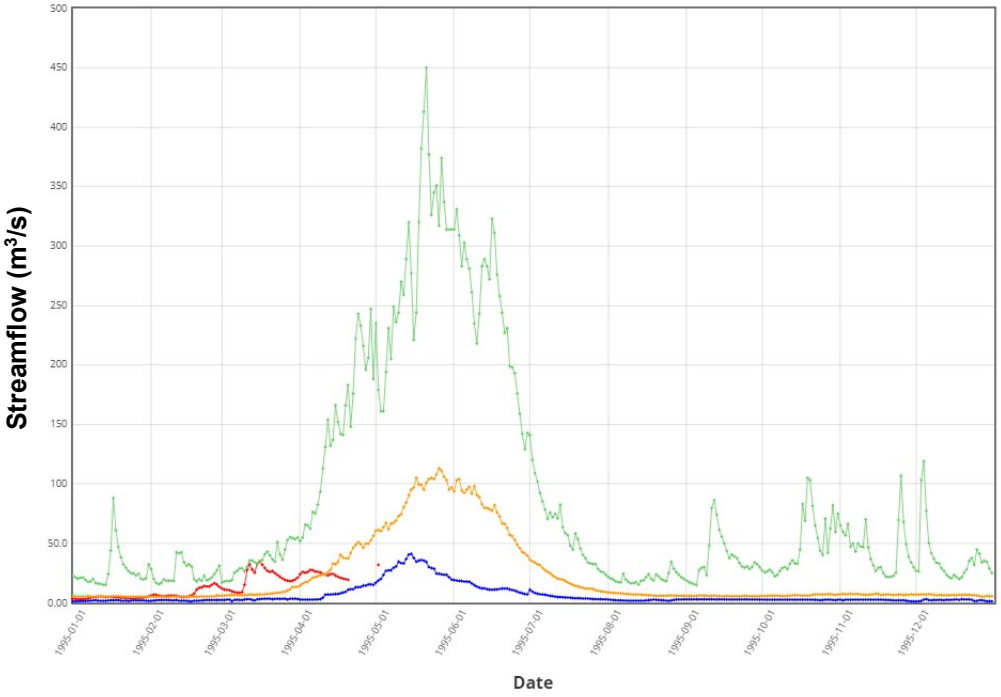


**Figure D-8. Example freshet-driven hydrologic regime for Goat River near Erickson (08NH004). Green line is the maximum streamflow, the blue line is the minimum streamflow, the orange line is the median, and the red line is the 1995 streamflow.**

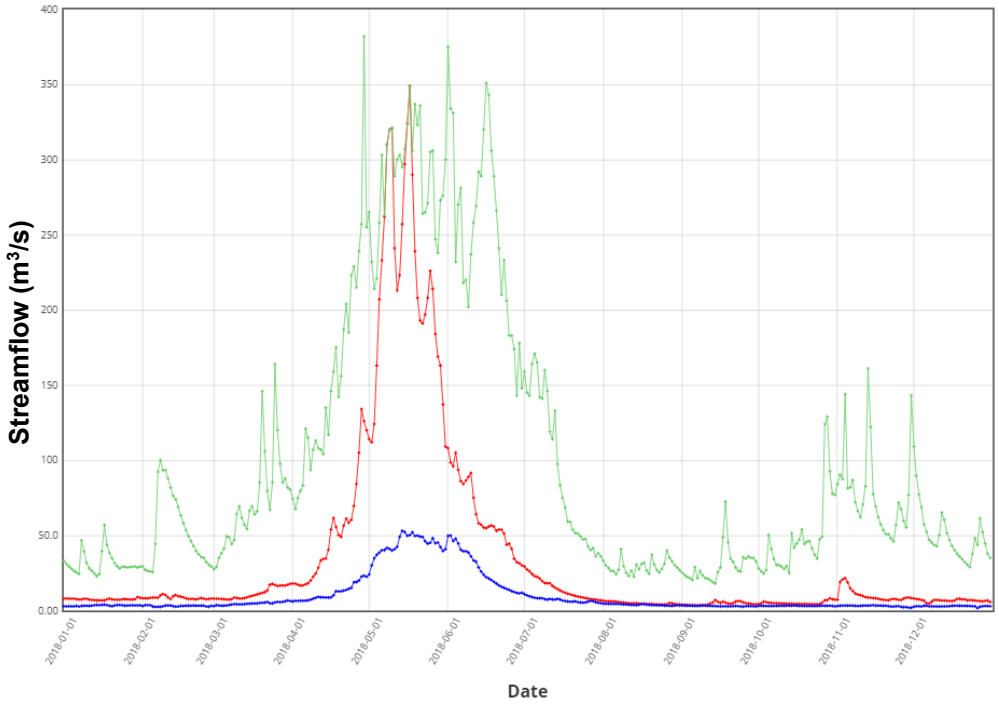


**Figure D-9. Example freshet-driven hydrologic regime for Salmo River near Salmo (08NE074). Green line is the maximum streamflow, the blue line is the minimum streamflow, and the red line is the 2018 streamflow.**

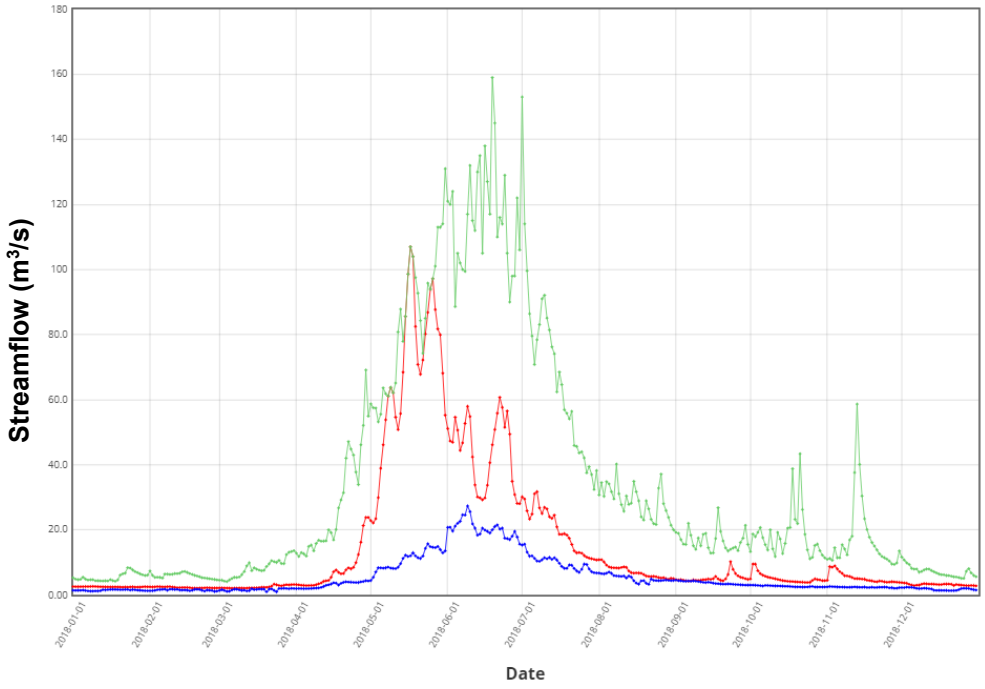


**Figure D-10. Example freshet-driven hydrologic regime for Kaslo below Kemp Creek (08NH005). Green line is the maximum streamflow, the blue line is the minimum streamflow, and the red line is the 2018 streamflow.**

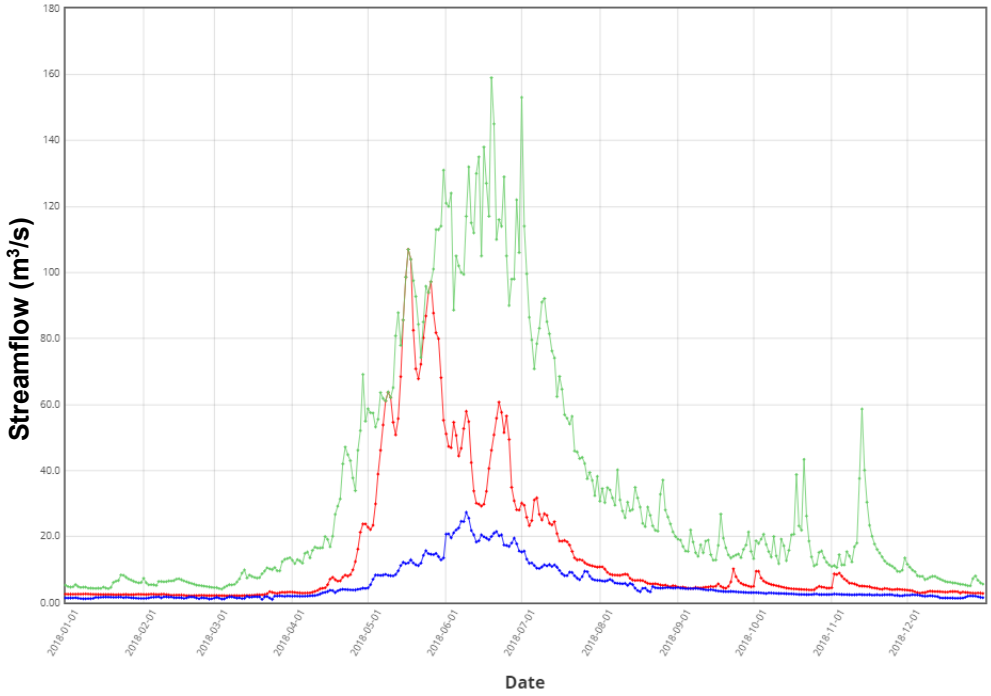


**Figure D-11. Example freshet-driven hydrologic regime for Slocan River near Crescent Valley (08NJ013). Green line is the maximum streamflow, the blue line is the minimum streamflow, and the red line is the 2018 streamflow.**

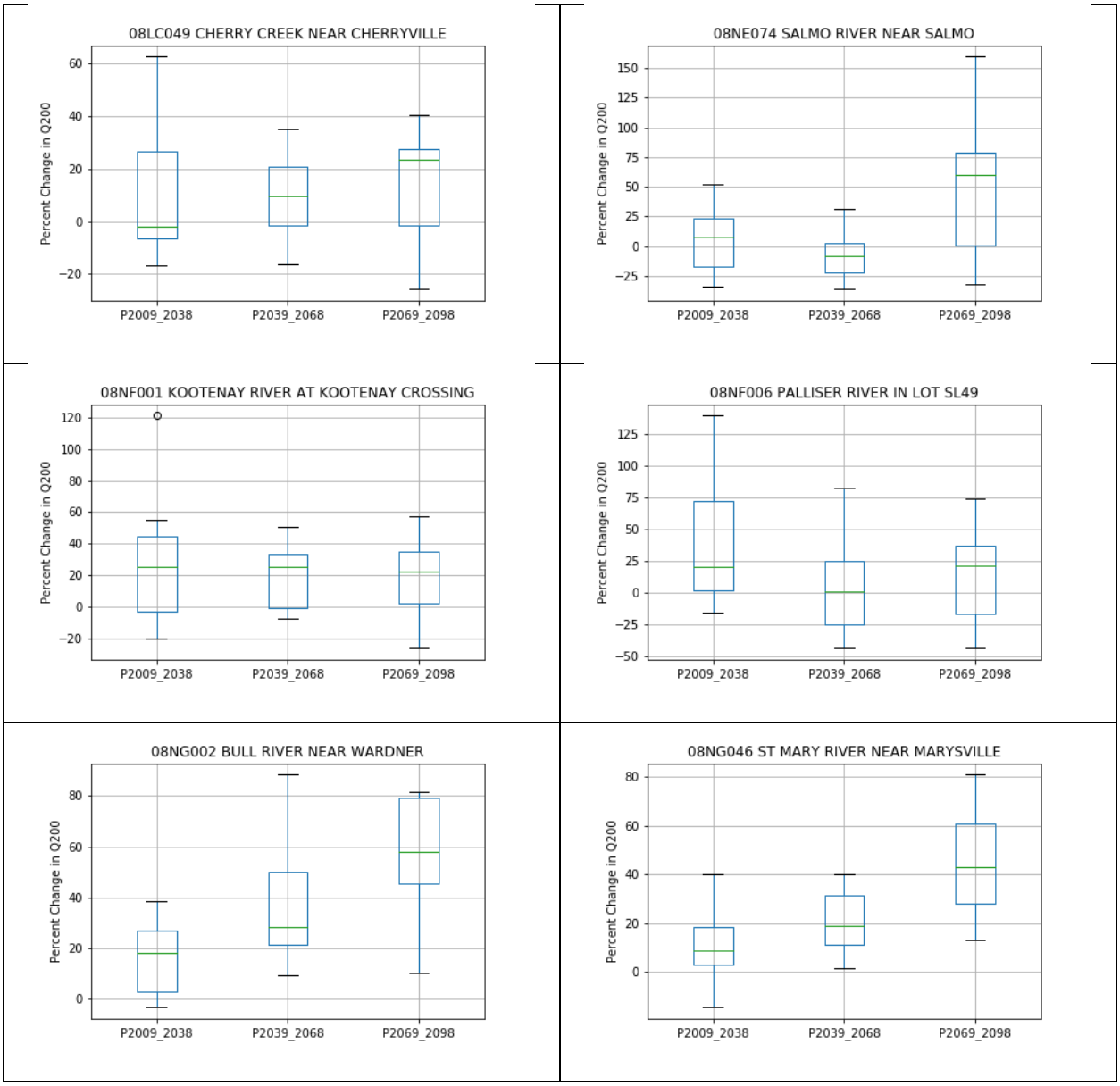


**Figure D-12a. Boxplots of the PCIC Hydrological Stations and their change in the magnitude of the 200-year flood for the three periods examined compared to the 1955-2009 historical period. Boxplots represent the interquartile range from the ensemble of 8 GCM models.**

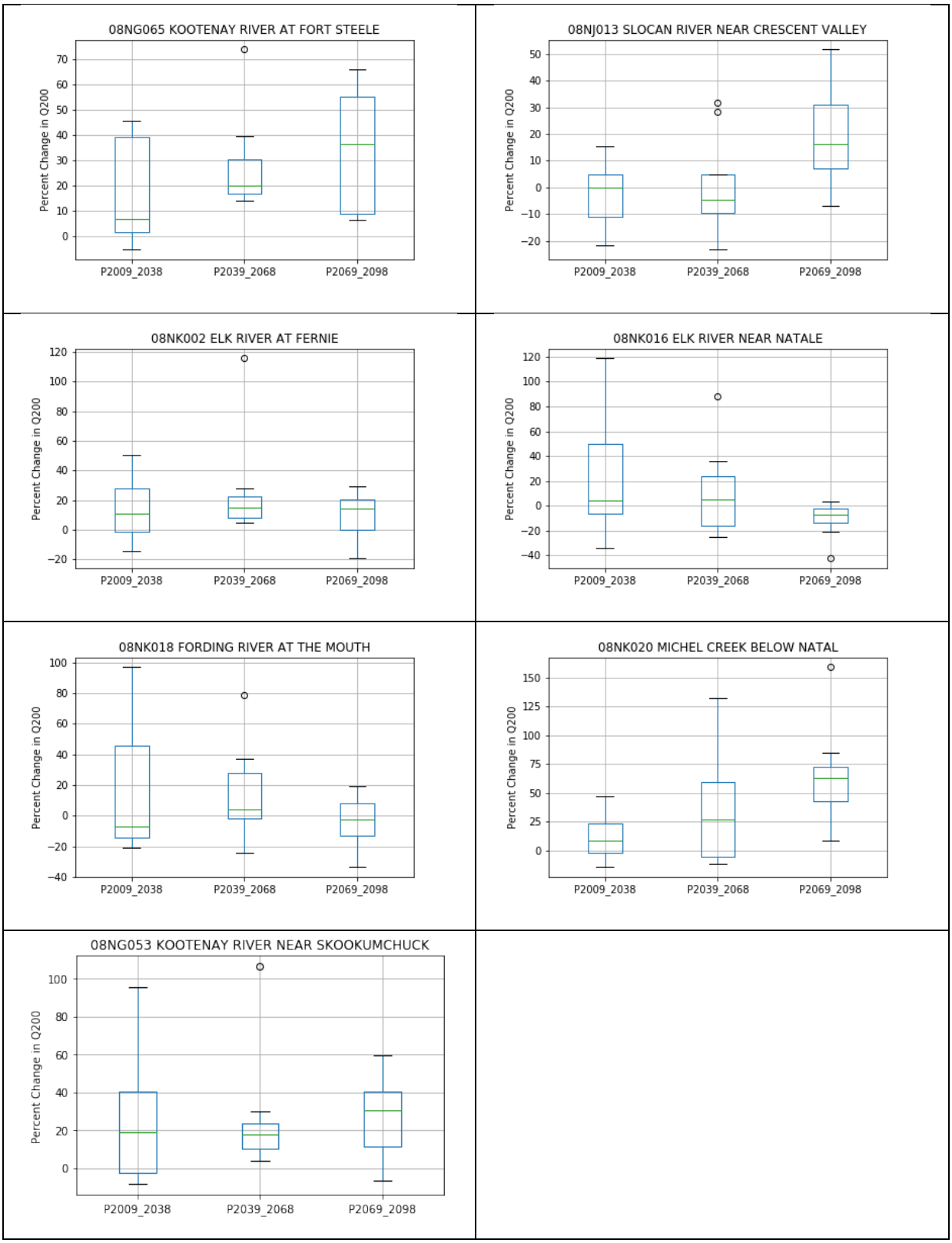


**Figure D-12b. Boxplots of the PCIC Hydrological Stations and their change in the magnitude of the 200-year flood (continued).**

# REFERENCES

Barnett, T. P., Pierce, D. W., Hidalgo, H. G., Bonfils, C., Santer, B. D., Das, T., Mirin, A. A. (2008). Human-induced changes in the hydrology of the western United States. *Science, 319*(5866), 1080–1083.

Columbia Basin Trust (CBT). (2017). *Water Monitoring and Climate Change in the Upper Columbia Basin – Summary of Current Status and Opportunities*.

Déry, S. J., Stahl, K., Moore, R., Whitfield, P., Menounos, B., & Burford, J. E. (2009). Detection of runoff timing changes in pluvial, nival, and glacial rivers of western Canada. *Water Resources Research, 45*, W04426. https://doi.org/10.1029/2008WR006975

Eaton, B. & Moore, R. (2010) Regional hydrology. In R. Pike, T. Redding, R. Moore, R. Winkler, K. Bladon (Eds), *Compendium of Forest Hydrology and Geomorphology in British Columbia, Land Management Handbook 66, Vol 1, BC* (Chap 4). Ministry of Forests and Range, Forest Science Program and FORREX Forum for Research and Extension in Natural Resources: Victoria, BC and Kamloops, BC, URL htto://www.for.gov.bc.ca/Lmh/Lmh66.htm

Engineers and Geoscientists BC (EGBC). (2018). *Professional Practice Guidelines – Legislated Flood Assessments in a Changing Climate in BC*. Version 2.1.

Farjad, B., Gupta, A., & Marceau, D.J. (2016). Annual and seasonal variations of hydrological processes under climate change scenarios in two sub-catchments of a complex watershed. *Water Resources Management, 30*(8), 2851-2865. https://doi.org/10.1007/s11269-016-1329-3

Harder, P., Pomeroy, J.W., & Westbrook, C.J. (2015). Hydrological resilience of a Canadian Rockies headwaters basin subject to changing climate, extreme weather, and forest management. *Hydrological Processes, 29*, 3905-3924. https://doi.org/10.1002/hyp.10596

Kang, D.H., Shi, X., Gao, H., & Déry, S. J. (2014). On the changing contribution of snow to the hydrology of the Fraser River basin, Canada. *Journal of Hydrometeorology, 15*(4), 1344-1365.

Knutti, R., Massin, D., & Gettelman, A. (2013). Climate model genealogy: Generation CMIP5 and how we got there. *Geophysical Research Letters, 40*(6), 1194-1199. https://doi.org/10.1002/grl.50256

Loukas, A. & Quick, M.C. (1999). The effect of climate change on floods in British Columbia. *Nordic Hydrology, 30*(3), 231-256. https://doi.org/10.2166/nh.1999.0013

Pacific Climate Impacts Consortium (PCIC). (2011). Hydrologic *Impacts of Climate Change in the Peace, Campbell and Columbia Watersheds, British Columbia, Canada: Hydrologic Modeling Project Final Report (Part II)*.

Pacific Climate Impacts Consortium (PCIC). (2012). Plan2Adapt. Retrieved from https://www.pacificclimate.org/analysis-tools/plan2adapt.

Pacific Climate Impacts Consortium (PCIC). (2013). Climate Summary for: Kootenay / Boundary Region. Retrieved from https://www.pacificclimate.org/sites/default/files/publications/Climate_Summary-Kootenay-Boundary.pdf

Pacific Climate Impacts Consortium (PCIC). (2014). Station Hydrologic Model Output. Downloaded from https://data.pacificclimate.org/portal/hydro_stn/map/ on November 2019.

Pacific Climate Impacts Consortium (PCIC). (2019). Statistically Downscaled Climate Scenarios. Downloaded from https://data.pacificclimate.org/portal/downscaled_gcms/map/ on November 2019. Method: BCCAQ v2.

Prein, A.F., Rasmussen, R.M., Ikeda, K., Liu, C., Clark, M.P, & Holland, G.J. (2017). The future intensification of hourly precipitation extremes. *Nature Climate Change, 7*, 48-52. http://dx.doi.org/10.1038/nclimate3168

Schnorbus, M.A., Bennett, K.E., Werner, A.T., & Berland, A.J. (2011). *Hydrologic Impacts of Climate Change in the Peace, Campbell and Columbia Watersheds, British Columbia, Canada*. Pacific Climate Impacts Consortium, University of Victoria, Victoria, BC, 157 p.

Schnorbus, M., Werner, A., & Bennett, K. (2014). Impacts of climate change in three hydrologic regimes in British Columbia, Canada. *Hydrological Processes, 28*, 1170-1189. https://doi.org/10.1002/hyp.9661

Shrestha, R.R., Schnorbus, M.A., Werner, A.T., & Berland, A.J. (2012). Modelling spatial and temporal variability of hydrologic impacts of climate change in the Fraser River basin, British Columbia, Canada. *Hydrological Processes, 26*, 1840–1860. https://doi.org/10.1002/hyp.9283.

Wang, T., Hamann, A. Spittlehouse, D.L., & Carroll, C. (2016). Locally downscaled and spatially customizable climate data for historical and future periods for North America. *PLoS One 11*, e0156720. https://doi.org/10.1371/journal.pone.0156720

Werner, A. T., 2011: BCSD downscaled transient climate projections for eight select GCMs over British Columbia, Canada. Pacific Climate Impacts Consortium, University of Victoria, Victoria, BC, 63 p.

Whitfield, P.H., Cannon, A.J., & Reynolds, C.J. (2002). Modelling streamflow in present and future climates: examples from the Georgia Basin, British Columbia. *Canadian Water Resources Journal, 27*(4), 427–456. https://doi.org/10.4296/cwrj2704427

Wood, A.W., Leung, L.R., Sridhar, V., & Lettenmaier, D.P. (2004). Hydrologic implications of dynamical and statistical approaches to downscaling climate model outputs. *Climate Change*, 62, 189–216. https://doi.org/10.1023/B:CLIM.0000013685.99609.9e.

# APPENDIX E
# HYDRAULIC ASSESSMENT METHODS

## E.1. INTRODUCTION

This appendix describes the approach used for the Kaslo Creek study area to develop 20, 50, 200 and 500-year flood events, and to estimate the corresponding flood inundation extents and hazard maps. The following sections describe the methods used to develop the hydraulic model including model selection, model domain, scenarios and sensitivity analyses.

## E.2. MODELLING SOFTWARE

Results of the hydraulic analysis including water surfaces profiles, water depths and flow velocities were estimated using the HEC-RAS version 5.0.7. HEC-RAS is a public domain hydraulic modeling program developed and supported by the United States Army Corps of Engineers. (Brunner & CEIWR-HEC, 2016).

For this study, which includes dike breach scenarios, a 2-D hydraulic model was selected. The 2-D model is suited for modelling overland flow that occurs during breach conditions. The 2-D model also provides more detailed resolution of flow depths and velocities than a 1-D model. A 2-D model also removes some of the subjective modelling techniques which are involved in the development of 1-D models such as defining ineffective flow areas, levee markers, and cross-section orientation.

## E.3. MODEL DOMAIN AND BOUNDARY CONDITIONS

The model domain covers a 2 km section of Kalso Creek (Figure E-1). The upstream model boundary is located in a steep gorge approximately 1.5 km upstream of the Highway 31 bridge crossing. The downstream of the model domain extends approximately 100 m out into Kootenay Lake so that the lake level boundary condition does not affect the hydraulics in the Kaslo River. The edges of the modelled domain were set to allow all flow scenarios to be modelled without interacting with the boundary.

The upstream boundary for Kaslo Creek was defined as an unsteady inflow hydrograph. The objective was to establish steady state conditions corresponding to the peak discharge but a warm-up, increasing from 0 $m^3/s$ to the peak discharge over 2 to 6 hours (shorter durations for lower peak discharges) was used. The Kaslo Creek watershed is gauged, and therefore a prorated flood frequency analysis was used to estimate flood quantiles (Appendix A). The downstream lake level boundary was at an elevation of 535 m, which is intermediate scenario between BC Hydro's minimum and maximum flood scenarios; and 0.5 m above the peak recorded reservoir level (July 4, 2012) since commissioning of the Libby Dam (BGC, January 15, 2020).


**Figure E-1. Kaslo Creek study area modelling domain.**

## E.4. HYDRAULIC ROUGHNESS

As is common with many hydraulic models, HEC-RAS uses the Manning's roughness coefficient (Manning's n) to represent roughness of the channel and floodplain. Manning's n values for Kalso Creek were selected with guidance from the literature, using empirical equations and calibration to a limited number of concurrent flow and water surface observations.

As part of a bridge hydraulics study conducted by BGC for Ministry of Transportation and Infrastructure (MOTI), BGG received survey data from MOTI that included surveyed highwater marks from the 2017 and 2018 floods. These events had a return period of approximately 5-years. (BGC, July 5, 2019). Additionally, BGC collected flood level observations from debris lines during a site visit in April 2019. The location and elevation of these flood lines were estimated with a handheld GPS to record the locations of the marks, and a tape measure and clinometer were used to measure the height from each mark to the top of the adjacent river bank. The elevations of the flood lines identified by BGC and MOTI and associated flow are not known precisely, but reasonable agreement between observed levels and estimated flows were achieved with a Mannings n of 0.05. As a secondary check Manning's n was estimated with Jarrett's steep-creek Manning's n equation (Jarrett ,1984).

The gradient of Kaslo Creek channel in the study area generally ranges between 0.5% to 2.5%. Jarrett (1984) allows estimation of n values based on readily estimated river parameters, as follows:

$$n = 0.39S^{0.38}R^{-0.16}$$

where S is the energy slope (assumed equal to the channel slope) and R is the hydraulic radius of the stream (in units of feet). Jarrett's equation is based on 75 observations of streams in Colorado. His streams were composed of bed material ranging from cobbles to small boulders. The range of energy slopes were 0.2 % to 9% and range of hydraulic radii were 0.15 to 2.1 m.

The main channel Manning's n value calculated from Jarrett (1984) varies along the length of the channel and values between 0.045 and 0.07 were calculated for six cross sections examined. Given the water level calibration information the results from Jarrett, a Manning's n of 0.06 was considered appropriate for modelling the Kaslo Creek channel. For reference, a Manning's n value of 0.075 was selected for modelling hydraulics in support of the dike design (Rungas, 1981). It is not known what hydraulic roughness values were used for the 1984 floodplain mapping. A sensitivity on the model results to the Manning's n is provided in Section E.7.

For modelling overland flow in urban areas, a Manning's n of 0.1 was selected based on review of literature. This value is higher that the in-channel value as it accounts for flow around obstructions such as trees, cars, houses and urban debris that may be entrained.

## E.5. MODEL MESHING

The HEC-RAS software for 2D modelling uses an irregular mesh to simulate the flow of water over the terrain. Irregular meshes are useful for development of numerically efficient 2D models to allow refinement of the model in locations where the flow is changing rapidly and/or where additional resolution is desired. With 2D models the objective is to define a model with sufficient accuracy and resolution that minimizes model runtime.

The default cell geometries created by HEC-RAS are rectangular, but other geometries can be created to accommodate complex terrain. Within HEC-RAS, a 2D mesh is generated based on the following inputs:

- The model perimeter (the model domain or extent of the model)
- Refinement areas to define sub-domains where the mesh properties (e.g., mesh resolution) is adjusted.
- Breaklines to align the mesh with terrain features which influence the flow such as dikes, ditches, terraces and embankments. HEC-RAS provides options to adjust the mesh resolution along breaklines if the modeler chooses.

From these inputs, HEC-RAS generates the mesh consisting of computational points at the cell centroid and the faces of the cells. The mesh was cleaned and checked for errors such a cell having more than 8 faces or overly large cells.

### E.5.1. Mesh Development

For the Kalso River Study area, a base model resolution of 10 m was selected. A refinement area was added to the Village overland flow area with a mesh resolution of 5 m. Breaklines were created along the stream centerline and along dike crests with 2 m cells and had between 4 and 6 repeats. Additional breaklines were also added in areas where 'leakage' was noted between

cells. Leakage is a result of the terrain features not aligning with cell faces and/or cells that are too large and allows water to non-physically flow between cells. The final mesh after refinement consisted of 27,000 computational cells. An example of the mesh developed is given in Figure E-2.

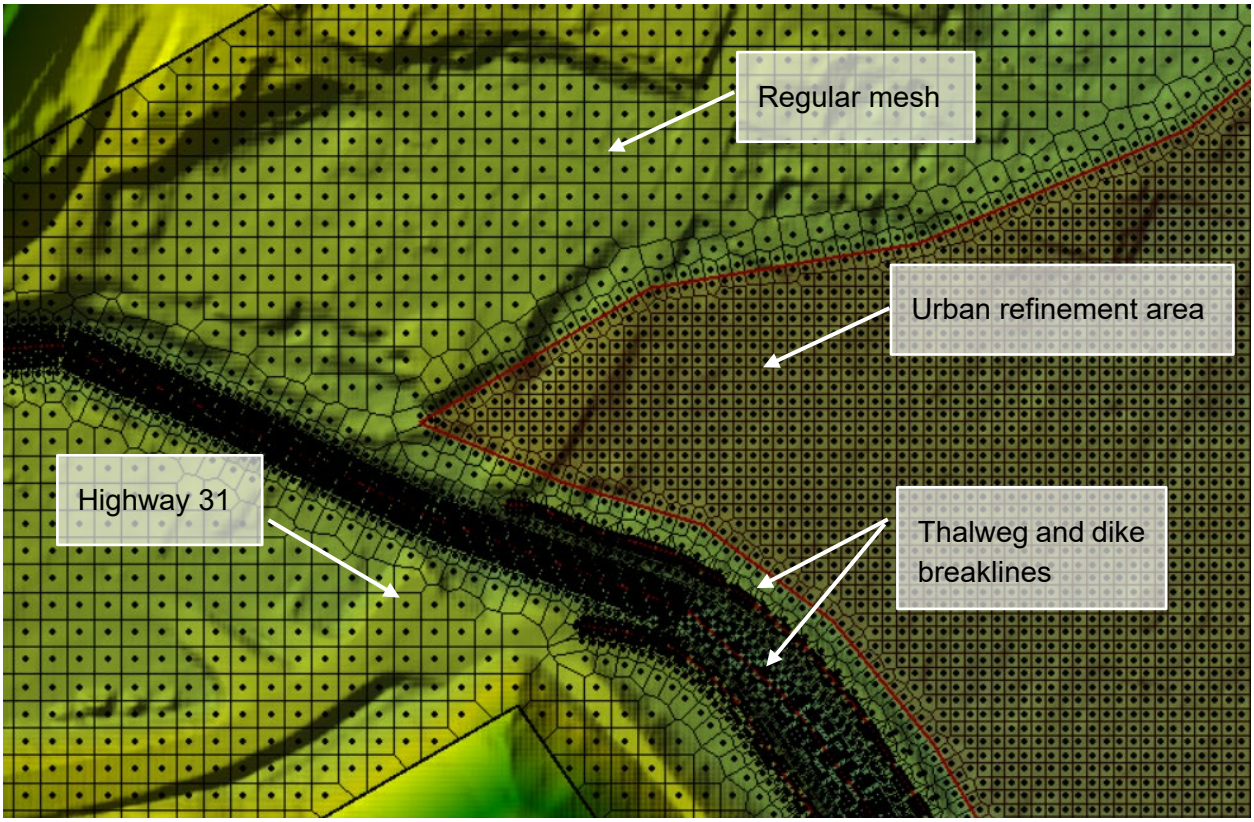


**Figure E-2. Example of the mesh used for the model showing the breaklines and refinement areas.**

### E.5.2. Dike Breach

Dike breach scenarios were assessed as there is a potential of dike failure caused by large woody debris either damaging the dike and/or causing a log jam that results in flow that overtops the dike. Dike modelling followed the guidance provided in the Floodplain Mapping Guideline and Specifications (WMA, 2004). A 200 m long breach was cut in the dike just downstream of the Highway 31 bridge. This location was selected as it provides the largest flood extent and FCL, but the following caveats should be noted:

1. The beach was not modelled dynamically. That is to say, the terrain was modified to include the final breach geometry and steady state conditions were determined. Velocities near the breach location could be higher than shown in the hazard maps as the breach develops.
2. Dike material eroded from the beach location are not included in the model and may affect flood conditions (inundation area and/or hazards)
3. A breach in other locations is expected to have a smaller inundation extent and FCL, but depths and velocities could be higher than shown in the hazard maps.

The location of the breach is shown on Figure E-3

**Figure E-3. Selected dike breach location.**

### E.5.3. Simulation Settings

The hydraulic model described above was run using a Courant controlled time step. The initial time step was 10 seconds, reducing to 0.16 seconds to maintain a maximum Courant number was 5. The model was run for between 4 to 12 hours using the diffusion wave equation. The results of this were saved and used as an initial condition for the model which was then run for 2 to 6 hours using the full momentum equation. The full momentum equations provide accurate representation of flow dynamics especially where sharp contraction, expansions or changes in flow direction are observed. However, as the diffusion wave equation is less computationally heavy, using diffusion wave initially helped prevent numerical errors. The full moment simulations were also run using a Courant controlled time step, but the maximum Courant number was reduced to 2. Steady state conditions were typically reached after 1 hour using the full momentum equation.

## E.6. MODELLING SCENARIOS

Six scenarios were selected to assess a range of conditions. Each scenario was modelled with climate-change adjusted discharges to represent projected future conditions. Dike breach scenarios were also assessed at Kaslo Creek. Although the dikes appear to have sufficient freeboard for the 200-year flood event, FLNRORD and others have noted concern about large woody debris either damaging the dike riprap and/or causing a log jam that overtops the dike. Modelled scenarios are summarized in Table E-1.

**Table E-1. Return period classes.**

| Scenario | Return Period (years) | AEP | Dike Breach | Objective |
|---|---|---|---|---|
| 1 | 20 | 0.05 | No | Determine FCL |
| 2 | 50 | 0.02 | No | Assess flood hazards |
| 3 | 200 | 0.005 | No | Assess flood hazards |
| 4 | 200 | 0.005 | Yes | Determine FCLs with dike breach |
| 5 | Used for model sensitivity assessment | | | |
| 6 | 500 | 0.002 | Yes | Assess flood hazards |

## E.7. SENSITIVITY ANALYSIS

Since the models are largely uncalibrated, a sensitivity analysis for Manning's n was performed. For the 200-year flood event (Scenario 3) an additional model run with a "high" Manning's n scenario with main channel's Manning's n value increased to n=0.075 (25% increase over the base case) to provide comparison to previous modelling (Rungas, 1981).

For the high Manning's n scenario the water surface elevation (WSE) was found to increase water levels by approximately 0.2 to 0.4 m in both the main channel and the floodplain. The effect of Manning's n on flood inundation extent is shown in Figure E-4. Increasing Manning's n by 25% result in reduced freeboard on dikes but did not result in overtopping. Approximately 1 m of freeboard remains in most areas. Similarly, the increased n reduces clearance at bridges but the soffit is not flooded.

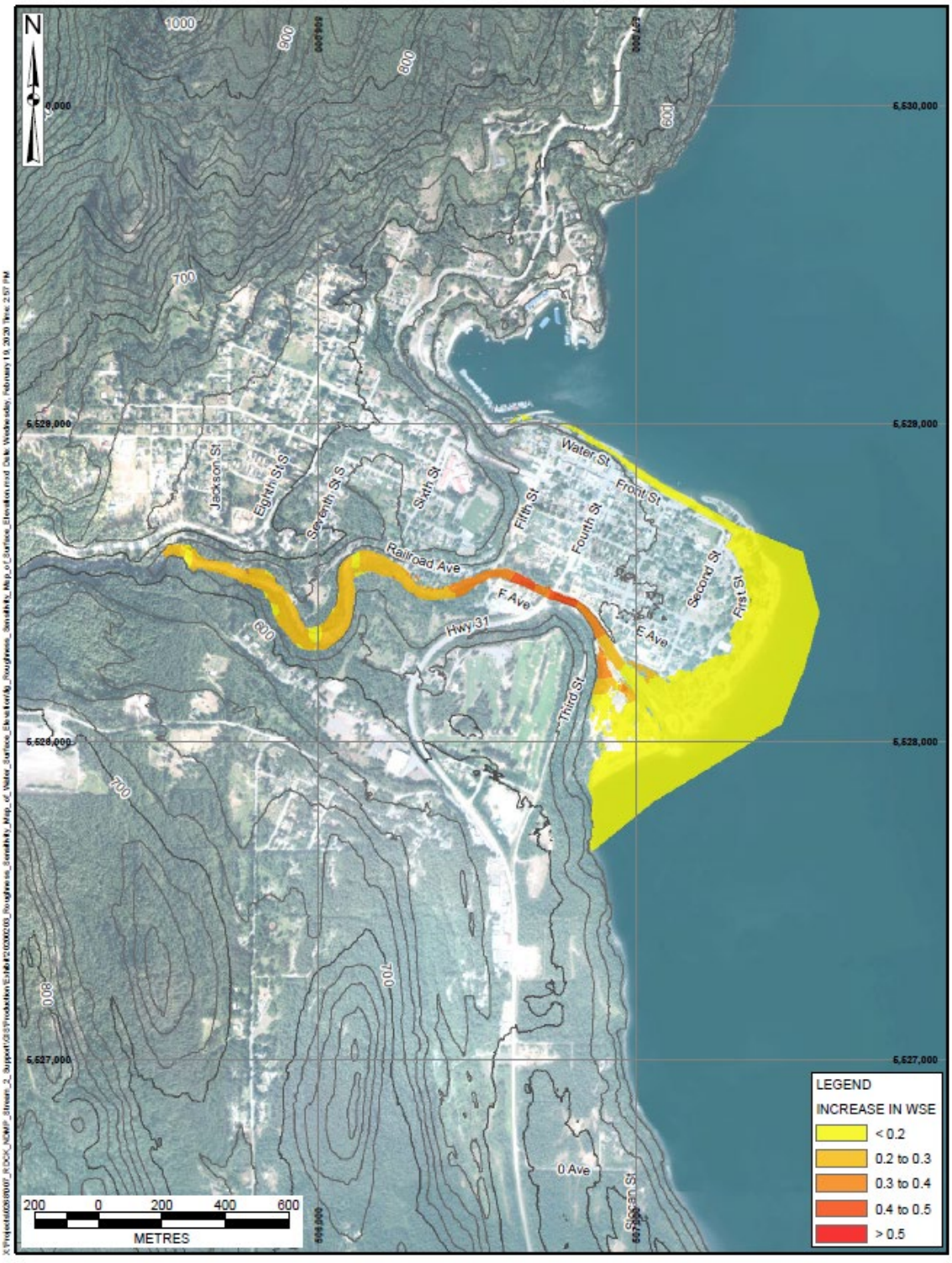


**Figure E-4. Change in WSE for 25% increase in Manning's n.**

# REFERENCES

BGC Engineering Inc. (2019, July 5). *Kaslo River Bridge Replacement* [Draft Report]. Prepared for BC Ministry of Transportation and Infrastructure.

BGC Engineering Inc. (2020, January 15). *Kootenay Lake Flood Impact Analysis* [Draft Report]. Prepared for Regional District of Central Kootenay.

Brunner, G. W., & CEIWR-HEC. (2016). HEC-RAS River Analysis System 2D Modeling User's Manual. Retrieved from www.hec.usace.army.mil

Jarrett, R. D. (1984). Hydraulics of high-gradient streams. Journal of hydraulic engineering, 110(11), 1519-1539.

Rungas, R., (1981). Kaslo River Flood Protection. Prepared for the BC Ministry of Environment, Water Management Branch, Victoria BC.

Water Management Consultants Inc. (2004, March 19). Floodplain Mapping: Guidelines and Specifications [Report]. Prepared for Fraser Basin Council, Vancouver BC.

# DRAWINGS

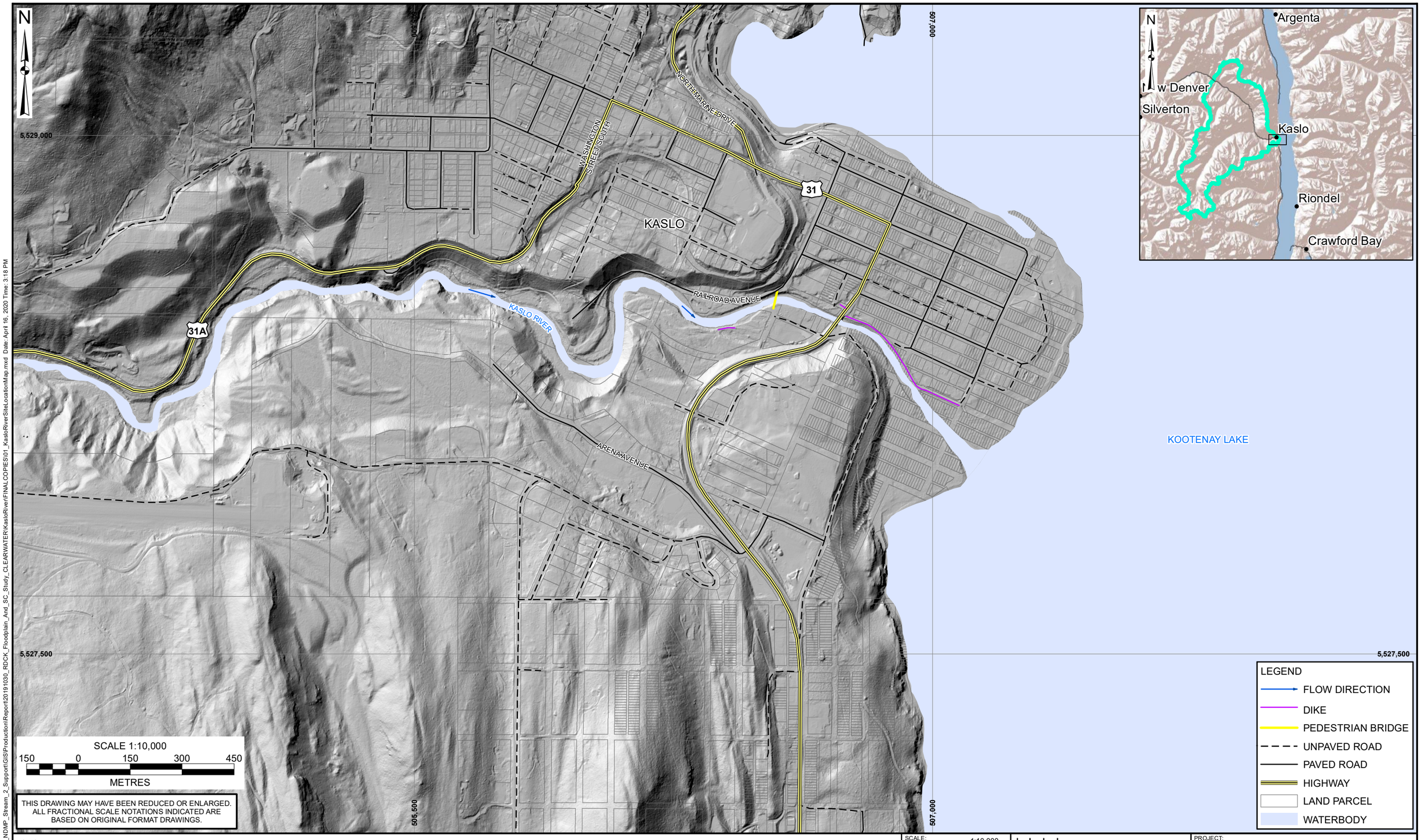


X:\Projects\0268\007_RDCK_NDMP_Stream_2_Support\GIS\Production\Report\20191030_RDCK_Floodplain_And_SC_Study_CLEARWATER\KaslоRiver\FINALCOPIES\01_KaslоRiverSiteLocationMap.mxd Date: April 16, 2020 Time: 3:18 PM

NOTES:
1. ALL DIMENSIONS ARE IN METRES UNLESS OTHERWISE NOTED.
2. THIS DRAWING MUST BE READ IN CONJUNCTION WITH BGC'S REPORT TITLED "RDCK FLOODPLAIN AND STEEP CREEK STUDY - KASLO RIVER ", AND DATED MARCH 2020.
3. BASE TOPOGRAPHIC DATA BASED ON LIDAR PROVIDED BY REGIONAL DISTRICT OF CENTRAL KOOTENAY DATED 2018.
4. COORDINATE SYSTEM IS WGS 1984 WEB MERCATOR AUXILIARY SPHERE. VERTICAL DATUM IS UNKNOWN.
5. DIKE LOCATIONS FROM FLOOD PROTECTION WORKS: STRUCTURAL WORKS DATASET PROVIDED BY BC MFLNRO (2017).
6. UNLESS BGC AGREES OTHERWISE IN WRITING, THIS DRAWING SHALL NOT BE MODIFIED OR USED FOR ANY PURPOSE OTHER THAN THE PURPOSE FOR WHICH BGC GENERATED IT. BGC SHALL HAVE NO LIABILITY FOR ANY DAMAGES OR LOSS ARISING IN ANY WAY FROM ANY USE OR MODIFICATION OF THIS DOCUMENT NOT AUTHORIZED BY BGC. ANY USE OF OR RELIANCE UPON THIS DOCUMENT OR ITS CONTENT BY THIRD PARTIES SHALL BE AT SUCH THIRD PARTIES' SOLE RISK.

| | |
|---|---|
| SCALE: | 1:10,000 |
| DATE: | MAR 2020 |
| DRAWN: | MW |
| CHECKED: | ES |
| APPROVED: | RM |

BGC ENGINEERING INC.
AN APPLIED EARTH SCIENCES COMPANY

CLIENT:

PROJECT: RDCK FLOODPLAIN AND STEEP CREEK STUDY
KASLO RIVER

TITLE: SITE LOCATION MAP

| PROJECT No.: | DWG No: |
|---|---|
| 0268-007 | 01 |

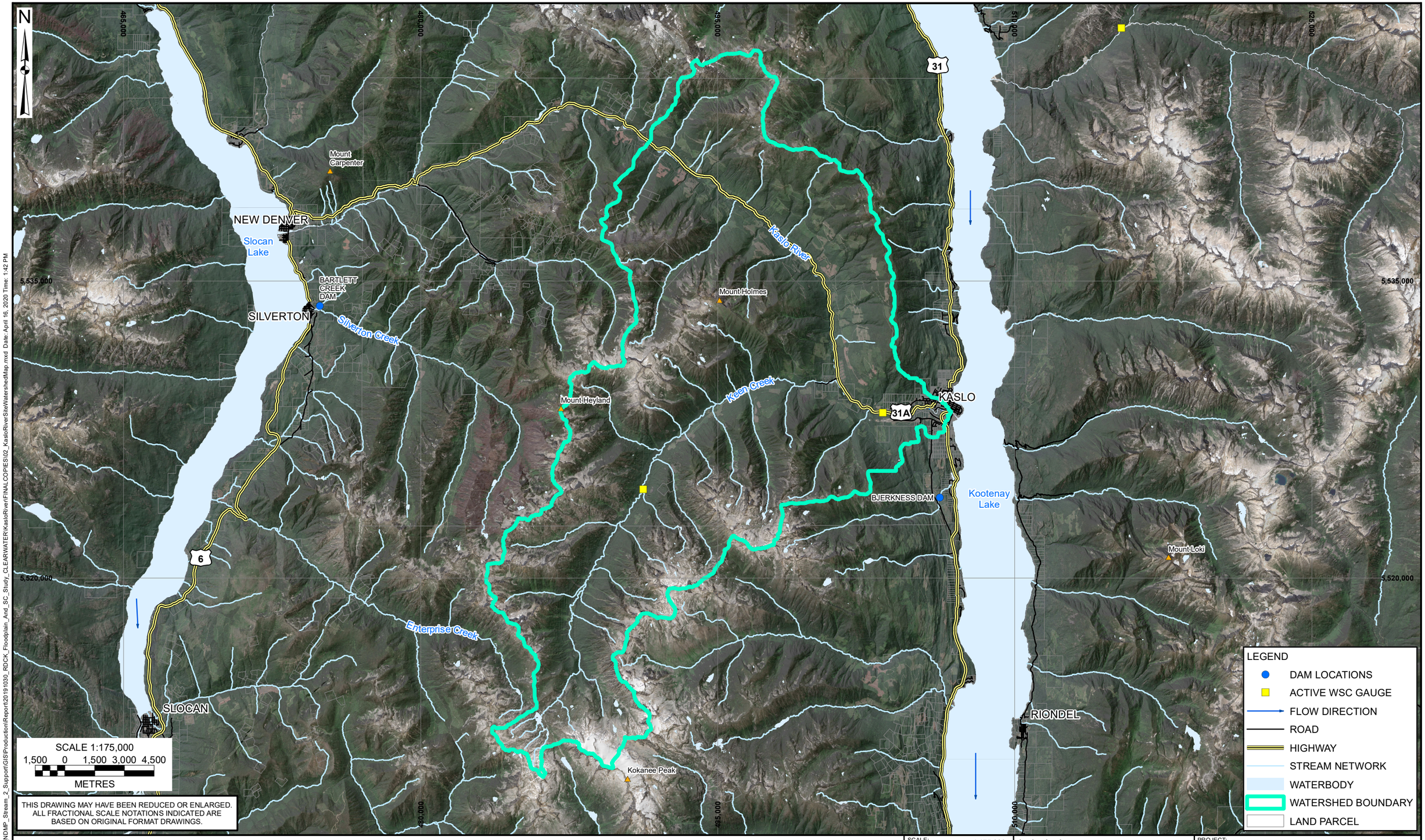


X:\Projects\0268\007_RDCK_NDMP_Stream_2_Support\GIS\Production\Report\20191030_RDCK_Floodplain_And_SC_Study_CLEARWATER\Kaslo\River\FINALCOPIES\02_KaslorRiverSiteWatershedMap.mxd Date: April 16, 2020 Time: 1:42 PM

NOTES:
1. ALL DIMENSIONS ARE IN METRES UNLESS OTHERWISE NOTED.
2. THIS DRAWING MUST BE READ IN CONJUNCTION WITH BGC'S REPORT TITLED "RDCK FLOODPLAIN AND STEEP CREEK STUDY - KASLO RIVER ", AND DATED MARCH 2020.
3. BASE IMAGERY PROVIDED BY THE SENTINEL 2 MISSON DATED AUGUST 2019.
4. COORDINATE SYSTEM IS NAD 1983 CSRS UTM Zone 11N. VERTICAL DATUM IS UNKNOWN.
5. UNLESS BGC AGREES OTHERWISE IN WRITING, THIS DRAWING SHALL NOT BE MODIFIED OR USED FOR ANY PURPOSE OTHER THAN THE PURPOSE FOR WHICH BGC GENERATED IT. BGC SHALL HAVE NO LIABILITY FOR ANY DAMAGES OR LOSS ARISING IN ANY WAY FROM ANY USE OR MODIFICATION OF THIS DOCUMENT NOT AUTHORIZED BY BGC. ANY USE OF OR RELIANCE UPON THIS DOCUMENT OR ITS CONTENT BY THIRD PARTIES SHALL BE AT SUCH THIRD PARTIES' SOLE RISK.

| | |
|---|---|
| SCALE: | 1:175,000 |
| DATE: | MAR 2020 |
| DRAWN: | MW |
| CHECKED: | ES |
| APPROVED: | RM |

BGC ENGINEERING INC.
AN APPLIED EARTH SCIENCES COMPANY

CLIENT:

PROJECT: RDCK FLOODPLAIN AND STEEP CREEK STUDY
KASLO RIVER

TITLE: WATERSHED OVERVIEW MAP

| PROJECT No.: | DWG No: |
|---|---|
| 0268-007 | 02 |


X:\Projects\0268007_RDCK_NDMP_Stream_2_Support\GIS\Production\Report\20191030_RDCK_Floodplain_And_SC_Study_CLEARWATER\KaslioRiver\FINAL COPIES\03_KaslioRiverSurveyLocations.mxd Date: April 16, 2020 Time: 1:23 PM

NOTES:
1. ALL DIMENSIONS ARE IN METRES UNLESS OTHERWISE NOTED.
2. THIS DRAWING MUST BE READ IN CONJUNCTION WITH BGC'S REPORT TITLED "RDCK FLOODPLAIN AND STEEP CREEK STUDY - KASLO RIVER", AND DATED MARCH 2020.
3. BASE TOPOGRAPHIC DATA BASED ON LIDAR PROVIDED BY REGIONAL DISTRICT OF CENTRAL KOOTENAY DATED 2018. CONTOUR INTERVAL IS 5M.
4. SURVEY DATE: AUGUST 9 TO 11, 2019 SURVEYED BY MIDWEST SURVEYS INC.
5. HORIZONTAL DATUM: NAD83 (CSRS) (2010), VERTICAL DATUM: CGVD 2013
6. GPS LOCATION EQUIPMENT: TRIMBLE R10 GNSS
7. TOPOGRAPHIC SURVEY EQUIPMENT: LEICA TCR 403 AND TRIMBLE S3 ROBOTIC TOTAL STATION
8. SONAR EQUIPMENT: ODOM ECHOTRAC CV-100 (TRANSDUCER) SOFTWARE USED TO GENERATE DEM: GLOBAL MAPPER 21.0 AND SURFER 16
9. PROJECTION: NAD 1983 CSRS UTM ZONE 11N.
10. DIKE LOCATIONS FROM FLOOD PROTECTION WORKS: STRUCTURAL WORKS DATASET PROVIDED BY BC MFLNRO (2017).
11. UNLESS BGC AGREES OTHERWISE IN WRITING, THIS DRAWING SHALL NOT BE MODIFIED OR USED FOR ANY PURPOSE OTHER THAN THE PURPOSE FOR WHICH BGC GENERATED IT.BGC SHALL HAVE NO LIABILITY FOR ANY DAMAGES OR LOSS ARISING IN ANY WAY FROM ANY USE OR MODIFICATION OF THIS DOCUMENT NOT AUTHORIZED BY BGC. ANY USE OF OR RELIANCE UPON THIS DOCUMENT OR ITS CONTENT BY THIRD PARTIES SHALL BE AT SUCH THIRD PARTIES' SOLE RISK.

| | |
|---|---|
| SCALE: | 1:5,000 |
| DATE: | MAR 2020 |
| DRAWN: | MW |
| CHECKED: | ES |
| APPROVED: | RM |

BGC ENGINEERING INC.
AN APPLIED EARTH SCIENCES COMPANY

CLIENT:

PROJECT: RDCK FLOODPLAIN AND STEEP CREEK STUDY
KASLO RIVER

TITLE: SURVEY LOCATIONS

PROJECT No.: 0268-007

DWG No: 03

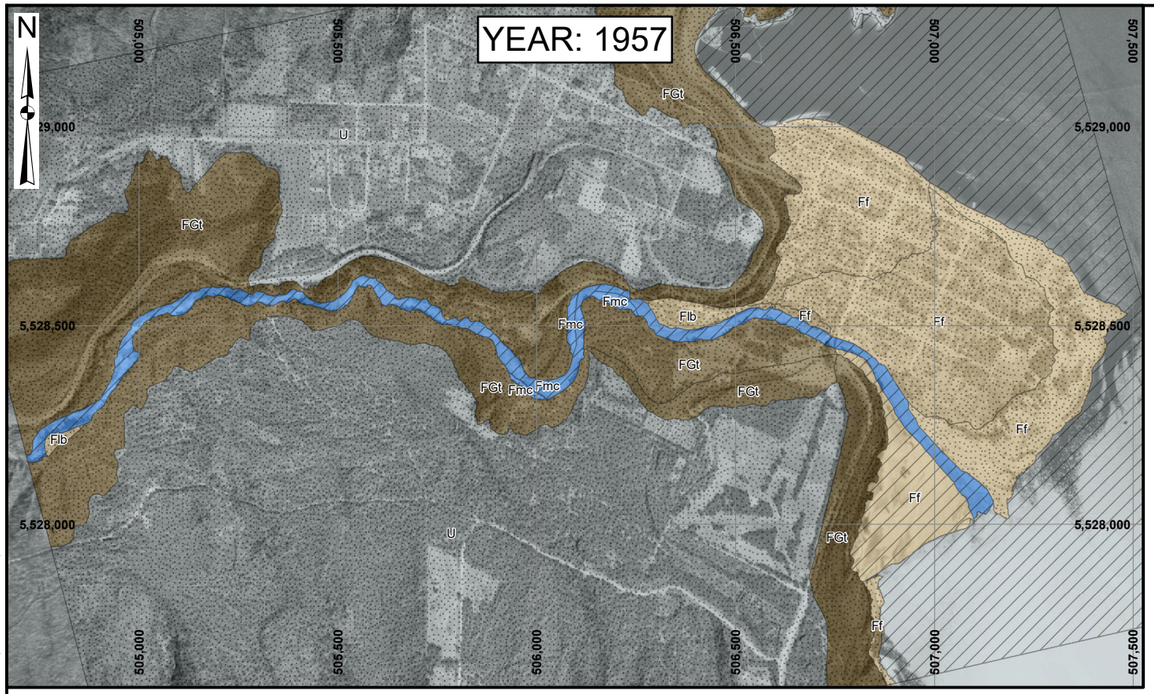


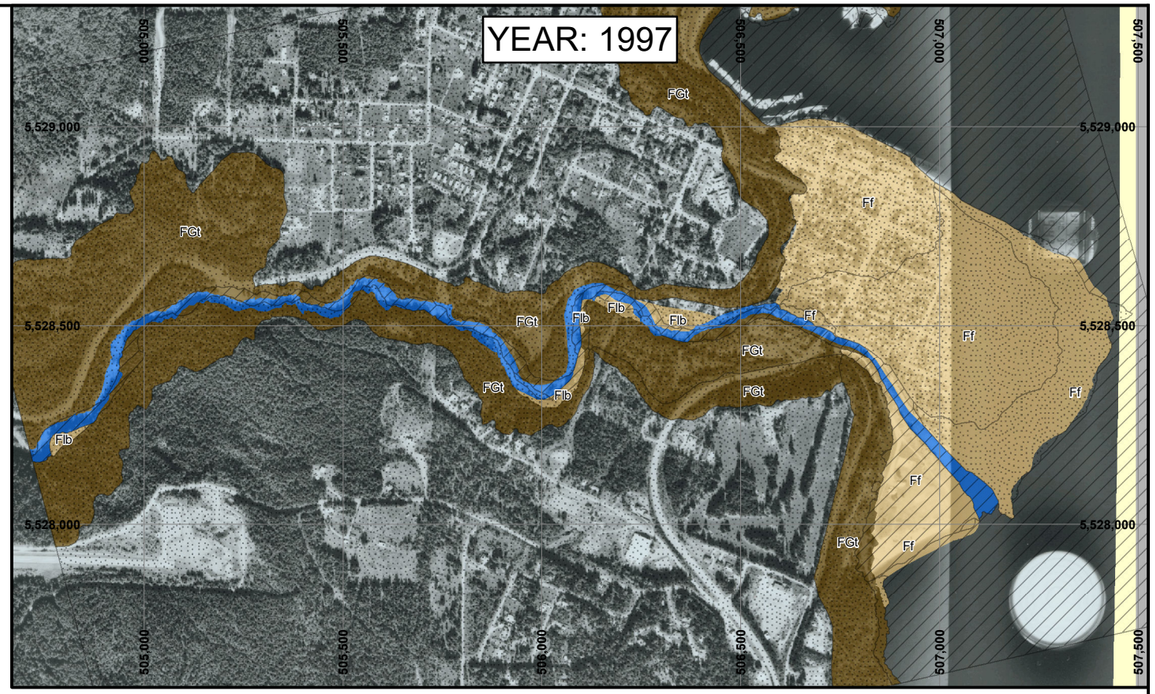





SCALE 1:15,000

150 75 0 150 300 450

METRES

NOTES:
1. ALL DIMENSIONS ARE IN METRES UNLESS OTHERWISE NOTED.
2. THIS DRAWING MUST BE READ IN CONJUNCTION WITH BGC'S REPORT TITLED "RDCK FLOODPLAIN AND STEEP CREEK STUDY - KASLO RIVER ", AND DATED MARCH 2020.
3. BASE TOPOGRAPHIC DATA BASED ON LIDAR PROVIDED BY REGIONAL DISTRICT OF CENTRAL KOOTENAY DATED 2018. BASE IMAGERY REFERENCES IN TABLE 4-2 OF REPORT.
4. COORDINATE SYSTEM IS NAD 1983 UTM ZONE 11N. VERTICAL DATUM IS UNKNOWN.
5. DIKE LOCATIONS FROM FLOOD PROTECTION WORKS: STRUCTURAL WORKS DATASET PROVIDED BY BC MFLNRO (2017). MAPPED UNITS DETERMINED BASED ON CRITERIA OUTLINED IN TABLE 4-3 OF REPORT. ACTIVITY LEVEL OF MAPPED UNITS DETERMINED BASED ON CRITERIA OUTLINED IN TABLE 4-4 OF REPORT. GROUND MOVEMENT LOCATIONS BASED ON GEOMORPHOLOGICAL INTERPRETATION OF LIDAR DATA.
6. UNLESS BGC AGREES OTHERWISE IN WRITING, THIS DRAWING SHALL NOT BE MODIFIED OR USED FOR ANY PURPOSE OTHER THAN THE PURPOSE FOR WHICH BGC GENERATED IT. BGC SHALL HAVE NO LIABILITY FOR ANY DAMAGES OR LOSS ARISING IN ANY WAY FROM ANY USE OR MODIFICATION OF THIS DOCUMENT NOT AUTHORIZED BY BGC. ANY USE OF OR RELIANCE UPON THIS DOCUMENT OR ITS CONTENT BY THIRD PARTIES SHALL BE AT SUCH THIRD PARTIES' SOLE RISK.

LEGEND

- ABANDONED-CHANNEL (Fac)
- ALLUVIAL FAN/DELTA (Ff)
- BACK-CHANNEL (Fbc)
- FLOOD-CHANNEL (Ffc)
- FLOODPLAIN (Fp)
- LATERAL AND POINT BARS (Flb)
- MID-CHANNEL BAR (Fmb)
- MAIN-CHANNEL (Fmc)
- SIDE-CHANNEL (Fsc)
- TERRACE (FGt)

ACTIVITY LEVEL

- ACTIVE
- INACTIVE
- GROUND MOVEMENT LOCATION
- DIKE

| | |
|---|---|
| SCALE: | 1:15,000 |
| DATE: | MAR 2020 |
| DRAWN: | MW |
| CHECKED: | ES/VC |
| APPROVED: | RM |

BGC ENGINEERING INC.
AN APPLIED EARTH SCIENCES COMPANY

CLIENT:

PROJECT: RDCK FLOODPLAIN AND STEEP CREEK STUDY
KASLO RIVER

TITLE: AIR PHOTO COMPARISON

| PROJECT No.: | DWG No: |
|---|---|
| 0268-007 | 04 |

X:\Projects\0268\007_RDCK_NDMP_Stream_2_Support\GIS\Production\Report\20191030_RDCK_Floodplain_And_SC_Study_CLEARWATER\KasloRiver\FINALCOPIES\04_KasloRiverAirPhotoComparison.mxd Date: April 16, 2020 Time: 3:14 PM

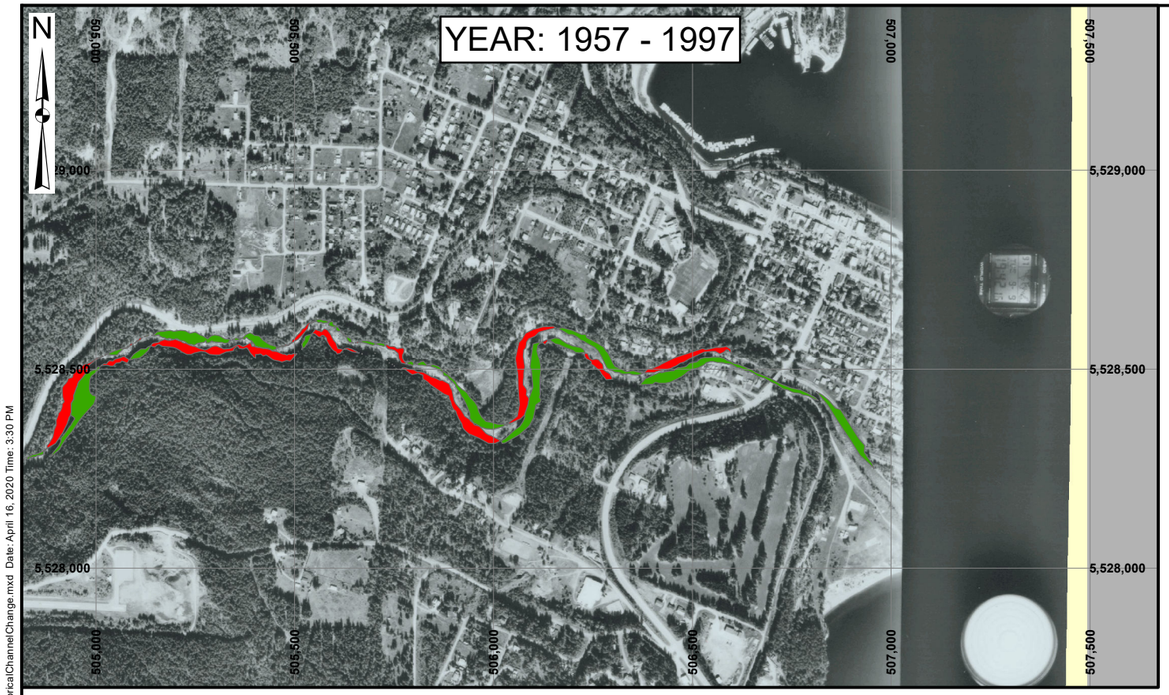


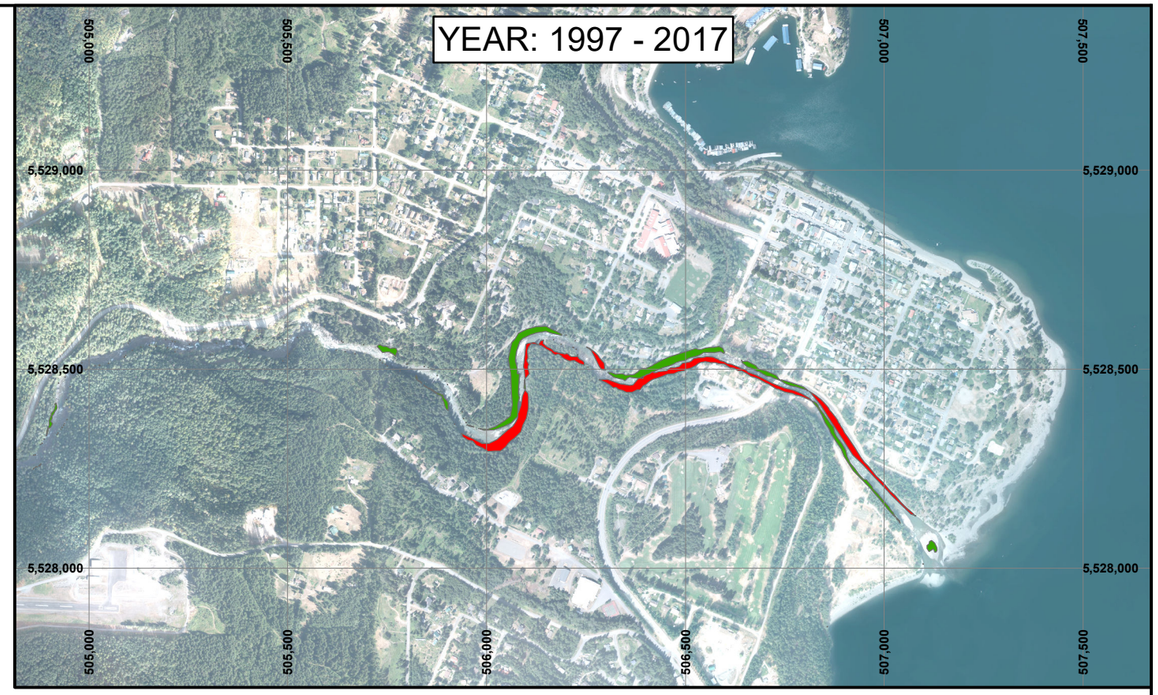


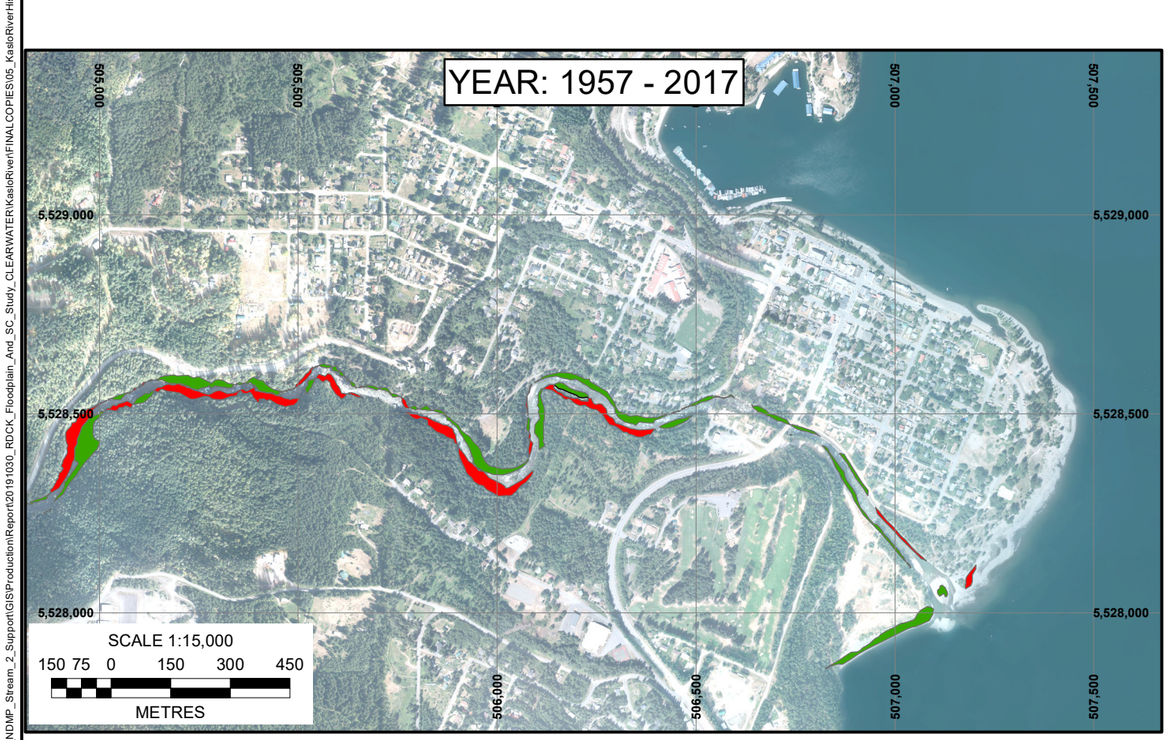


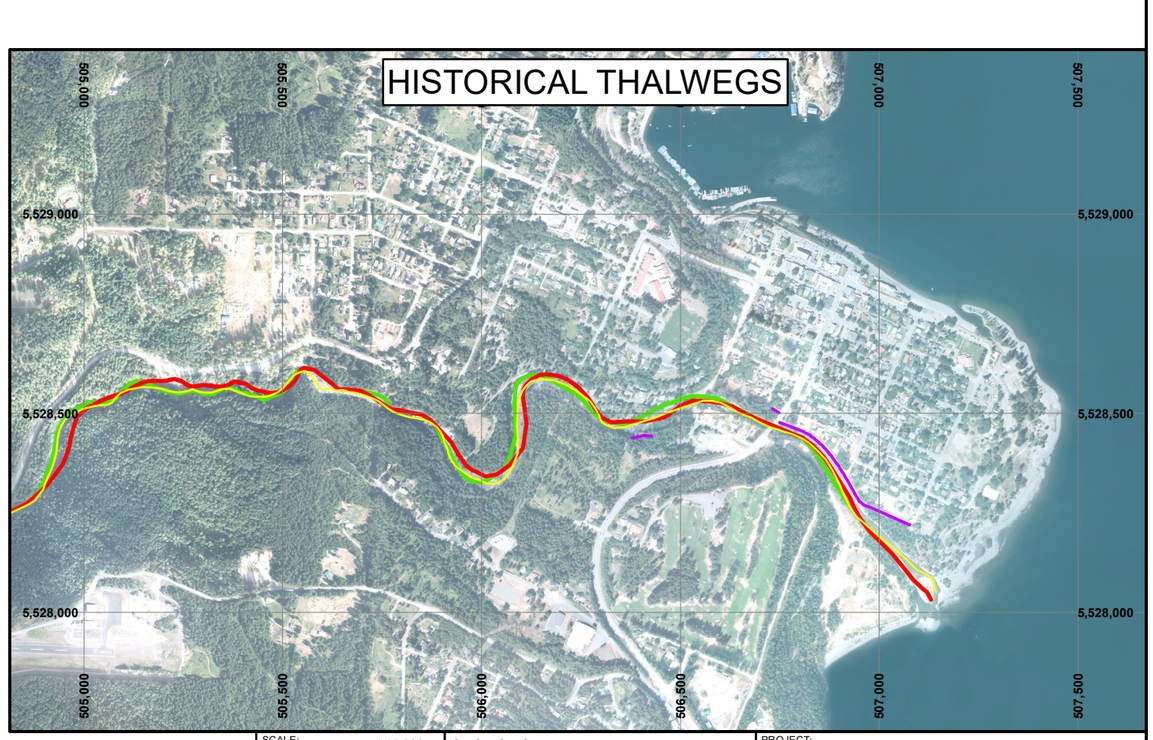


NOTES:
1. ALL DIMENSIONS ARE IN METRES UNLESS OTHERWISE NOTED.
2. THIS DRAWING MUST BE READ IN CONJUNCTION WITH BGC'S REPORT TITLED "RDCK FLOODPLAIN AND STEEP CREEK STUDY - KASLO RIVER ", AND DATED MARCH 2020.
3. BASE TOPOGRAPHIC DATA BASED ON LIDAR PROVIDED BY REGIONAL DISTRICT OF CENTRAL KOOTENAY DATED 2018. BASE IMAGERY REFERENCES IN TABLE 4-2 OF REPORT.
4. COORDINATE SYSTEM IS NAD 1983 UTM ZONE 11N. VERTICAL DATUM IS UNKNOWN.
5. DIKE LOCATIONS FROM FLOOD PROTECTION WORKS: STRUCTURAL WORKS DATASET PROVIDED BY BC MFLNRO (2017). CHANGE DETECTION CRITERIA DESCRIBED IN TABLE 4-5 OF REPORT. HISTORICAL THALWEGS INTERPRETED FROM PHOTOGRAPHS AND MANUALLY DIGITIZED.
6. UNLESS BGC AGREES OTHERWISE IN WRITING, THIS DRAWING SHALL NOT BE MODIFIED OR USED FOR ANY PURPOSE OTHER THAN THE PURPOSE FOR WHICH BGC GENERATED IT. BGC SHALL HAVE NO LIABILITY FOR ANY DAMAGES OR LOSS ARISING IN ANY WAY FROM ANY USE OR MODIFICATION OF THIS DOCUMENT NOT AUTHORIZED BY BGC. ANY USE OF OR RELIANCE UPON THIS DOCUMENT OR ITS CONTENT BY THIRD PARTIES SHALL BE AT SUCH THIRD PARTIES' SOLE RISK.

LEGEND
- CHANNEL THALWEG (2019)
- CHANNEL THALWEG (1997)
- CHANNEL THALWEG (1957)
- DIKE
- BANK EROSION, CHANNEL MIGRATION
- DEPOSITION, STABILIZATION

| | |
|---|---|
| SCALE: | 1:15,000 |
| DATE: | MAR 2020 |
| DRAWN: | MW |
| CHECKED: | ES/VC |
| APPROVED: | RM |

BGC ENGINEERING INC.
AN APPLIED EARTH SCIENCES COMPANY

CLIENT:

PROJECT: RDCK FLOODPLAIN AND STEEP CREEK STUDY
KASLO RIVER

TITLE: HISTORICAL CHANNEL CHANGE

PROJECT No.: 0268-007

DWG No: 05

X:\Projects\0268\007_RDCK_NDMP_Stream_2_Support\GIS\Production\Report\20191030_RDCK_Floodplain_And_SC_Study_CLEARWATER\KasloRiver\FINALCOPIES\05_KasloRiverHistoricalChannelChange.mxd Date: April 16, 2020 Time: 3:30 PM

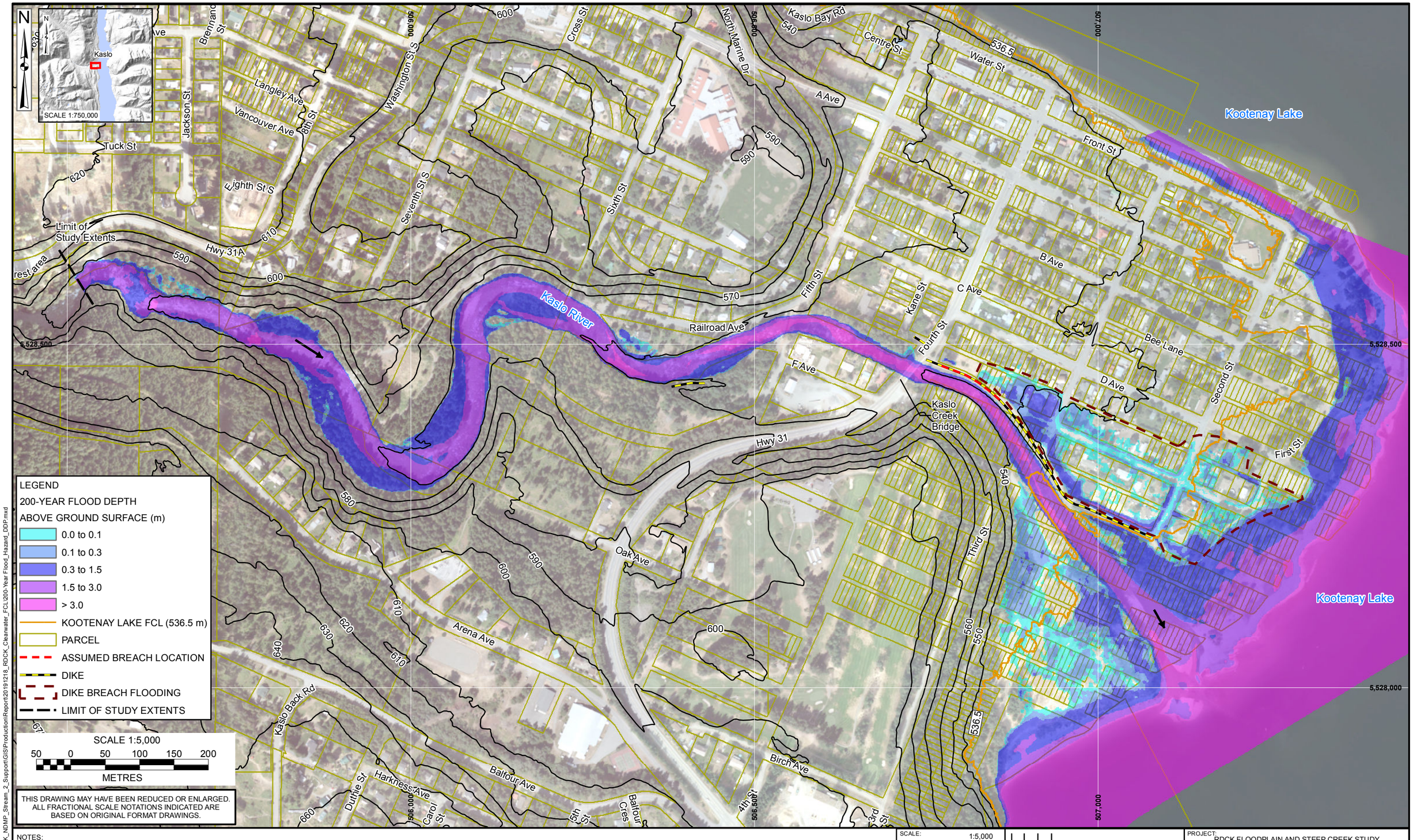


THIS DRAWING MAY HAVE BEEN REDUCED OR ENLARGED. ALL FRACTIONAL SCALE NOTATIONS INDICATED ARE BASED ON ORIGINAL FORMAT DRAWINGS.

NOTES:
1. ALL DIMENSIONS ARE IN METRES UNLESS OTHERWISE NOTED.
2. THIS DRAWING MUST BE READ IN CONJUNCTION WITH BGC'S REPORT TITLED "RDCK FLOODPLAIN AND STEEP CREEK STUDY KASLO RIVER", AND DATED MARCH 2020.
3. BASE TOPOGRAPHIC DATA BASED ON LIDAR PROVIDED BY RDCK DATED 2017 AND 2018. CONTOUR INTERVAL IS 10 m. ORTHOPHOTO PROVIDED BY RDCK AND DATED 2017 AND 2018.PARCEL DATA FROM PARCELMAP BC. DIKE DATA FROM DATA BC. FLOOD DEPTH BASED ON THE 200-YEAR FLOOD USING THE INSTANTANEOUS PEAK DISCHARGE ADJUSTED FOR CLIMATE CHANGE AND A KOOTENAY LAKE ELEVATION OF 535 m.
4. PROJECTION IS NAD 1983 UTM ZONE 11N. VERTICAL DATUM IS CGVD2013.
5. UNLESS BGC AGREES OTHERWISE IN WRITING, THIS DRAWING SHALL NOT BE MODIFIED OR USED FOR ANY PURPOSE OTHER THAN THE PURPOSE FOR WHICH BGC GENERATED IT. BGC SHALL HAVE NO LIABILITY FOR ANY DAMAGES OR LOSS ARISING IN ANY WAY FROM ANY USE OR MODIFICATION OF THIS DOCUMENT NOT AUTHORIZED BY BGC. ANY USE OF OR RELIANCE UPON THIS DOCUMENT OR ITS CONTENT BY THIRD PARTIES SHALL BE AT SUCH THIRD PARTIES' SOLE RISK.

| | |
|---|---|
| SCALE: | 1:5,000 |
| DATE: | MAR 2020 |
| DRAWN: | LL |
| CHECKED: | PG, TJP |
| APPROVED: | RM |

BGC ENGINEERING INC.
AN APPLIED EARTH SCIENCES COMPANY

CLIENT:

PROJECT: RDCK FLOODPLAIN AND STEEP CREEK STUDY
KASLO RIVER

TITLE: 200-YEAR FLOOD HAZARD
(SHEET 1 OF 1)

| PROJECT No.: | DWG No: |
|---|---|
| 0268 007 | 06 |

X:\Projects\0268\007_RDCK_NDMP_Stream_2_Support\GIS\Production\Report\20191218_RDCK_Clearwater_FCL\200-Year Flood_Hazard_DDP.mxd

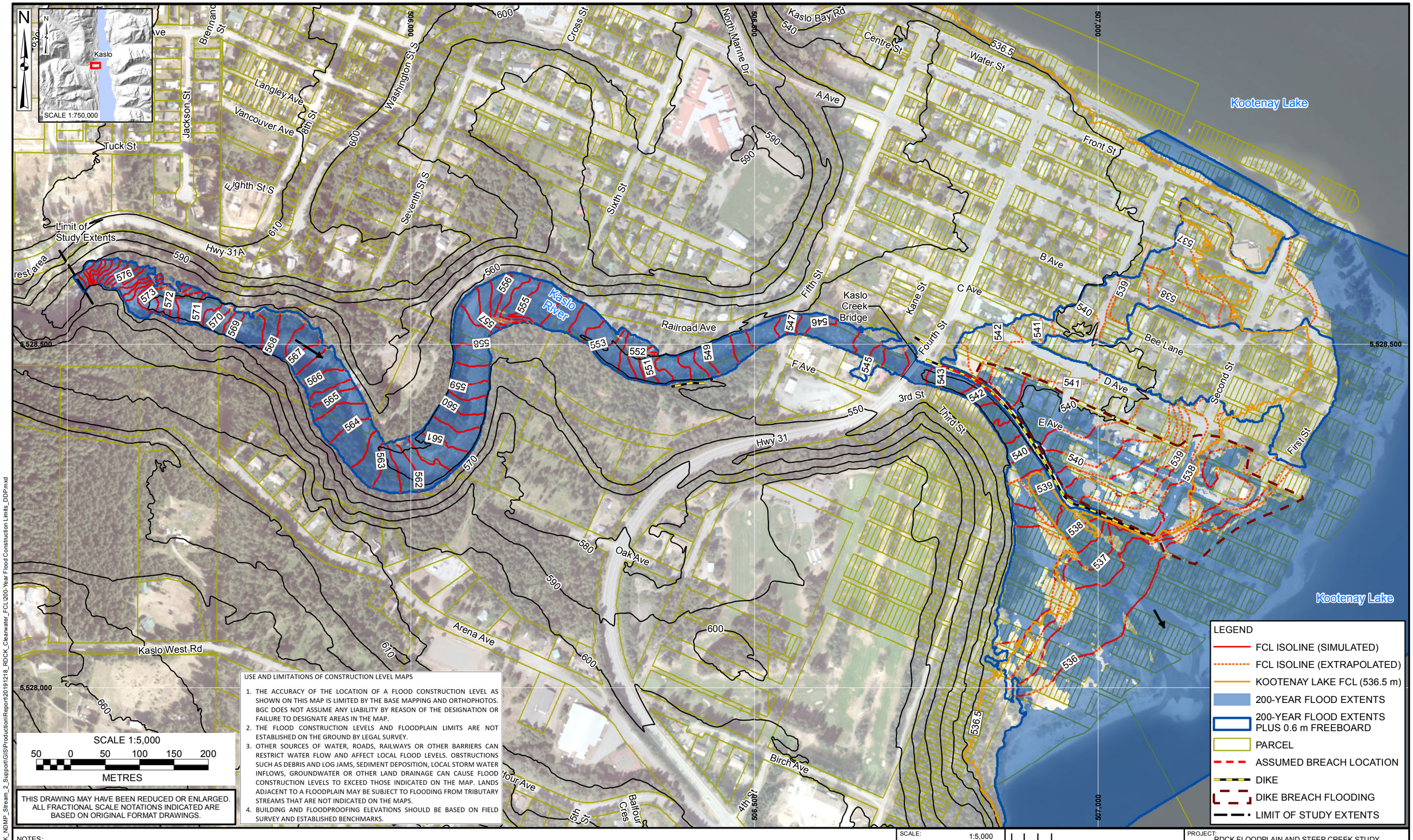


THIS DRAWING MAY HAVE BEEN REDUCED OR ENLARGED. ALL FRACTIONAL SCALE NOTATIONS INDICATED ARE BASED ON ORIGINAL FORMAT DRAWINGS.

USE AND LIMITATIONS OF CONSTRUCTION LEVEL MAPS

1. THE ACCURACY OF THE LOCATION OF A FLOOD CONSTRUCTION LEVEL AS SHOWN ON THIS MAP IS LIMITED BY THE BASE MAPPING AND ORTHOPHOTOS. BGC DOES NOT ASSUME ANY LIABILITY BY REASON OF THE DESIGNATION OR FAILURE TO DESIGNATE AREAS IN THE MAP.
2. THE FLOOD CONSTRUCTION LEVELS AND FLOODPLAIN LIMITS ARE NOT ESTABLISHED ON THE GROUND BY LEGAL SURVEY.
3. OTHER SOURCES OF WATER, ROADS, RAILWAYS OR OTHER BARRIERS CAN RESTRICT WATER FLOW AND AFFECT LOCAL FLOOD LEVELS. OBSTRUCTIONS SUCH AS DEBRIS AND LOG JAMS, SEDIMENT DEPOSITION, LOCAL STORM WATER INFLOWS, GROUNDWATER OR OTHER LAND DRAINAGE CAN CAUSE FLOOD CONSTRUCTION LEVELS TO EXCEED THOSE INDICATED ON THE MAP. LANDS ADJACENT TO A FLOODPLAIN MAY BE SUBJECT TO FLOODING FROM TRIBUTARY STREAMS THAT ARE NOT INDICATED ON THE MAPS.
4. BUILDING AND FLOODPROOFING ELEVATIONS SHOULD BE BASED ON FIELD SURVEY AND ESTABLISHED BENCHMARKS.

NOTES:
1. ALL DIMENSIONS ARE IN METRES UNLESS OTHERWISE NOTED.
2. THIS DRAWING MUST BE READ IN CONJUNCTION WITH BGC'S REPORT TITLED "RDCK FLOODPLAIN AND STEEP CREEK STUDY KASLO RIVER", AND DATED MARCH 2020.
3. BASE TOPOGRAPHIC DATA BASED ON LIDAR PROVIDED BY RDCK DATED 2017 AND 2018. CONTOUR INTERVAL IS 10 m. ORTHOPHOTO PROVIDED BY RDCK AND DATED 2017 AND 2018. PARCEL DATA FROM PARCELMAP BC. DIKE DATA FROM DATA BC. FLOOD CONSTRUCTION LEVEL BASED ON THE WATER SURFACE ELEVATION FROM THE 200-YEAR FLOOD USING THE INSTANTANEOUS PEAK DISCHARGE ADJUSTED FOR CLIMATE CHANGE PLUS 0.6 m FREEBOARD AND A KOOTENAY LAKE ELEVATION OF 535 m.
4. PROJECTION IS NAD 1983 UTM ZONE 11N. VERTICAL DATUM IS CGVD2013.
5. UNLESS BGC AGREES OTHERWISE IN WRITING, THIS DRAWING SHALL NOT BE MODIFIED OR USED FOR ANY PURPOSE OTHER THAN THE PURPOSE FOR WHICH BGC GENERATED IT. BGC SHALL HAVE NO LIABILITY FOR ANY DAMAGES OR LOSS ARISING IN ANY WAY FROM ANY USE OR MODIFICATION OF THIS DOCUMENT NOT AUTHORIZED BY BGC. ANY USE OF OR RELIANCE UPON THIS DOCUMENT OR ITS CONTENT BY THIRD PARTIES SHALL BE AT SUCH THIRD PARTIES' SOLE RISK.

| | |
|---|---|
| SCALE: | 1:5,000 |
| DATE: | MAR 2020 |
| DRAWN: | LL |
| CHECKED: | PG, TJP |
| APPROVED: | RM |

BGC ENGINEERING INC.
AN APPLIED EARTH SCIENCES COMPANY

CLIENT:

PROJECT: RDCK FLOODPLAIN AND STEEP CREEK STUDY
KASLO RIVER

TITLE: 200-YEAR FLOOD CONSTRUCTION LEVEL
(SHEET 1 OF 1)

| PROJECT No.: | DWG No: |
|---|---|
| 0268 007 | 07 |

X:\Projects\0268\007_RDCK_NDMP_Stream_2_Support\GIS\Production\Report\20191218_RDCK_Clearwater_FCL\20D-Year Flood Construction Limits_DDP.mxd